

UNIVERSITÉ DU QUÉBEC EN ABITIBI-TÉMISCAMINGUE

ADAPTIVE SWITCHED BEAM RECONFIGURABLE ANTENNA FOR WIRELESS
SENSOR NETWORK APPLICATIONS.

MÉMOIRE

PRÉSENTÉ

COMME EXIGENCE PARTIELLE
DE LA MAÎTRISE EN INGÉNIERIE

Par

MUKENDI LEINGTHONE MUAMBA

Jury d'évaluation

Examineur Externe : Prof. Gilles Y. Delisle, Université Laval

Examineur Externe : Prof. Michel Misson, Université Clermont Auvergne

Examineur Interne : Prof. Nahi Kandil, Université du Québec en
Abitibi-Témiscamingue

Directeur de Recherche : Prof. Nadir Hakem, Université du Québec en
Abitibi-Témiscamingue

© Copyright by Mukendi Leingthone Muamba, 2018



BIBLIOTHÈQUE

Cégep de l'Abitibi-Témiscamingue
Université du Québec en Abitibi-Témiscamingue

Mise en garde

La bibliothèque du Cégep de l'Abitibi-Témiscamingue et de l'Université du Québec en Abitibi-Témiscamingue a obtenu l'autorisation de l'auteur de ce document afin de diffuser, dans un but non lucratif, une copie de son œuvre dans Depositum, site d'archives numériques, gratuit et accessible à tous.

L'auteur conserve néanmoins ses droits de propriété intellectuelle, dont son droit d'auteur, sur cette œuvre. Il est donc interdit de reproduire ou de publier en totalité ou en partie ce document sans l'autorisation de l'auteur.

Warning

The library of the Cégep de l'Abitibi-Témiscamingue and the Université du Québec en Abitibi-Témiscamingue obtained the permission of the author to use a copy of this document for non-profit purposes in order to put it in the open archives Depositum, which is free and accessible to all.

The author retains ownership of the copyright on this document. Neither the whole document, nor substantial extracts from it, may be printed or otherwise reproduced without the author's permission.

BIBLIOTHÈQUE

Cégep de l'Abitibi-Témiscamingue
Université du Québec en Abitibi-Témiscamingue

Mise en garde

La bibliothèque du Cégep de l'Abitibi-Témiscamingue et de l'Université du Québec en Abitibi-Témiscamingue a obtenu l'autorisation de l'auteur de ce document afin de diffuser, dans un but non lucratif, une copie de son œuvre dans Depositum, site d'archives numériques, gratuit et accessible à tous.

L'auteur conserve néanmoins ses droits de propriété intellectuelle, dont son droit d'auteur, sur cette œuvre. Il est donc interdit de reproduire ou de publier en totalité ou en partie ce document sans l'autorisation de l'auteur.

Warning

The library of the Cégep de l'Abitibi-Témiscamingue and the Université du Québec en Abitibi-Témiscamingue obtained the permission of the author to use a copy of this document for non-profit purposes in order to put it in the open archives Depositum, which is free and accessible to all.

The author retains ownership of the copyright on this document. Neither the whole document, nor substantial extracts from it, may be printed or otherwise reproduced without the author's permission.

ABSTRACT

The ability to tune resonances, change polarization and modify their radiation patterns has made reconfigurable antennas development imperative in modern telecommunication systems and they are widely used as additional features in wireless communication system. Their agility and diversity have expanded their horizons for different types of applications especially in cognitive radio, satellites and many other applications. Reconfigurable antennas satisfy the requirements for increased functionality, such as direction finding, beam steering, radar, control and command, within a confined volume.

The integrations of reconfigurable antennas with radio frequency (RF) switches are needed to perform the switchable ability among many other reconfiguration techniques.

In this project, a new reconfigurable Frequency Selective Surface (FSS) screen is proposed to create a switched beam reconfigurable antennas. Indeed, the transmission/reflection responses of each planar FSS are carefully delineated to elaborately reshape the screens to a cylindrical form. The cylindrical shape is deliberately chosen to achieve the desired sweeping beam performances over all azimuth angles. Then, by precisely controlling the active elements integrated into the cylindrical FSS, the radiated field of an RF-source at the center of the cylinder is controlled to achieve the desired functionality.

Validation for Adaptive Switched Beam Reconfigurable Antenna (ASBRA) is achieved by comparing the simulated and measured radiation patterns parameters. The measured half-power beam width is 72° while 40° for the simulated. The simulated realized gain is around 15 dB while the measured gain is around 12.5 dBi at the frequency range of 2.4GHz.

ABSTRACT

La possibilité de syntoniser les résonances, de modifier la polarisation et de modifier leurs diagrammes de rayonnement a rendu impératif le développement d'antennes reconfigurables dans les systèmes de télécommunication modernes et elles sont largement utilisées en tant que fonctionnalités supplémentaires dans les systèmes de communication sans fil. Leur agilité et leur diversité ont élargi leurs horizons pour différents types d'applications, en particulier dans les domaines de la radio cognitive, des satellites et de nombreuses autres applications. Les antennes reconfigurables répondent aux exigences d'une fonctionnalité accrue, telles que la direction, la direction du faisceau, le radar, le contrôle et la commande, dans un volume confiné.

Dans ce projet, nous proposons de créer de nouveaux écrans reconfigurables à surface sélective en fréquences (FSS) pour créer des antennes reconfigurables à faisceaux commutés. En effet, les réponses de transmission / réflexion de chaque FSS planaire sont soigneusement délimitées pour remodeler minutieusement les écrans en une forme cylindrique. La forme cylindrique est délibérément choisie pour obtenir les performances de balayage souhaitées sur tous les angles d'azimut. Ensuite, en contrôlant avec précision les éléments actifs intégrés dans le FSS cylindrique, le champ rayonné d'une source RF au centre du cylindre est commandé pour obtenir la fonctionnalité désirée.

La validation de l'antenne reconfigurable à faisceau commuté est obtenue en comparant les paramètres des diagrammes de rayonnement simulés et mesurés. La largeur de faisceau mesurée est de 72° alors qu'elle est de 40° pour la simulation. Le gain simulé réalisé est d'environ 15 dB et le gain mesuré est d'environ 12,5 dBi dans la gamme de fréquences de 2,4 GHz.

ACKNOWLEDGEMENT

Specially dedicated to my beloved ones who always inspired and motivated me along my excellent journey of education

*To Almighty God who was, is and is to come for his kindly love towards
. ‘Yahweh Jirreh my provider’*

Specially my gratefulness and appreciation goes to my project supervisor Professor Dr. Nadir Hakem, for welcoming me to his research team, for his confidence during the entire thesis, for his guidance, motivations, support and constructive comments in accomplishing this project;

‘I say Thank you so very much Professor.’

I gratefully acknowledge my thesis committee members Professor Gilles Delisle, Professor Nahi Kandil and Professeur Michel Misson for their insights, remarks and suggestions on my dissertation on this research, which will be a valuable experience for my future career.

I would like to thank the engineer of the LRTCS laboratory, Mr. Mohamed Ailas, for realization of the experimental prototype.

I thank as well my thesis advisors Taieb El karkraoui and Alex Mouapi Researchers at the UQAT and Joseph Kabuya and Iris Kapinga researchers at Laval university for their encouragements, confidence and the high quality of advises during the project

*My precious Parents
Mukendi Tubongo Louis and Justine Kenda*

*My Wife 'baby douce' Jessica Malila and my beautiful Children Linciah, Beracah and
Akilimali*

*'For your understanding, patience and supports through this period of time. Without your
kind cares and patience, the difficulties of my master objectives and being far from of
family would never be endured'*

*My awesome brothers
Cyrille Mukendi & Desanges Mashata, André Mukendi & Cathy Meta and
Joseph Kabuya & Iris Kapinga*

*My lovely sisters
Claudine Ngalula & Seraphin Mulumba, Prisca Ntumba & Serge Cimanga
Rosie Ngoya & Hyppolite Salambua*

*My wonderful Parents in law
Christophe Tshimpe Ditumbule and Perpetue Malila Muenyi*

*My brothers in law
Christian Tshimpe & Christelle, Thierry Tshimpe, Steve Tshimpe and Nicky Tshimpe.*

*My Sisters in law
Patricia Tshimpe & Jeff Muzingu, Vanessa Tshimpe & Billy Mwepu, Laetitia Tshimpe &
Linné Nkongolo.*

*My nephews and nieces
Eli Énoch, Piris, Joris, Johann, Percy, Joyce, Elroy, Brian, Kenny, Gradi, Ariella,
Daniella, Paris, Prunelle, Elmer, Nehema and Damaris*

*My Pastor
Pierre Paradis & Linda Lacoste.*

*My Best Friends
Francis Royer & Katy Lacoste, Sylvain Lacoste & Melanie Guay.*

*"We don't remember days, but
we remember moments"*

Much Love

TABLE OF CONTENTS

ACKNOWLEDGMENTS	i
ABSTRACT.....	ii
TABLE OF CONTENTS.....	v
LIST OF FIGURES	ix
LIST OF TABLES	xiii
LIST OF ABBREVIATIONS.....	xiv
LIST OF SYMBOLS	xv
LIST OF APPENDICES.....	xvi
1. CHAPTER ONE: GENERAL INTRODUCTION.....	1
1.1 Project background	1
1.2 Motivation.....	1
1.3 State of the Art of Wireless Sensor Network.....	2
1.3.1 Definition of WSN.....	2
1.3.2 Architecture of sensor node	3
1.3.3 Protocols	5
1.3.4 Deployment.....	6
1.3.5 Scalability	6
1.3.6 Power consumption.....	7
1.3.7 Applications of WSN	8
1.4 Problem identification.....	9
1.4.1 Introduction.....	9
1.4.2 Technical and organizational challenges	10
1.4.2.1 Shape of beam	10
1.4.2.2 Choice of structure.....	11
1.4.2.3 Switching mode	11
1.4.2.4 Power source.....	11
1.5 Problem remedies and project objectives	12
1.5.1 Main objectives.....	12
1.5.2 Specifics objectives.....	12
1.6 Organization of the thesis and original contribution.....	12
1.6.1 Scope and limitation of the project	12
1.6.2 Thesis organization	13

2. CHAPTER 2: FUNDAMENTAL KNOWLEDGE OF RECONFIGURABLE ANTENNAS	15
2.1 State of the art on antenna.....	15
2.1.1 Type of antenna.....	16
2.1.1.1 Wire antennas.....	16
2.1.1.2 Aperture antennas	16
2.1.1.3 Array antennas	16
2.1.1.4 Printed antennas	16
2.1.2 Fundamental antenna parameters.....	17
2.1.2.1 Bandwidth.....	17
2.1.2.2 S-parameters	18
2.1.2.3 Radiation pattern.....	19
2.1.2.3.1 Antenna field region	20
2.1.2.3.2 Reactive near-field region.....	21
2.1.2.3.3 Radiating near-field or Fresnel region	21
2.1.2.3.4 Radiating far-field or Fraunhofer region.....	21
2.1.2.3.5 Characteristic impedance of EM waves.....	22
2.1.2.4 Velocity of propagation	22
2.1.2.5 Directivity	23
2.1.2.6 Antenna efficiency.....	23
2.1.2.7 Gain.....	24
2.1.2.8 Polarization	24
2.1.2.9 Half power beam width.....	25
2.2 Reconfigurable antenna	26
2.2.1 Introduction.....	26
2.2.1.1 Frequency reconfigurable antenna.....	27
2.2.1.2 Polarization reconfigurable antenna	28
2.2.1.3 Radiation pattern reconfigurable Antenna.....	29
2.2.2 Principles of reconfigurability and RF switch technologies	29
2.2.2.1 Reconfiguration by switching.....	30
2.2.2.1.1 Electrically reconfigurable antenna	30
2.2.2.1.2 RF- MEMS.....	30
2.2.2.1.3 Varactors	31
2.2.2.1.4 PIN diodes.....	32

2.2.2.2 Reconfigurability by changing material.....	33
2.2.2.2.1 Tunable conductivity	33
2.2.2.2.2 Tunable permittivity.....	33
2.2.2.2.3 Tunable permeability	34
2.2.2.3 Optically reconfigurable antennas	34
2.2.2.4 Reconfiguration by structural alteration	34
2.2.3 Comparison between different techniques and practical issues.....	35
2.3 Propagation channel.....	36
2.3.1 Propagation in free space	37
2.3.2 Multipath propagation	38
2.4 Summary.....	38
3. CHAPTER THREE: A REVIEW OF RECONFIGURABLE ANTENNA	
BASED ON FSS	39
3.1 Introduction.....	39
3.2 Periodic structures.....	39
3.2.1 Analysis of periodic structures.....	40
3.2.1.1 Structure EBG	40
3.2.1.1.1 Historic on periodic structure	40
3.2.1.1.2 Theoretical notion	42
3.2.1.1.2.1 Floquet's-Bloch's mode	42
3.2.1.1.2.2 Dispersion diagram or Brillouin diagram	43
3.2.1.1.2.3 Fabry perrot resonator	48
3.2.2 Structure EBG	49
3.2.3 Structure FSS	50
3.2.3.1 Passive periodic structure	52
3.2.3.1.1 Continuous band FSS structure	52
3.2.3.1.2 Discontinuous band FSS structure	54
3.2.4 Active FSS structure	55
4. CHAPTER FOUR: DESIGN AND FABRICATION PROCESS OF THE	
ASBRA	58
4.1 Project methodology	58
4.2 Cylindrical FSS screen.....	60
4.2.1 Design of cylindrical reflector.....	60

4.2.2 Source of radiation design	62
4.2.3 FSS Unit cell design.....	64
4.2.4 PIN diode integration.....	65
4.2.4.1 PIN diode representation using lumped element	65
4.2.4.2 PIN diode representation using PEC pad.....	66
4.3 Parametric study of ASBRA.....	67
4.3.1 Effect of the radius of the cylindrical reflector	68
4.3.2 Effect of the number of FSS unit cell elements	71
4.3.3 Effect of the width of FSS Elements.....	72
4.3.4 Effect of the band gap aperture	73
4.3.5 Effect of lumped elements	74
4.3.6 Effect of the opening angle	76
4.4 Antenna matching.....	81
4.5 Fabrication process	83
4.6 Measurement process.....	86
4.6.1 Return loss measurement	86
4.6.2 Radiation pattern measurement.....	88
4.7 Summary.....	91
5. CHAPTER FIVE: RESULTS ANALYSIS AND DISCUSSION	93
5.1 Introduction.....	93
5.2 Analysis and discussion of the ASBRA.....	93
5.2.1 Input return loss	93
5.2.2 Realized gain.....	95
6. CHAPTER SIX: CONCLUSION	98
6.1 Conclusion	98
6.1.1 Key contribution	99
6.1.2 Future Research	99
7. REFERENCES	100
8. PUBLICATIONS	110
9. APPENDICES.....	112

LIST OF FIGURES

Figure 1.1 Wireless Sensor Network	3
Figure 1.2 Physical architecture of sensor node	3
Figure 1.3 Commercial WSN nodes	5
a. MICA2 Dot	5
b. Waspote plug & sensor	5
Figure 1.4 Power consumption of a MICAz node	7
Figure 1.5 Antenna beam patterns in switched beam systems.....	11
Figure 2.1 Two port network definition.....	19
Figure 2.2 Coordinate system for antenna analysis.	20
Figure 2.3 Field regions of an antenna.....	21
Figure 2.4 Rotation of a plane electromagnetic wave at $z = 0$ as a function of time.....	25
Figure 2.5 Two-dimensional of power pattern.	26
Figure 2.6 The block diagram of the reconfigurable antenna.	27
Figure 2.7 Telecommunication infrastructure	28
Figure 2.8 Types of RF-MEMS switches.	30
Figure 2.9 (a) Electrical Equivalent Circuit, (b) Symbol of Varactor diode.	31
Figure 2.10 Intrinsic region of the Pin diode.....	32
Figure 2.11 The principle of a crystalline solar cell	33
Figure 3.1 Structure Yablonovite.....	41
Figure 3.2 Structure woodpile.....	41
Figure 3.3 One-dimensional periodic structure.	42
Figure 3.4 Surface wave dispersion pattern of metal strips.	44
Figure 3.5 Two-dimensional crystalline structure.	46
Figure 3.6 (a) Centered cubic cell. (b) Wigner-Zeitez cell.....	47
Figure 3.7 Fabry-Perot cavity	48
Figure 3.8 Resonant cavity.	48
Figure 3.9 EBG antenna of Temelkuran.....	49
Figure 3.10 EBG antenna with fault	50

Figure 3.11 EBG Lens antenna.....	50
Figure 3.12 High impedance surface: (a) Mushroom cell, (b) Comb teeth.....	51
Figure 3.13 Artificial magnetic wall.....	52
Figure 3.14 Periodic continuous strip structure.....	53
Figure 3.15 Electrical model of a continuous band structure.....	54
Figure 3.16 Periodic structure with discontinuous bands.....	54
Figure 3.17 Electrical model of a discontinuous strip structure.....	55
Figure 3.18 Active FSS Structure.....	56
Figure 4.1 Flow chart of overall process of the ASBRA.....	59
Figure 4.2 Geometry of the proposed cylindrical FSS antenna.....	60
Figure 4.3 Geometry of a corner reflector into a semi-cylindrical reflector.....	61
Figure 4.4(a) Frequency response of the dipole.....	62
Figure 4.4(b) realized gain response of the dipole.....	63
Figure 4.4(c) Radiation pattern response of the dipole.....	63
Figure 4.4(d) Radiation pattern of the dipole in azimuth plane.....	63
Figure 4.5 Fss Unit cell of the Reconfigurable Beam Switching antenna.....	64
Figure 4.6(a) ASBRA representation using lumped element in CST.....	65
Figure 4.6(b) Pin diode electrical model (a)RLC-Serial (b) RLC-Parallel.....	65
Figure 4.6(c) Lumped element circuits that are developed in CST software.....	66
Figure 4.7 ASBRA representation in CST using PEC pad.....	66
Figure 4.8(a) Effect of the radius R on the resonance frequency of the cavity.....	69
Figure 4.8(b) Effect of the radius R on the H-plane radiation pattern of the cavity.....	69
Figure 4.8(b) Effect of the radius R on the H-plane radiation pattern of the cavity.....	70
Figure 4.8(c) Effect of the radius R on the E-plane radiation pattern of the cavity.....	70
Figure 4.9 Effect of the number of FSS elements (NFSS=6,9,12,15).....	71
Figure 4.10 Effect of the unit cell FSS width.....	72

Figure 4.11 Effect of the width of the gap.....	73
Figure 4.12 Effect of the diode capacitance on the structure.....	74
Figure 4.13 Effect of the diode capacitance on the radiation pattern... ..	75
Figure 4.14 Effect of the capacitance on directivity... ..	75
Figure 4.15 Opening angle of the radiating structure.... ..	75
Figure 4.16 Radiation diagrams in the azimuth plane at 2.45 GHz.....	76
Figure 4.17 Normalized radiation diagrams in the E- plane at 2.45 GHz.... ..	76
Figure 4.18 Directivity according to the opening angle... ..	77
Figure 4.19 S11 according to the opening angle.....	77
Figure 4.20 Radiation pattern according to the opening angle.....	78
Figure 4.21 Switching beam in the all azimuth angles	78
Figure 4.22 Reconfiguration in the H-plane... ..	79
Figure 4.23 Realized gain of the ASBRA.....	80
Figure 4.24 ASBRA radiation pattern in CST.....	81
Figure 4.25 Matching circuit	81
Figure 4.26 Return loss without and with matching circuit.....	82
Figure 4.27 Realized gain without and with matching circuit.	82
Figure 4.28 VectorStar MS4647A VNA Front Panel – Rear panel.....	85
Figure 4.29 Measuring the S11 of the dipole alone.....	86
Figure 4.30 Measuring the S11 of overall structure... ..	87
Figure 4.31 Power received and radiation pattern measurement set-up.... ..	87
Figure 4.32 LNA RLNAOIMIOG.....	88
Figure 4.33 Anritsu MG3692B.....	88
Figure 4.34 The Lab-volt 9506-00.....	89
Figure 4.35 The Lab-volt 9506-00 setup in the Laboratory.....	89
Figure 5.1 Simulated and measured S11 for ASBRA.....	90

Figure 5.2 Realized gain results for measured and simulated ASBRA.....	94
Figure 5.3 Measuring the dipole alone.....	94
Figure 5.4 Measuring the all structure.....	95
Figure 5.5 Radiation pattern of the dipole.....	96
Figure 5.6 Radiation pattern of the simulated and the fabricated ASBRA	97

Table 1.1 Commercial WSN node specifications.....	5
Table 2.1 Comparison between different switches.....	36
Table 4.1 The value of lumped elements as a PIN diode.....	66
Table 4.2 LNA Parameters RLNAOIMIOG.....	89
Table 4.6 Steps of fabrication process.....	84
Table 5.1 Comparison of bandwidth between simulation and measurement.....	94
Table 5.2 Previous researches on reconfigurable antenna.....	98

ASBRA - Adaptive Switched Beam Reconfigurable Antenna
WLAN - Wireless Local Area Network
UWB - Ultra Wide Band
CR - Cognitive Radio
VSWR - Voltage Standing Wave Ratio
RL - Return Loss
BW - Bandwidth
HPBW - Half Power Bandwidth
FR-4 - Fire Retardant Type 4
FSS - Frequency Selective Surface
GHz - Gigahertz
UV - Ultra-Violet
CST - Computer Simulation Technology
EM - Electromagnetic
SNR - Signal Noise Ratio
GSM - Global System for Mobile Communications
WIFI - Wireless Fidelity
RF - Radio Frequency
MEMS - Micro Electro Mechanical Systems
PBG - Photonic Band Gap
EBG - Electromagnetic Band Gap
LHM - Left Hand Material
TEM - Transverse ElectroMagnetic
TE - Transverse Electrique
TM - Transverse Magnétique
QoS - Quality of Service
MAC - Media Access Control
HART - Highway Addressable Remote Transducer Protocol
UAV - Unmanned Aerial Vehicles
FP - Fabry-Pérot

f_l - Low frequency

f_h - High frequency

τ - Scaling factor

E - Electric field.

H - Magnetic field.

h - Substrate thickness.

t - Copper thickness

ϵ_r - Relative permittivity of material.

$\tan \delta$ - Tangential loss of material.

dB - Decibel

mm - millimeter

R - Resistor

L - Inductor

C - Capacitor

Γ - the reflection coefficient.

V_0^- - reflected voltage wave

V_0^+ - incident voltage wave

CHAPTER ONE

GENERAL INTRODUCTION

1.1. Project background

The field of telecommunications is in perpetual evolution and the dynamics of development are constantly needed to improve flexibility, ergonomics and speed of information transfer. Therefore, wireless communication is essential for several reasons such as security, location and productivity.

The unsupervised or random deployment of a wireless sensor network requires the installation of an antenna system capable of adapting itself to the context of the conditions of propagation of the wireless signal. By adapting their operating characteristics such as the radiation pattern and by altering the current flow using switching elements such as Pin-diodes, the reconfigurable antennas have the ability to desirably improve energy efficiency and to avoid the effects of interference and multi-channel discoloration effects. Thus, the introduction of a reconfigurable antenna instead of an omnidirectional antenna makes it possible to transmit or receive the radio signal with longer ranges and faster throughput while reducing the amount of energy required establishing communication at its minimum.

This project proposes the design and development of an adaptive narrow band antenna using FSS technic with the integration of the PIN-diode to form the switched beam reconfigurable antenna. Depending on the switching state, the ASBRA enables the selection between several beams and achieves the desired performance that allows reconfigurable directive beams over the entire azimuth plane with equidistant angles. This thesis describes the ASBRA's development including the literature review, the simulation design until the fabrication and measurement process.

1.2. Motivation

Nowadays, the importance of communication in an emergency response scenario is well known due to the frequency of recent incidents such as disasters and their wide range of sever impact throughout the world. Human civilization has always been devastated by natural disasters, such as earthquakes, volcanoes, tsunamis, landslides, floods, forest fires, weather and climatic conditions (irma, harvey, hurricanes , tornadoes, extreme heat or cold, etc.) or artificial disasters such as large-scale terrorism, chemical spills, nuclear radiation

eruptions, public service failures, epidemics, accidents, explosions and urban fires, etc. ... which is a serious disruption to the functioning of a community or society. Such emergencies require a rapid and effective response from various stakeholders (team of pumps, firemen, paramedics, doctors...) responsible for intervening in the sectors concerned; So it allows us to anticipate our actions.

One of the most important components to help respond to these emergencies is the antenna. It must be selective in the sense that it must correspond to the frequency band given in a particular direction to send the most possible information, to reduce collisions, increase communication distance and optimize power consumption; It must also be economical in the sense that its output must be as ideal as possible in terms of efficiency and gain which leads to smart antenna in the literal sense of the term. As a result, intensive research has been conducted in many directions to find other alternatives and approaches in this field. One of these alternatives is to use a FSS in reconfigurable antennas. This approach offers more features for an antenna, more versatility, less cost and significant savings in size and space [1, 2]. So research in this area is very important and is one of the most popular areas nowadays. Our motivation is to investigate a new FSS structure with the use of RF switch technology to actively and intelligently change the operating beam of an antenna including minimization of active switching components and an overall reduction in antenna design complexity.

1.3. State of the Art of Wireless Sensor Network

1.3.1. Definitions of Wireless Sensor Network

A sensor is a small autonomous device capable of performing simple measures on its immediate environment. WSN are a new class of distributed systems [3] that consists of dispersed group of devices which use sensors to monitor environmental conditions. WSN were originally designed to facilitate military operations, but their applications have since grown to cover several domains such as medical, industrial and, more recently, home networks. Although this development was initially fueled by military research areas, today, as recent technological advances, the possibility of producing low-cost sensors has increased considerably, which brings us to the challenge of scaling networks to a larger number of nodes. As shown in *Figure 1.1*, WSN is a group of very small devices, named node, varying from dozens elements to several thousands.

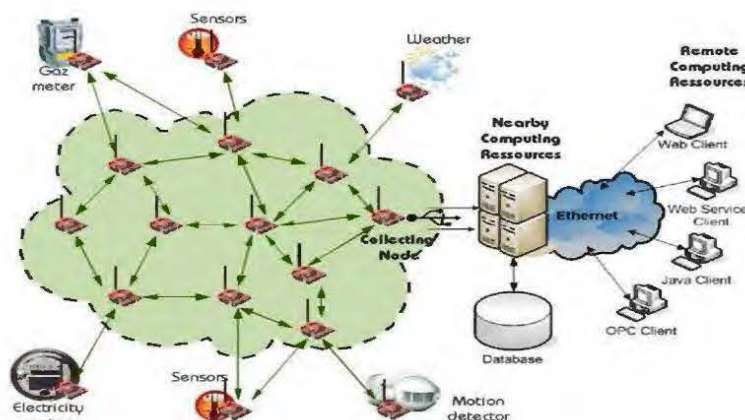


Figure 1.1 Wireless Sensor Network. [3]

In these networks, every node is capable of watching its environment and reacting if necessary by sending the information collected with the aid of wireless connection in one or several points of collection (Sink Puits). According to the system, nodes can communicate directly with the Puits Sink, or then act as relay for the transmission of information.

1.3.2. Architecture of a sensor node

According to [4], a generalized diagram of a WSN architecture is presented. The authors divide the architecture into four major core units as shown in *figure 1.2*.

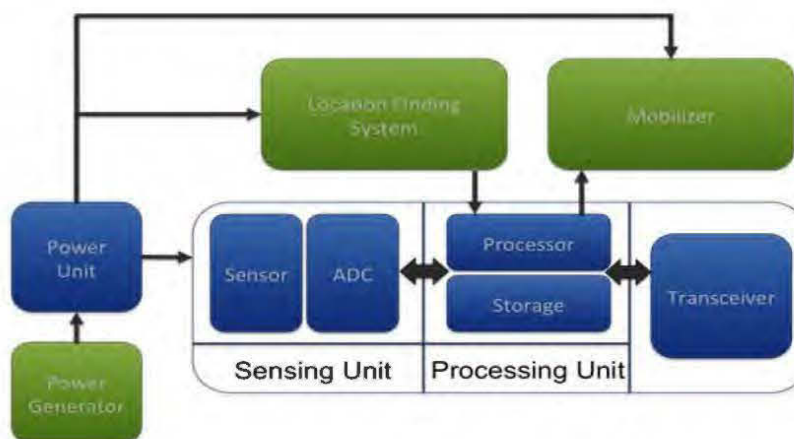


Figure 1.2 Physical Architecture of a sensor node [4]

It is possible to distinguish:

- **A Sensing unit or Capture unit:** it is the interface to the physical world responsible for carrying out data acquisition which provide the means to gather and send physical quantities and are converted by analog to digital converters to be analyzed and processed by the processing unit;

- **A processing unit:** this is the processor that is responsible for processing all relevant data and executing the code that describes the behavior of the sensor node; frequently known as micro-processor, this unit is responsible for controlling the other units' functionalities. However, it may also contain memory and several inputs/outputs, hence, its alternative title of micro-controller
- **A Transceiver unit or Communication unit:** it is composed of a (radio module) transmitter/receiver antenna(s) allowing communication between the different nodes of the network.
- **A Power unit or unit of energy:** this is responsible for maintaining the electric activity of the sensor node. This may be achieved by a network cell or by recharging a battery via energy harvesting, such as solar energy with solar cells.
- **Location finding system:** Used to determine the location of the sensor with high accuracy.
- **Mobilizer:** This is responsible to move the sensor node when it is required to carry out the task

The first important requirements of WSN is the node's lifetime, the network should be power efficient and fulfill its task as long as possible. The energy savings can be obtained from the optimization of software or hardware used on the system. Using energy harvesting from the environment is also a good solution to increase the WSN lifetime. Besides, the WSN should be based on low cost devices because the number of node can be up to thousands or more. Sensor network should be very flexible to adapt to the different conditions and scalable to support large number of nodes.

The system should be self-reconfigured to guarantee the network connection when the failure of individual nodes occurs. The reprogramming of sensor nodes is also important to update the new configuration and improve the performance of system. Finally, a sensor network should be able to protect itself and its data. For the secure data transmission, the encryption keys have to be established among sensor nodes.

There are many different types of sensors that are used on WSN such as:

Temperature, Humidity, Vehicular movement, Lightning condition, Pressure, Soil makeup, Noise level, The existence of certain kinds of objects, Mechanical stress levels, The current characteristics such as speed, direction, and size of an object.

In [4], I.F. Akyildiz et al. categorized the WSN application into military, environment, health, home and other commercial areas. In addition, space exploration, chemical processing and disaster relief are also considered as the expanding categories.

Several wireless sensor network commercial solutions are listed below:

Platform	Application	Processor speed	RAM	RF range	Data rate
MICA	Educational	8-16 MHz	4 kB	2.4 - 2.48 GHz	38.4/250 kB/s
LOTUS	Industrial	10-100 MHz	64 kB	2.4 GHz ISM	250 kB/s
TelosB	Educational	8 MHz	10 kB	2.4 - 2.48 GHz	250 kB/s
IRIS	OEM Edition	8 MHz	8 kB	2.4 GHz ISM	250 kB/s
LOTUS	Industrial	8 MHz	4 kB	433 MHz ISM	250 kB/s
Waspnote	Versatile	14.7 MHz	8 kB	2.4 GHz ISM	250 kB/s

Table 1.1: Commercial WSN node specifications. Adapted from [3].



(a) MICA2 Dot. (b) Waspnote Plug & Sensor

Figure 1.3 Commercial WSN nodes [3].

1.3.3. Protocols

As WSN evolved, several key factors such as robustness, efficiency and reliability arose to challenge the QoS. As these factors require mass expertise in all fronts of networking stack, from physical radio design to channel access schemes, routing protocols, and distributed data-processing algorithms [5], the IEEE introduced in 2003 a standard which specifies physical layer and MAC. The major features of IEEE 802.15.4 standard rely upon specifications in the physical and MAC layers for low-rate nearby communications. The standard defines, among others, which these networks should be capable of providing up to

250 kbps of data transfer rate with simple QoS requirements. The reason why this standard uses low transmission rates is because sensor network applications do not usually need high data transfer rates and consequently would clearly benefit from low-power solutions to prolong the lifetime. The list below briefly reviews the solutions that are based on the 802.15.4 standard:

1. ZigBee
2. Wireless HART (Highway Addressable Remote Transducer Protocol)
3. 6LoWPAN (IPv6 over Low power wireless personal area network)

Most commercial WSN solutions use one of these three standards. However, each may be better suited for a particular application. For instance, ZigBee networks are targeted for home automation, smart energy, building automation, telecommunication services and health care while Wireless HART is suited for automation and industrial applications.

1.3.4. Deployment

With the increasing number of nodes deployed in WSN infrastructures, the ability to collect sensor information has been part of a strategy to succeed in real-world applications. This not only reduces the overall costs, but can also prolong network lifetime. According to [6], node deployment can be classified as:

- **Static deployment:** nodes remain static during the network lifetime. This method may be sub classified as either controlled or random deployment [7]. The mentioned reference also exposes demonstrate optimization goals for this node deployment method such as: area coverage, network connectivity, network lifetime, and data fidelity.
- **Dynamic deployment:** nodes may re-arrange their position due to application-level requires location changes.

For instance, authors in [8] present design strategies of using Unmanned Aerial Vehicles UAVs to deploy wireless sensor networks for post-disaster monitoring, which perfectly exemplifies the random-static deployment mentioned above. As referred to earlier, the interest consists in network for agriculture, and for this reason a controlled-static” deployment is used in order to optimize the performance of the network.

1.3.5. Scalability

Wireless sensor networks may grow to contain hundreds of nodes; this creates scalability necessitate in-place routing protocols for managing and controlling scalable and adaptive networks. Several routing protocols, studied in [9] and [10] addresses these problems and

assesses those which are the best routing protocols using quantitative metrics such as throughput, latency, energy consumption, and delay.

1.3.6. Power consumption

As referred to earlier, the power unit is a key element in the WSN node structure. However, it is also the principle time limiting factor in the lifetime of a network. Currently, batteries are the major source of energy in WSNs and/or power buffer, in the case of energy harvesting WSN nodes. In [11], the authors show the different energy sources suitable for scavenging, energy conversion devices and a wide comparison of practical energy harvesting devices such as vibration based or solar based devices. In fact, in the WSN of interest, solar energy scavenging is used with a solar cell module.

The greatest part of the power is spent by peripherals, specifically radio modules, as *figure. 1.4* illustrates.

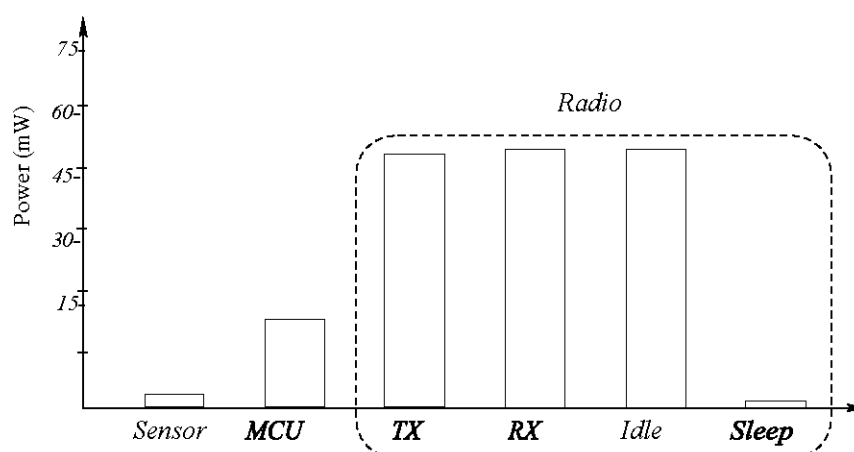


Figure 1.4 Power consumption of a MICAz node [11].

Currently, solutions to overcome this problem are based on batteries which may, in the case of nodes failure in a low density network, be quickly drained.

Dynamic Voltage Scaling is another processing power-saving technique. It adapts the power supply voltage and clock frequency of the microprocessor which depends upon the workload, leading to lower energy consumption without affecting the overall performance.

1.3.7. Application of Wireless sensor network

The sensor arrays can be made up of different types of sensors depending on the application. In general, the main applications of wireless sensor networks can be military, environmental, sanitary or domestic [12].

- **The military field** is the first to be interested in the WSNs, in order to study the movements of the enemy troops, or to analyze a battlefield before embarking on it. However, due to application-level requirements, robustness, scalable self-organization, network connectivity, energy consumption, fault tolerance, and end-to-end message security are the major concerns. These type of WSNs can be applied in three military operation scenarios:
 - battlefield: large-scale and non-manually deployed;
 - urban-warfare and force-protection: medium-scale and manually deployed;
 - other-than-war: any scale, both manually or non-manually deployed.

In [13], a battlefield scenario requesting distribution of thousands of tactical sensors in a specific area using UAV dropping and/or artillery deployment methods is presented.

It has a self-organizing initialization period and after that the information is reported to a UAV sink node. Also [14] report, among others, several examples of military WSN applications such as perimeter protection, sniper detection and localization,” chemical, biological and explosive vapor detection with micro cantilever array sensors”. [15]

- **In the environmental field**, the WSNs are used to detect and prevent natural disasters such as fires, to understand the evolution of natural habitats and movements of animal populations with a view to knowledge and protection of species or in agricultural environments to optimize soil management. The most commonly used sensors are:

- Atmospheric pressure sensor
- Leaf wetness sensor
- Humidity sensor
- Temperature sensor
- Luminosity sensor
- Soil moisture sensor
- Soil temperature sensor
- Ultraviolet radiation sensor
- Anemometer
- Pluviometer
- Dielectric permittivity sensor

- **In the biomedical field**, the implantation of autonomous sensors in the human body or in the habitat would enable the physiological data to be collected and stored continuously and sent to a competent medical center, distance of a convalescent patient,

or facilitating early diagnosis and disease prevention. In the case of human applications, WSNs are applied in hospitals and homes.

Several applications are listed below.

- emergency response
- provision of interfaces for the disabled
- integrated patient monitoring
- drug administration
- tracking and monitoring doctors and patients in hospitals
- Sudden Infant Death Syndrome (SIDS) detection
- premature infant thermal regulation
- Finally, WSNs are also useful in monitoring difficult or **structural environments** such as bridges, vehicles or industrial environments for the purpose of detecting alterations and preventing disasters which is part of our work.

The industrial applications can be divided based on specific production requirements.

- Industrial environmental sensing: pollution, hazard, security
- Condition monitoring: structural health, equipment condition, human error monitoring
- Process automation: evaluation, improvement

1.4. Problem identification

1.4.1. Introduction

Antenna development play a key role in wireless technology since the rapidly increasing number of users in broadcasting, telecommunications, navigation, radar, sensors, military and for wireless communication. The increasing number of users may lead to congestion of existing spectrum such as Wireless Local Area network (WLAN). Most WLANs use the same frequency band in the narrow range of 2.4 to 2.5 GHz. They link many systems together, thus resulting in better communication and compatibility. In addition, most of these systems use the miniature sleeve dipole antenna. Although the use of these antennas is relatively simple (buy-plug-play), their performances are limited (about 0 dBi of gain). This type of antenna provides an omnidirectional radiation pattern.

The ability to receive signals from almost every direction (azimuth plane) is the main advantage of omnidirectional antenna.

On the other hand, they lead to serious problems of interference, lower capacity, prominent decrease in connection speeds and sometimes lack of connectivity due to the unavailability of free access channels [16]. In addition, this type of antenna is very sensitive in multipath environments when the fading effect is important. In this case, the drop in the quality of transmission channels will lead to more packet errors. Thus, the packets have to be resent and the overall power consumption will increase. The introduction of directional antenna instead of an omnidirectional antenna is as an interesting solution that makes it possible to transmit or receive the radio signal with longer ranges and faster throughput while reducing the amount of energy necessary to establish communication.

The main advantage of this solution is a higher gain because radiated power is focused and it propagates the signal in one or more specify directions. Besides, the effect of noise from unwanted signals is reduced, thus channel quality is improved. However, the larger dimension is a classical drawback of this antenna type. Additionally, in the networks that contain hundreds or thousands of sensor nodes, the restriction on the number of signal propagation direction is its fatal weaknesses. This is a reason that lead our research towards directional antenna in the field of WSN.

1.4.2. Technical and organizational challenges

1.4.2.1. Shape of beam

Switched beam antenna systems form multiple fixed beams with increased sensitivity in some directions. It is very beneficial for many applications such as base stations of mobile networks where the quality of coverage is a requirement.

The adaptive beamforming technique represents a spatial form of adaptive signal processing (see *figure.1.5*). This technique can be used in wireless communication systems that work in a challenging environment with multiple sources of interference leading to amplify the target signal and attenuate the interference signals. The optimization of the transmission to the desired user (directivity) makes it possible to obtain less energy consumption and lower amplification costs.

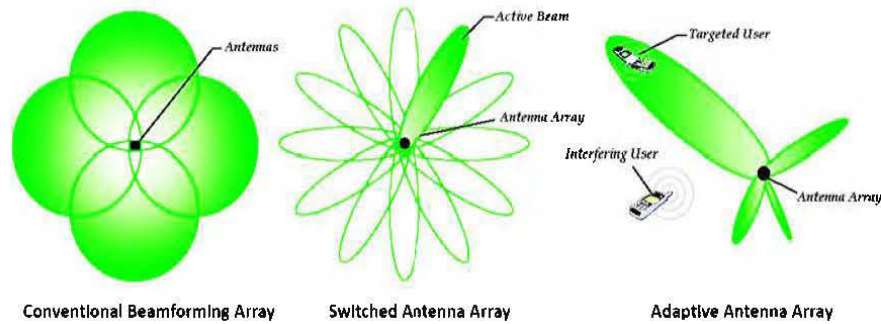


Figure 1.5 Antenna beam patterns in Switched beam systems

(<https://www.networkcomputing.com/wireless-infrastructure/how-does-mu-mimo-work/74896423>)

1.4.2.2. Choice of Structure

The fundamental idea behind reconfigurable antennas is to improve the performance of the wireless communication system by increasing the gain in a chosen direction. FSS are structures whose behavior changes with frequency, they have particular electromagnetic characteristics making them act as electric or magnetic wall, radiating structure or decoupling device. Often, these are periodic structures illuminated by a wave parallel to their normal. As a result, their use in the antenna field has as many advantages as applications. FSS-based antennas are a solution to achieve a certain dimension reduction and thus arrive at compact antennas [17, 18].

1.4.2.3. Switching mode

Taking into account the frequency range, the ability to handle high power with low distortion, loss, low cost, high speed, fast switching, high isolation, ease of polarization, less current. [19,20]

1.4.2.4. Power source

An intelligent antenna system can improve considerably by reducing multi-path discoloration, extending battery life, increasing system capacity, extending the coverage area and increasing transmission rate. With a non-uniform radiation pattern, there is a new gain challenge in the desired direction which is also an important factor in deciding the required power. We address the issue of controlling the energy efficient topology in a wireless network with directional switched beam antennas. [21,22].

1.5. Problem remedies and project objectives

In this work, a new class of reconfigurable FSS screens is proposed to create a reconfigurable antenna. Indeed, the transmission/reflection responses of each planar FSS are carefully delineated to elaborately reshape the screens to a cylindrical form. The cylindrical shape is deliberately chosen to achieve the desired sweeping beam performances over all azimuth angles. Then, by precisely controlling the active elements integrated into the cylindrical FSS, the radiated field of an RF-source at the center of the cylinder is controlled to achieve the desired functionality.

1.5.1. Main objectives

The main objective is to design and develop a cylindrical ASBRA with an EBG technic and FSS structure that can provide an agile and reconfigurable radiation pattern using a single radiation source capable of covering instantaneously all azimuth angles. These features will be used in the intelligent systems demanding a high gain to enhance the performance of the system by increasing the SNR.

1.5.2. Specifics objectives

As specific objectives, the designed and fabricated ASBRA with integration of real PIN diodes and biasing circuits must operate at 2.4GHz and 5.8GHz. It must be able to sweep whole azimuth angles over minimum bandwidth using a directive pattern with high realized gain. The back-lobe level of the radiation-pattern in the directive case would be expected to be less than 20dB. In the design process, the number of active elements needs to be kept as minimum as possible to decrease the antenna cost and also enhance its radiation performances. The parameters of the ASBRA are characterized in term of input return loss, radiation pattern, half power beam width and gain for both simulation and measurement.

1.6. Organisation of the thesis

1.6.1. Scope and Limitation of the Project

The thesis deals with using switchable FSS properties to form a ASBRA. This research is important because it overcomes the problems associated with communication system performances by combining several functions in a single element

- The significance of this thesis results arises from the following points:
 - To improve the reconfigurable antenna performance and its functionality, new switchable FSS are proposed in the 2.4GHz frequency bands.

- To increase the functionality of the reconfigurable antenna by achieving narrow bandwidth along with suitable back lobe level and low side lobe level in the directive radiation pattern case.
- Due to the switchable FSS size, the antenna size is reduced and more directive positions are achieved in the whole azimuth plane with enhanced performance.
- The main scopes of this research are:
 - Literature review and previous research study reconfigurable antenna
 - Design, simulate and analyze ASBRA antenna using CST Microwave Studio Software and for comparison and validation of the optimized results, Ansoft HFSS.
 - Fabricate and measure the ASBRA. The fabrication part includes soldering the PIN diode.
 - Analyze and compare the results between simulation and measurement
 - Scientific publications and mémoire publications.
- The limitations of this research are:
 - There are multiple parameters that can be tuned for reconfigurable antenna. However, this research only focuses on switched beam reconfigurable from wideband to narrowband.
 - The measurements of the antenna are based on available facilities at UQAT. Since there is a lack of anechoic chamber at UQAT, the labvolt systems were used for radiation pattern measurement. Hence, only front lobes of radiation patterns are compared with the simulation.
 - The switching mechanism of this antenna is using the Arduino board

1.6.2. Thesis organization

Chapter One: General introduction

The first chapter consists of the general introduction, project background, problem statement, objectives, scope of study, project contribution and the WSN applications. Some possible solutions are presented in detail in the following chapters.

Chapter Two: Fundamental knowledge of reconfigurable antennas

This chapter gives an overview of literature review on the reconfigurable antenna. The basics of the antenna properties such as radiation pattern, bandwidth, gain and half power bandwidth are presented. The reconfigurability concept is introduced and explained to get a narrow band operation before the integration of PIN diodes.

Besides, the circuit representation of PIN diode and its biasing circuit have also been explained for reconfigurable purposes and some overview of previous studies is also presented.

Chapter Three: A review of reconfigurable antenna based on FSS

This chapter discusses the passive antenna, the active antenna integrated with lumped element and the geometry of these antennas is introduced together with the use of FSS.

Chapter Four: Design and fabrication process of the ASBRA

The ASBRA's methodology is introduced. The design, simulation and experimental results for the ASBRA performance are presented. The antenna performance is examined and the impact of each influential parameter on the antenna performance is justified in details. The antenna is characterized by its parameters and is compared to other similar antennas in literature to prove this enhancement.

Chapter Five: Result analysis and discussion

The ASBRA is fabricated and the measurement results are reported and compared with the theoretical results in terms of return loss and radiation pattern. A discussion of these results is presented clearly.

Chapter Six: Conclusions

The thesis is concluded with a short summary and general assessment of the project's findings, some key contribution and provides recommendations for future work.

CHAPTER TWO

FUNDAMENTAL KNOWLEDGE OF RECONFIGURABLE ANTENNAS

2.1. State of the Art

What is an Antenna?

The IEEE defines an antenna as:

'a means for radiating or receiving radio waves' [23]

Radio waves are electromagnetic waves that travel in a vacuum or air at the speed of light and can be represented by sine waves. The distance a wave travels to complete one cycle is known as the wavelength, λ . This parameter is of great importance when designing antennas and is analyzed throughout this project.

$$\lambda = \frac{c}{f} (m). \quad (2.1)$$

Where c is the speed of light (3×10^8 m/s.) and f is the frequency (Hz).

Back to 1873 when James Clerk Maxwell presented 'A Treatise on Electricity and Magnetism' [24]. This work drew from empirical and theoretical work that had already been carried out by scientists such as Gauss, Ampere, Faraday, and others. Maxwell took the theories of electricity and magnetism and unified them. The equations he derived are presented below in differential form.

$$\nabla \cdot \vec{E} = \frac{-\partial \vec{B}}{\partial t} - \vec{M} \quad (2.2)$$

$$\nabla \cdot \vec{H} = \frac{-\partial \vec{B}}{\partial t} + J \quad (2.3)$$

$$\nabla \cdot \vec{D} = \rho \quad (2.4)$$

$$\nabla \cdot \vec{B} = 0 \quad (2.5)$$

Where: E is the electric field intensity (V/m).

H is the magnetic field intensity (A/m).

D is the electric flux density (C/m²).

B is the magnetic flux density (Wb/m²).

M is the (fictitious) magnetic current density (V/m²).

J is the electric current density (A/m²)

ρ is the electric charge density (C/m³)

Maxwell's four equations are the guarantors of the conversion and ensure the propagation of the electromagnetic field from the source to the point of reception. The passive nature of the antenna thus makes it a reciprocal device that also converts electromagnetic quantities to electrical signals. Maxwell's equations allow the calculation of the radiated fields from a known charge or current distribution. They also give a description of the behavior of the fields around a known current distribution or a known geometry. Maxwell's equations can then be used to understand the fundamental principles of antennas.

2.1.1. Type of Antennas

There are many types of antennas developed for many different applications; they can be classified into four distinct groups

2.1.1.1. Wire antennas

The wire antennas are typified by the TV antennas, car antennas, etc. The wire antennas may include dipoles, loops, helical dipoles, bushings, Yagi-Uda networks. Wire antennas usually have a low gain and operate at lower frequencies (HF to UHF). They have the advantages of low cost, ease of manufacture and simple design.

2.1.1.2. Aperture antennas

Aperture antennas have a physical opening through which electromagnetic waves propagate. The pattern has a narrow primary beam which leads to a higher gain. These types of antennas are very useful in space applications, as they can easily be embedded on the skin of an aircraft or spacecraft. Examples of such antennas include a parabolic reflector, horn antennas, lens antennas and circular apertures.

2.1.1.3. Array Antennas

Array antennas consist of a matrix of discrete sources which radiate individually. The pattern of the array is determined by the relative amplitude and phase of the excitation fields of each source and the geometric spacing of the sources. Typical elements in an array are dipoles, monopoles, slots in waveguides, open-ended and microstrip radiators.

2.1.1.4. Printed Antennas

Printed antennas are made via photolithographic methods, with both the feeding structure and the antenna fabricated on a dielectric substrate. Printed antennas form the bulk of the ASBRA structures discussed in this thesis.

2.1.2. Fundamental Antenna Parameters

Antenna parameters play an important role in antenna performance. These parameters can be altered in the process of designing the antenna to increase the performance and the criteria that is needed for a dedicated application. There are many parameters that can be measured from an antenna. In this project, only certain parameters will be discussed in detail due to the lack of equipment, but the parameters discussed in this work are sufficient enough to analyze the performance of the prototype antenna.

The most fundamental antenna parameters are;

1. Bandwidth
2. S-parameters
3. Radiation pattern
4. Directivity
5. Efficiency
6. Gain
7. Polarization
8. Half power beam width

All of the parameters mentioned above are necessary to fully characterize an antenna, and to establish whether the antenna is optimised for its purpose.

2.1.2.1. Bandwidth

The term 'impedance bandwidth' is used to describe the bandwidth over which the antenna has acceptable losses due to mismatch. The impedance bandwidth can be measured by the characterization of both the VSWR and RL at the frequency band of interest. Both VSWR and RL are dependent on measuring (Γ). Γ is defined as the ratio of the amplitude of the reflected voltage wave (V_0^-) normalized to the amplitude of the (V_0^+) at a load [25] and is defined by the following equation.

$$\Gamma = \frac{v_o^+}{v_o^-} \quad (2.6)$$

The VSWR is defined as the ratio between the voltage maximum and voltage minimum of the standing wave created by the mismatch at load on a transmission line.

$$VSWR = \frac{|Z_L|}{|Z_0|} = \frac{1+|\Gamma|}{1-|\Gamma|} \quad (2.7)$$

The return loss (RL) is the magnitude of the ratio of the reflected wave to that of the

incident wave, and is defined in dB as:

$$RL = -20\text{Log} |\Gamma|. \quad (2.8)$$

The scattering parameter is equivalent to Γ . It is common for S_{11} to be defined in dB as:

$$S_{11} = 20\text{Log} |\Gamma|. \quad (2.9)$$

The maximum acceptable mismatch for an antenna is normally 10% of the incident signal. For the reflection coefficient, this equates to $\Gamma = 0.3162$. For VSWR the impedance bandwidth lies between $1 < \text{VSWR} < 2$, and RL value must be greater than 10dB or $S_{11} < -10$ dB. A description of S-parameters is given in the following section.

The range of operating frequency within the selected return loss or VSWR is called the bandwidth of the antenna. There are two ways to represent a bandwidth which is for broadband antenna and narrowband antenna. For broadband antenna, the bandwidth is defined as a ratio of the upper-to-lower frequencies of acceptable operation. It's also can be calculated by using these formulas:

$$\frac{f_1}{f_2} < 2 \text{ (Narrow band) and } \frac{f_1}{f_2} > 2 \text{ (Broadband)}$$

In this project, the designed antenna is a broadband type of antenna. The bandwidth percentage is calculated as shown in *equation 2.10*

$$BW \% = \frac{f_u - f_l}{\sqrt{(f_u \cdot f_l)}} \cdot 100\% \quad (2.10)$$

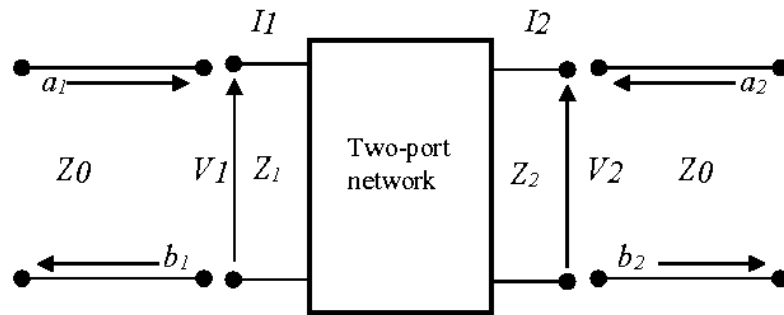
where:

f_u = upper frequency bandwidth

f_l = lower frequency bandwidth

2.1.2.2.S-Parameters

When designing antennas as part of a network, or on their own, it is advantageous to create a model which allows the designer insight into the performance of the system/antenna. It is common to extract useful data via a Vector Network Analyzer (VNA). The data is normally presented in the form of S-parameters. The S-Parameters are defined by measuring the voltage travelling waves between the N-ports. To explain this concept, it is best to look at a two port network shown by *Figure 2.1*



$V_1 =$ Voltage at port 1, $V_2 =$ Voltage at port 2, $I_1 =$ Current at port 1, $I_2 =$ Current at port 2; $Z_0 =$ Characteristic impedance, $Z_1 =$ port 1 impedance, $Z_2 =$ port 2 impedance, $a_1 =$ signal incident at port 1, $b_1 =$ signal reflected at port 1, $a_2 =$ signal incident at port 2, $b_2 =$ signal reflected at port 2

Figure 2.1 Two port network definition

The input reflection coefficient, when port 2 is matched, $S_{11} = \frac{b_1}{a_1} \Big|_{b_2=0}$

The reverse transmission gain, when port 1 is matched, $S_{12} = \frac{b_1}{a_2} \Big|_{a_1=0}$

The output reflection coefficient, when port 1 is matched, $S_{22} = \frac{b_2}{a_2} \Big|_{a_1=0}$

The forward transmission gain, when port 2 is matched, $S_{21} = \frac{b_2}{a_1} \Big|_{a_2=0}$

Typically, when using S-parameters to characterize antennas the reflection coefficients and forward transmission gain are most frequently used. Ideally reflection coefficients should tend towards zero ($S_{11}=S_{22}=0$) as this means that there is no power being reflected back due to a good match to the characteristic impedance of the feeding structures, usually 50Ω . The forward transmission gain should ideally tend towards one.

2.1.2.3. Radiation Pattern

An antenna radiation pattern is defined in the IEEE Standard Definitions [23] as:

“A mathematical function or a graphical representation of the radiation properties of the antenna as a function of space coordinates. In most cases, the radiation pattern is determined in the far-field region and is represented as a function of the directional coordinates. Radiation properties include power flux density, radiation intensity, field strength, directivity, phase or polarisation.”

Primarily, when measuring the radiation pattern, the property of most interest is the energy radiated relative to the antennas position [25].

This is usually measured using spherical coordinates as shown in *Figure 2.2*.

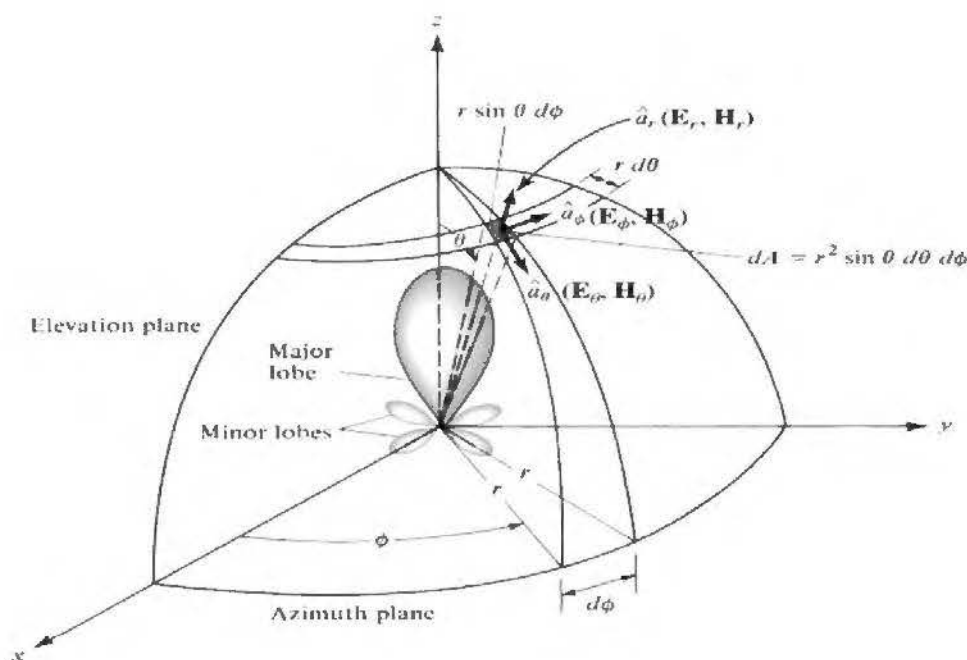


Figure 2.2 Coordinate system for antenna analysis.

(<http://slideplayer.com/slide/8562653/>)

The antenna under test is placed at the origin and is rotated through $\phi = 0^\circ - 360^\circ$ and $\theta = 0^\circ - 180^\circ$ while the power is measured in the far-field. As shown in *Figure 2.2*, the x-z plane is considered the elevation plane and is normally aligned with the electric field vector and is called the E-plane. The x-y plane is normally aligned with the magnetic field vector and is termed the H-plane.

2.1.2.3.1. Antenna Field Region

As an antenna radiates, there are changes to the electromagnetic field structure as the radiation moves away from the antenna at a distance R. These changes can be split into three distinct groups and are shown in *Figure 2.3*

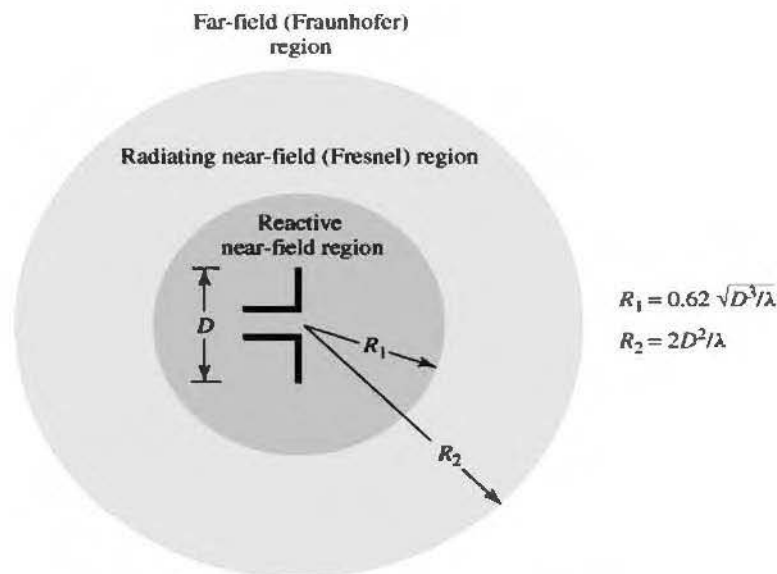


Figure 2.3. Field regions of an antenna

(<http://totalecer.blogspot.com/2016/02/radiating-field-regions-of-antenna.html>)

2.1.2.3.2. Reactive near-field region

The reactive near-field region, sometimes called the antenna region, is considered to be the volume of the field in the immediate vicinity of the antenna. For the majority of antennas this region exists at $R < 0.62 \sqrt{D^3/\lambda}$ from the antenna, where R is radius and D is the maximum antenna dimension. Confined within this region is a high amount of non-propagating energy, or reactive power.

2.1.2.3.3. Radiating near-field or Fresnel region

The radiating near-field, or Fresnel region does not display spherical power flow and varies as a function of distance, R , from the antenna. Also, the longitudinal component of the electric field may be significant, for example, if using the dipole from *figure 2.3*. The boundaries for this region are between where $R \geq 0.62 \sqrt{D^3/\lambda}$ and $R < 2D^2/\lambda$, and where D is the largest dimension. If the antenna is very small compared to wavelength this region may not exist.

2.1.2.3.4. Radiating far-field or Fraunhofer region

In the radiating far-field or Fraunhofer region the field components are transverse to the radial direction from the antenna and all the power flow is directed outwards in a radial fashion. In this region the shape of the field pattern is independent of the distance, R , from the antenna. The inner boundary is taken to be the distance $R = 2D^2/\lambda$, where D is the largest dimension of the antenna.

2.1.2.3.5. Characteristic impedance of EM waves

To help differentiate between near-field and far-field regions it is useful to analyse the characteristic impedance of plane waves. The characteristic impedance of a plane wave for a lossless medium is given by:

$$\begin{aligned} Z_0 &= \sqrt{\frac{\mu}{\epsilon}} (\Omega) \\ \mu &= \mu_0 \mu_r \\ \epsilon &= \epsilon_0 \epsilon_r \end{aligned} \quad (2.11)$$

where:

ϵ_0 = Permittivity of free space = 8.854×10^{-12} (F/m)

ϵ_r = Relative permittivity of the dielectric material

μ_0 = Permeability of free space = $4\pi \times 10^{-7}$ (H/m)

μ_r = Relative permeability of the magnetic material

For plane waves, this impedance is also known as the intrinsic impedance of the medium. In free space, where $Z_0 = 377 \Omega$, the E-field and H-field are orthogonal to each other and orthogonal to the direction of propagation. If the wave is in the near-field, in a free space environment, $Z_0 \neq 377 \Omega$ since the fields are not orthogonal to each other, or in the direction of propagation.

2.1.2.4. Velocity of Propagation

Another useful differentiation between the far-field and near-field regions, which gives an insight into the property of electromagnetic waves, is the velocity of propagation (m/s). The velocity of propagation of a plane wave, sometimes known as phase velocity, is the speed at which a wave moves through a medium and is given, for a lossless medium, by:

$$v_p = \frac{1}{\sqrt{\epsilon\mu}} = \frac{\omega}{k} (ms^{-1}) \quad (2.12)$$

where:

ω = frequency (rad/s)

$\beta = \sqrt{\mu\epsilon}$ = wavenumber (m^{-1})

For a plane wave travelling in free space, the velocity is equal to the speed of light, $c = 2.998 \times 10^8$ m/s. As with the wave impedance, for the wave to be planar (i.e. in the far-field) in free space then the phase velocity must equal the speed of light.

2.1.2.5. Directivity

Antenna directivity in the IEEE Standard Definitions of Terms for Antennas [26] as:

“The ratio of the radiation intensity in a given direction from the antenna to the radiation intensity averaged over all directions. The average radiation intensity is equal to the total power radiated by the antenna divided by 4π . If the direction is not specified, the direction of the maximum radiation intensity is implied.”

Essentially, this means that the directivity of an antenna is the ratio of the radiation intensity in a given direction over that of an isotropic source. This can be written as:

$$D = \frac{U}{U_0} = \frac{4\pi U}{Prad} \quad (2.13)$$

where,

U = radiation intensity (W/unit solid angle)

U_0 = radiation intensity of an isotropic source (W/unit solid angle)

$Prad$ = total radiated power (W)

If the antenna was to radiate in all directions (isotropic radiator) then its directivity would be unity. As an isotropic radiator cannot be realized practically, the most comparable antenna has directivity different from any other antenna that have a higher directivity which means their patterns are more focused in a particular direction.

2.1.2.6. Antenna Efficiency (η)

Like other microwave components, antennas can suffer from losses. The total antenna efficiency takes into account the losses at the input terminals, and within the structure of the antenna itself. The mismatch or reflection efficiency (η_r) is directly related to the return loss (Γ) and can be defined as:

$$\eta_r = (1 - |\Gamma|^2). \quad (2.14)$$

The radiation efficiency (η) is a measure of how much power is lost in the antenna due to conductor and dielectric losses. These losses reduce the radiation in any given direction and can be expressed as:

$$\eta = \frac{Prad}{Pin} \quad (2.15)$$

2.1.2.7. Gain

Antenna gain, G , is the product of efficiency and directivity, and is defined in the IEEE Standard Definitions of Terms for Antennas [27] as:

“The ratio of the intensity, in a given direction, to the radiation intensity that would be obtained if the power accepted by the antenna were radiated isotropically. The radiation intensity corresponding to the isotropically radiated power is equal to the power accepted by the antenna divided by 4π ”.

This can be expressed as:

$$G = \frac{4\pi U(\phi, \theta)}{P_{in}} \quad (2.16)$$

Unless specified, it is assumed that the antenna is receiving a signal in the direction of maximum gain. It is also common for the gain to be expressed in decibels and referenced to an isotropic source ($G = 1$), as shown in Equation 2.15.

$$G \text{ (dBi)} = 10 \text{ Log } (G/1). \quad (2.17)$$

2.1.2.8. Polarization

The polarization of an antenna is the orientation of the electric field vector of the radiated wave and is defined in the IEEE Standard Definitions of Terms [28] as:

“The property of an electromagnetic wave describing the time-varying direction and relative magnitude of the electric-field vector; specifically, the figure traced as a function of time by the extremity of the vector at a fixed location in space, and the sense in which it is traced, as observed along the direction of propagation”

Polarization is the curve traced by the tip of the electric field vector viewed in the direction of propagation. *Figure 2.4* shows a typical trace as a function of time [29].

The polarization of the wave may be linear, circular, or elliptical. The instantaneous electric field of a plane wave, travelling in the negative z direction, may be written as:

$$E(z, t) = E_x(z, t)\hat{x} + E_y(z, t)\hat{y}. \quad (2.18)$$

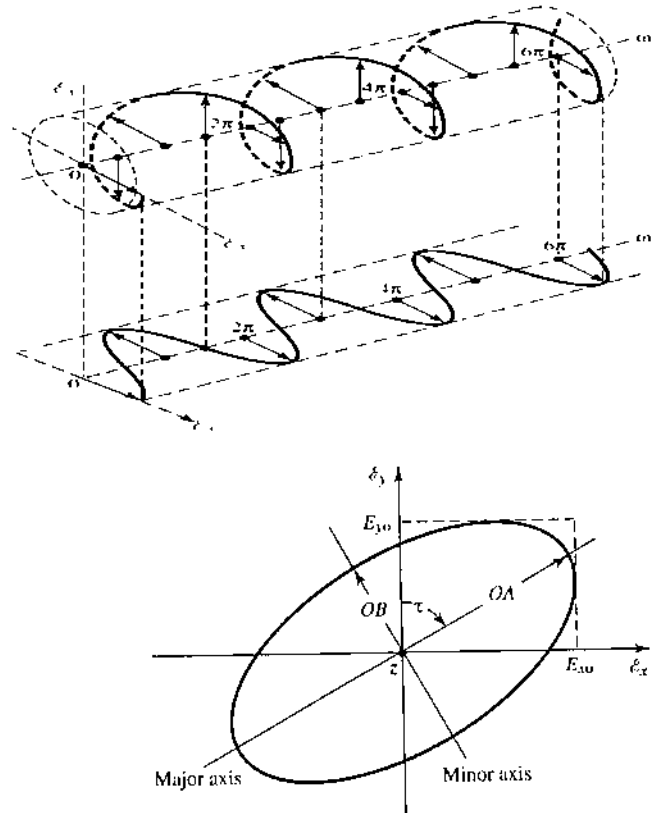


Figure 2.4. Rotation of a plane electromagnetic wave and its polarization ellipse at $z = 0$ as a function of time

(<http://slideplayer.com/slide/8562653/>)

The instantaneous components are related to their complex counterparts by:

$$E_x(z, t) = E_y \cos(\omega t + \beta z + \theta_x) \quad (2.19)$$

$$E_y(z, t) = E_x \cos(\omega t + \beta z + \theta_y). \quad (2.20)$$

Where E_x and E_y are the maximum magnitudes and θ_x and θ_y are the phase angles of the x and y components, ω is the angular frequency

2.1.2.9. Half-Power Beam-width

The HPBW can be defined as half the maximum value that is calculated between two angles from the main lobe [30]. In other words, the HPBW is measured at the main beam, by calculating the angle of the gain which has the value of the maximum value minus 3 dB as shown in *Figure 2.4*. The beam width is an important parameter for the antenna and is usually referred to when users use it.

The beam width is always used as a trade-off between the side lobe levels to analyze the antenna performance and β is the propagation constant.

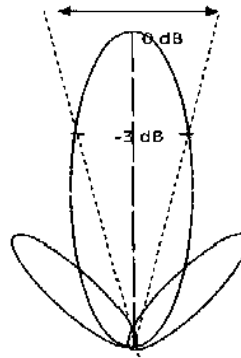


Figure 2.5: Two-dimensional of power pattern.

(<http://slideplayer.com/slide/8562653/>)

2.2. Reconfigurable antenna

The antenna is an essential element to create a telecommunication system by allowing its adaptation with the external environment and providing links to very great distances. The control of fundamental antenna parameters such as frequency, radiation pattern and polarization makes it possible to create a reconfigurable antenna that can increase the spectral efficiency of the system and optimize the quality of wireless communication thus create an intelligent antenna [30,31]. An intelligent antenna is based on the control of the current flowing in the desired directions, which alters its overall structure.

The antenna can potentially operate at different frequencies, radiate in other directions, or perhaps adapt its radiation pattern according to the environment or need. The structures of the antennas and the material that invent them take up the challenge of designing intelligent antennas.

The idea is to have a smart system capable of changing its functional characteristics in a stand-alone way according to the user's need and to explore a new structure with a low fabrication cost, light weight and compatible with integrated circuits devices. As soon as these antenna is built and placed on a certain platform, it can be reconfigured remotely without having to rebuild the antenna or platform on which the structure is mounted.

Designing reconfigurable antennas addresses three challenging questions.

- 1) Which reconfigurable property (frequency, radiation pattern or polarization) needs to be modified?
- 2) How are the different radiating elements of the antenna structure reconfigured to achieve the required property?
- 3) Which reconfiguration technique minimizes the negative effects on antenna radiation / impedance characteristics.

There are several advantages in using reconfigurable antennas as summarized below [32]:

- 1) Ability to support more than one wireless standard.
 - a) minimizes cost;
 - b) minimizes volume requirement;
 - c) simplifies integration;
 - d) good isolation between different wireless standards.
- 2) Lower front end processing.
 - a) no need for front end filtering;
 - b) good out-of-band rejection.
- 3) Best candidate for software-defined radio.
 - a) capability to adapt and learn;
 - b) automated via a microcontroller or a field programmable gate array (FPGA).
- 4) Multifunctional capabilities.
 - a) change functionality as the mission changes;
 - b) act as a single element or as an array;
 - c) provide narrow band or wideband operation.

Three main types of reconfigurable antennas exist as frequency [33-36], polarization [37-39], radiation pattern [40-42], and/or two or more of parameters [43-45] in a single antenna. The block diagram of the reconfigurable antenna is shown in *Figure 2.6*.

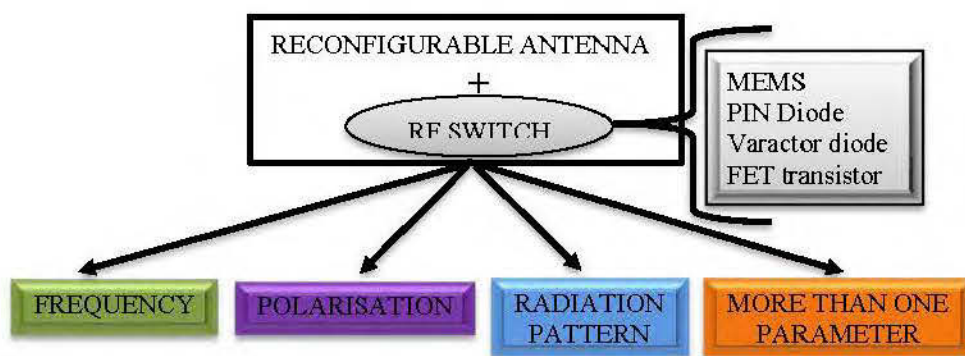


Figure 2.6. The block diagram of the reconfigurable antenna. [42]

In the sections to follow herein, the classification of reconfigurable antennas, their various reconfiguration techniques, the advantages and disadvantages of each technique, and some of the most recent applications of reconfigurable antennas are discussed.

2.2.1. Frequency reconfigurable Antenna

Several telecommunication devices such as Smart Phone and computers are equipped with applications or services that operate on different frequency bands such as GSM, WIFI, Bluetooth and FM Radio as illustrated in *Figure 2.7*.

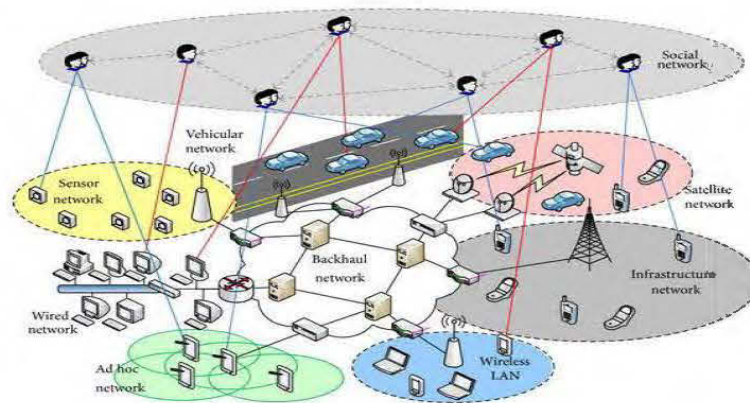


Figure 2.7. *Telecommunication infrastructure*

(<https://www.hindawi.com/journals/jcs/2013/972352/fig1/>)

Each application requires an antenna according to the wavelength and its supply circuit operating in the requested frequency band. As the number of applications increases, the number of antennas increases, which will complicate the system platform in terms of size, technological complexity, cost and interference between standards communications.

Reconfigurable multifrequency antennas is a solution that reduces the number of antennas and integrates them in a single antenna and simultaneously cover several frequency bands. The frequency reconfiguration can be performed continuously or by means of switch. Both methods are based on changing the effective electrical length of the radiator or, on the other hands, the effective current distribution on the radiator. By using continuous variation, the frequency of the antenna can be reconfigured smoothly over a specific bandwidth; while, for discontinuous cases, reconfiguration is realized by switching between different bands [46]. Mechanically changing the antenna structure and material properties are other approaches, which can continuously change the frequency of the antenna. However, each method has its own advantages and drawbacks that according to their potentials for the desired application are chosen.

2.2.2. Polarization reconfigurable antenna

The change in the polarization of an antenna causes an increase in its immunity against interference which degrades the quality of the signal because of the nature of the electromagnetic environment and increase the sensitivity especially at the level of reception against reflections multiple paths [46].

Generally, a fixed circular polarization is obtained from an excitation orthogonal antenna of two antennas linked by a coupler which provides a phase difference of 90° between the two antennas therefore, it makes possible to replace the old system which provides only one fixed polarization (either right or left) and reduce the size of the system and its complexity. The switching of polarization is a technique which makes it possible to maintain the signal-to-noise ratio at a fixed value defined by a given application. The change in the polarization must not influence other parameters such as the adaptation or shape of the radiation pattern.

2.2.3. Radiation pattern reconfigurable Antenna

Reconfigurable radiation pattern antennas play a very important role in wireless telecommunication systems by their spatial filtering characteristics. They allow to increase the capacity of the channel by focusing the energy in the useful direction and to avoid the interfering signals by the insertion of the zeros in these directions. This can be achieved even by changing the amplitude and phase of the electric or magnetic currents on the structure. However, because of changing in the current distribution, it is expected to have some variation in the frequency response of the antenna as well. This is the main technical point that should be considered in the design process to minimize the effect of pattern/gain reconfiguration on the frequency response and hence matching bandwidth.

2.3. Principles of Reconfigurability and RF Switch Technologies

The radiation of an antenna comes from the particular way that the current is distributed on the antenna structure leading to the change of fields around the antenna and thus also the far- field radiated. Obviously all properties of the radiation characteristics of an antenna such as its frequency of operation, the far field pattern field and polarization can be reconfigured. These changes can be made by modifying the antenna geometry or its material properties. Unfortunately, it is very difficult to configure them independently of each other. The change of one will affect others as well, that why careful design and analysis are important to ensure that we understand what effect a particular change in antenna will have. Reconfigurable Antennas based on:

- Redirecting their surface currents are called electrically reconfigurable.
 - Radio-frequency microelectromechanical systems (RF-MEMS) [47- 48].
 - PIN diodes [49 – 50].
 - Varactor [51 – 52]
- Photoconductive switching elements are called optically reconfigurable antennas [53 – 54].
- Altering the structure are called physically reconfigurable antennas [55– 56].

- The use of smart materials such as ferrites and liquid crystals are called materials reconfigurable antennas [57].

2.3.1. Reconfiguration by Switching

Optical switches, high frequency PIN-Diodes, FETs, and radio frequency micro-mechanical switches (MEMS) are some kinds of commonly used means applied to connect or disconnect different parts of the antenna. These components are applicable to reconfigure frequency, polarization, or radiation pattern. Inter-modulation harmonic level, losses, and speed are the main important issues for our approaches, which determine the component type for the desired operating requirements of our project.

2.3.1.1. Electrically reconfigurable antennas

An electrically reconfigurable antenna relies on electronic switching components (RF-MEMS, PIN diodes, or Varactors) to redistribute the surface currents, and alter the antenna radiating structure topology despite the numerous issues surrounding such as the nonlinearity effects of switches, interference, losses, and negative effect of the biasing lines used to control the state of the switching components on the antenna radiation pattern.

2.3.1.1.1. RF-MEMS

RF-MEMS are tiny mechanical switches made on a substrate (silicon, quartz, glass) [58]. *Figure 2.8* shows three types of RF MEMS switches in their on and off positions. The cantilever beam in *Figures 2.8 (a) and 2.8 (b)* is anchored to a post on the left, while the other end of the beam is suspended above the drain. An electrostatic force pulls the beam down when a voltage is applied, and creates an electrical path between the beam and the drain. *Figures 2.8 (c)-2.8(f)* show a RF MEMS membrane switch, which consists of a flexible, thin, metal membrane, anchored to posts at both ends.

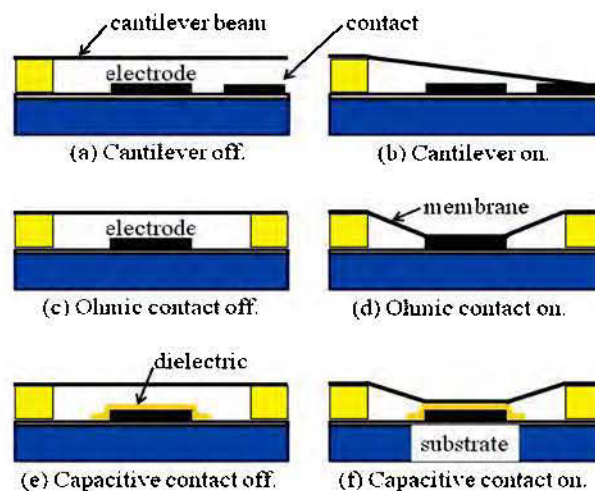


Figure 2.8. Types of RF-MEMS switches. [58]

A potential applied to the bias electrode pulls the membrane down and closes the circuit. An ohmic contact is a metal-to-metal connection, while a capacitive contact has a dielectric between the two metal contacts. Ohmic switches have a higher bandwidth than capacitive switches. Switching speeds for electro-statically driven capacitor structures are 10 μs . Recently, RF-MEMS switches with piezoelectric films have been developed, and have fast switching times (1-2 μs). The cantilever device travels 6 μm between the on and off states. RF-MEMS switches have low power consumption, low insertion loss, and high isolation, like mechanical switches, but are small, lightweight, and low cost, like semiconductor switches [59]. On the other hand, RF-MEMS switches have high losses at mm-wave frequencies, limited power-handling capability (~ 100 mW), and they may need expensive packaging to protect the movable MEMS bridges against the environment.

2.3.1.1.2. Varactors

Varactor Diode is a reverse biased p-n junction diode, whose capacitance can be varied electrically. As a result, these diodes are also referred to as varicaps, tuning diodes, voltage variable capacitor diodes, parametric diodes and variable capacitor diodes. It is well known that the operation of the p-n junction depends on the bias applied which can be either forward or reverse in characteristic. It is also observed that the span of the depletion region in the p-n junction decreases as the voltage increases in case of forward bias. On the other hand, the width of the depletion region is seen to increase with an increase in the applied voltage for the reverse bias scenario. Under such condition, the p-n junction can be considered to be analogous to a capacitor where the p and n layers represent the two plates of the capacitor while the depletion region acts as a dielectric separating them as shown in *figure 2.9*

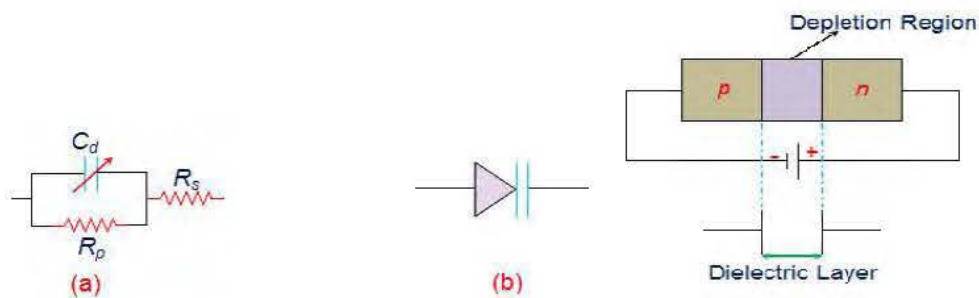


Figure 2.9 (a) Electrical Equivalent Circuit, (b) Symbol of Varactor diode.

(<https://www.electrical4u.com/varactor-diode/>)

However, because of packaging parasitic elements and losses, the application of these components is limited, especially for the components based on the semiconductor technologies.

2.3.1.1.3. PIN Diodes

A PIN diode is a component with a wide, undoped intrinsic semiconductor region between a p-type semiconductor and an n-type semiconductor region. The p-type and n-type regions are typically heavily doped because they are used for ohmic contacts.

The wide intrinsic region is in contrast to an ordinary p-n diode. The wide intrinsic region makes the PIN diode an inferior rectifier (one typical function of a diode), but it makes it suitable for attenuators, fast switches, photodetectors, and high voltage power electronics applications. It has heavily doped p-type and n-type regions (used for ohmic contacts), which are separated by a wide, lightly-doped intrinsic region.

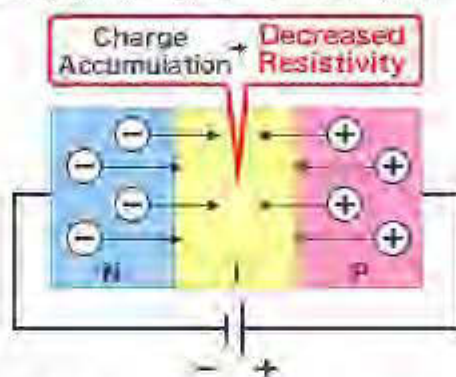


Figure 2.10. *intrinsic region of the Pin diode*

(https://www.electronics-tutorials.ws/diode/diode_2.html)

Forward biasing a PIN diode creates a very low resistance at high frequencies, while reverse biasing results in an open circuit.

- The PIN diode is current controller,
- PIN diodes have the ability to control large RF signal power while using much smaller levels of control power.
- PIN diodes are less susceptible to electrostatic-discharge damage.

The off-capacitance of PIN diodes is a function of reverse voltage: the more negative the voltage, the less capacitance. The useful upper-frequency-response limit of PIN diodes can be much higher, due to lower off-state capacitance (C_{off}) for a given on resistance (R_{on}).

2.3.1.2. Reconfigurability by changing material

Antennas are also made reconfigurable through a change in the substrate characteristics by using materials such as liquid crystals or ferrites. The change in the material is achieved by a change in the relative electric permittivity or magnetic permeability. In fact, a liquid crystal is a nonlinear material whose dielectric constant can be changed under different voltage levels, by altering the orientation of the liquid crystal molecules.

As for a ferrite material, a static applied electric/magnetic field can change the relative material permittivity. In these methods, by applying a DC voltage, the electrical properties of the dielectrics are changed, leading to alter the EM response of the structure. For example, the propagation of the wavelength in the RF structure or the impedance will be changed by permittivity (ϵ_r) or permeability (μ_r) changes and the ability to grant the structure will be based fundamentally on the magnitudes of ϵ_r and μ_r [58].

2.3.1.2.1. Tunable conductivity

Through changes in temperature, bias, or light the conductivity in semiconductors can be tuned. It is varying depending on the bandgap energy, the level of doping, and defects in the material. Shining light with a photon energy greater than the bandgap on an intrinsic semiconductor increases the free-electron and hole-charge carriers, which in turn increases the semiconductor's conductivity. Solar cells are a good example [58]

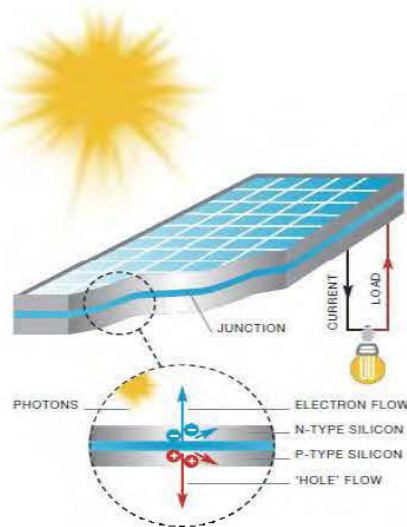


Figure 2.11. *The principle of a crystalline solar cell*
(<http://www.thinksolar-us.com/myth-solar-power-systems/>)

2.3.1.2.2. Tunable permittivity

A number of approaches have been explored to achieve economical solutions for a high ability to tune with low losses and fast response, for the purpose of controlling microwave filters and phased arrays. The relative “tunability” of the permittivity of a system is defined as:

$$\eta_t = \frac{\epsilon_r(0) - \epsilon_r(E)}{\epsilon_r(0)} \quad (2.21)$$

where $\epsilon_r(0)$ and $\epsilon_r(E)$ are the small-signal relative permittivity's without bias and with a bias of strength E [V/cm], respectively.

2.3.1.2.3. Tunable permeability

Similar to the tunable response in dielectric materials, the magnetic permeability decreases with the application of a static field [59]. Ferromagnetic materials and LCs are bulkier than ferroelectric materials and they create more losses than ferroelectrics. Moreover, creating higher cross polarization level in ferromagnetic is other reason to not widely apply these materials directly as radiators in the antenna applications.

2.3.1.3. Optically reconfigurable antennas

An optical switch is formed when laser light is incident on a semiconductor material (silicon, gallium arsenide). This results in exciting electrons from the valence to the conduction band and thus creating a conductive connection [60]. Integrating such a switch into an antenna structure and using it to reconfigure the antenna behavior is called an optically reconfigurable antenna. The linear behavior of optical switches, in addition to the absence of biasing lines, compensates for their lossy aspect and the need for laser light to activate them. The activation or deactivation of the photoconductive switch by shining light from the laser diode does not produce harmonics and intermodulation distortion due to their linear behavior. Moreover, these switches are integrated into the antenna structure without any complicated biasing lines which eliminates unwanted interference, losses, and radiation pattern distortion. Despite all these advantages, optical switches exhibit lossy behavior and require a complex activation mechanism.

2.3.1.4. Reconfiguration by structural alteration

Antennas can also be reconfigured by physically altering the antenna radiating structure. The tuning of the antenna is achieved by a structural modification of the antenna radiating parts. The importance of this technique is that it does not rely on any switching mechanisms, biasing lines, or optical fiber/laser diode integration. On the other hand, this technique depends on the limitation of the device to be physically reconfigured.

The advantages of using physical reconfiguration techniques lie in the fact that they do not require bias lines or resort to laser diodes or optical fibers. However, their disadvantages include slow response, cost, size, power source requirements and the complex integration of the reconfiguring element into the antenna structure. [60,62]

2.3.2. Comparison between different techniques and the practical issues.

The study on the reconfiguration properties shows that the reconfiguration mechanisms are usually achieved by means of mechanical or electrical approaches. In the mechanical method, the structure of the radiator is moved by electromechanical actuators in order to reshape the antenna structure. Piezo-electric actuators or micro-machined plastic

deformation are some kinds of recently proposed methods to reconfigure the frequency and radiation-pattern. This method delivers a wide range of frequency of operation limited by the practical constraints and it can continuously sweep the desired property through a bandwidth or switch between different regimes. In addition, it provides low loss, linear behavior at high frequencies, which are remarkable merits to alleviate the inter-modulation (IMD) harmonic problem. However, needing to a specific complex actuation system and being low speed are the main drawbacks of this approach. On the other hand, in the electrical methods there is no any movement in the configuration and the changes in the overall shape is electronically achieved. Indeed, this is realized by connecting/disconnecting different parts of the structure, changing the elements of the equivalent electrical circuit model of the antenna via variable capacitors or by changing the material properties. Optical switches, high frequency PIN-Diodes, FETs, and radio frequency micro-mechanical switches (MEMS) are some kinds of commonly used means applied to connect or disconnect different parts of the antenna. These components are applicable to reconfigure frequency, polarization, or radiation pattern. Inter-modulation (IMD) harmonic level, losses, and speed are the main important issues for these approaches, which determine the component type for the desired operating requirements. Among these drawbacks, the undesired natural parasitic elements introduced by component packaging and soldering, for instance in PIN-Diodes and FETs, are the main reasons in limiting their applications. This leads to increase the elements nonlinearity and hence increase the IMD problem. MEMS technology is the potential approach to get rid of the losses and parasitic elements by packing the reconfiguration mechanism and antenna structure during the fabrication process [63]. However, this method is not practical for all applications and is not extensively available in the market. Alternatively, variable capacitors are other components that are usually used to continuously reconfigure the frequency response of the antenna over a specific bandwidth. This can be realized by chip variable capacitors integrated into the structure. These capacitors are usually based on the semiconductor or MEM technologies. However, because of packaging parasitic elements and losses, the application of these components is limited and based on the semiconductor technologies.

	Technology	Tuning range	Power consumption	Bias	Speed	IMD
Semi-conductors	<ul style="list-style-type: none"> • Schottky (GaAs) • HBV(GaAs) • Abrupt p-n junction (Si) • PIN-Diode 	High	<ul style="list-style-type: none"> • <1 mW • <1 mW • <5 mW • <0.1 mW 	<ul style="list-style-type: none"> • <5 V • <20 V • <30 V • <10 V 	<ul style="list-style-type: none"> • <1 ns • <5 ns • <10 ns • <1 μs 	<ul style="list-style-type: none"> • Fair • Poor • Poor • Poor
Magnetic	<ul style="list-style-type: none"> • Remnant magnetization • Magneto-static (spin)wave 	<ul style="list-style-type: none"> • - • - 	<ul style="list-style-type: none"> • Low • Low 	<ul style="list-style-type: none"> • Current (Gall) • - 	<ul style="list-style-type: none"> • <5 ms • <5 ms 	<ul style="list-style-type: none"> • - • -
Ferroelectric	<ul style="list-style-type: none"> • Thin film • Thick film • Bulk 	<ul style="list-style-type: none"> • Moderate to high • Moderate to high • Moderate to High 	<ul style="list-style-type: none"> • Negligible • Negligible • Negligible 	<ul style="list-style-type: none"> • <30 V • <1000 V • <15 KV 	<ul style="list-style-type: none"> • <1 ns • <10 ns • <1 μs 	<ul style="list-style-type: none"> • Low • Low • Low
Liquid crystal	Cavity/Bulk	Moderate	Negligible	<40 V	<10 ms	-
Optical	Photoconductivity	-	<10 mW	Current (I.D. IJTD)	10 fs-10 ms	-
Mechanical	<ul style="list-style-type: none"> • MEM Varactor • Piezo-transducer 	<ul style="list-style-type: none"> • Low • High 	<ul style="list-style-type: none"> • Negligible • Negligible 	<ul style="list-style-type: none"> • <50 V • >100 V 	<ul style="list-style-type: none"> • >10 μs • >100 μs 	<ul style="list-style-type: none"> • Excellent • Good

Table 2.1 Comparison between different switches. [63]

2.4. Propagation channel

In the field of wireless networks, the channel characterizing the propagation of the electromagnetic wave in space has a distinctive importance. It is therefore essential to have knowledge of the mechanisms involved in the channel of propagation and its interactions with the environment in order to predict chances and conditions of establishing a radio link between the transmitter and receiver.

A radio transmission system makes it possible to transform a signal electrical emitted $e(t)$ into an electric signal received $r(t)$ by means of waves electromagnetic. The propagation channel is the place that transforms the waves electromagnetic waves during their propagation. At this point, it is important to differentiate the propagation channel, which only takes into account interactions of the transmitted signal with the environment traversed and the transmission channel, which includes the effects induced by the transmitting and receiving antennas.

Propagation in free space

Generally, the propagation environment influences the wave electromagnetic emitted. In free space, the transmission system is characterized by the absence of obstacles. The power density W in a free space is expressed as a function of the distance between the transmitter

and receiver, the gain of the transmitting antenna G_e and the power of the transmitted signal P_e .

$$W = \frac{P_e G_e}{4 \pi d^2} \quad (2.22)$$

The signal strength available at the terminals of a reception antenna P_r is connected to the power density W by the following relation:

$$P_r = W \frac{\lambda^2 G_r}{4 \pi} \quad (2.23)$$

where G_r represents the gain of the receiving antenna and λ represents the wavelength at the working frequency. The attenuation of the signal in free space can be calculated using both previous formulas as follows:

$$\frac{P_r}{P_t} = G_t G_r \left(\frac{c}{4 \pi f d} \right)^2 \quad (2.24).$$

where c , the speed of light is expressed as $C = f \cdot \lambda$.

It should be noted that the above formula is valid only when the receiving antenna is considered in the far field of the transmitting antenna. This condition is verified when the distance (d) between the antennas is greater than the distance of Fraunhofer which is connected to the largest dimension (D) of the transmitting antenna:

$$d_f = 2 \frac{D^2}{\lambda} \quad (2.25)$$

where D is the size of the transmitting antenna. The loss in free space is given by the following relation: $P_L = 10 \log_{10} \frac{(P_r)}{(P_t)} = -10 \log_{10} [G_t G_r \left(\frac{\lambda}{4 \pi d} \right)^2]$ (2.26)

2.4.1. Multipath propagation

In a wireless system, the environment of the transmission system interferes with the wave transmitted according to different mechanisms. The receiver can receive the same signal of several different paths since the transmitted signals can be reflect on a surface like the ground, the buildings ... etc. In practice, it is often two or more phenomena apply simultaneously to the trajectory of the signal. This effect is called multipath propagation. Indeed, there are four main phenomena: reflection, refraction, diffraction, diffusion waveguides that have a direct impact on signal propagation [61].

The waves emitted during the radio communication generally undergo a combination of these various phenomena. The received signal is a sum of all arriving routes to the receiver and this sum can be constructive or destructive. Barriers can be considered as a benefit or a disadvantage. For example, when a transmitter and receiver are in direct view LOS,

reflection disrupts the link. However, in the case of the NLOS channel, the diffraction and diffusion ensure the continuity of the connection.

An analyze of power of the received signal as a function of the distance between the transmitter and the receiver, three types of variations of the received power can be deduced:

- path loss: due to distance, it can be calculated deterministically or with a model empirical when the environment is complicated.
- Shadowing or slow fading: slow variations due to successive attenuations produced by large local obstacles that cause diffraction.
- Fast fading or multi-fading: rapid variations caused by the paths due to constructive addition or destructive signals that cannot be deterministic.

2.5. Summary

In chapter 2, firstly a literature review on the reconfigurable antennas is carried out to clearly the concept. The possible reconfigurable antenna characteristics and their impacts in improving the overall system performances are explained. And finally, the most commonly used reconfiguration methods are also described and compared to each other, and finally the chapter is ended up with some remarks on practical considerations. Following to the research survey presented in the first chapter, comprehensive studies on periodic structures and in particular frequency selective surfaces are presented in chapter 3.

CHAPTER THREE

A REVIEW OF RECONFIGURABLE ANTENNA BASED ON FREQUENCY SELECTIVE SURFACE

3.1. Introduction

An antenna is a passive device that converts an electrical signal transported by a conductive support: transmission lines, waveguide, or more overall material: optical fibers, to turn it into a signal electromagnetic capable of propagating without specifically requiring a material support and ensuring links at very great distances.

In theory, any conductor wire with a proper size compare to the wavelength of the signal can act as an antenna and create the electromagnetic field that induce a current on its surface; however, an agile antenna is based on the control of current flowing through it in the desired directions which modifies the overall structure. The antenna can potentially operate at different frequencies, radiate in different directions, or possibly adapt its radiation pattern according to the environment or the need. Acting on the structures of the antennas and the materials that compose them makes it possible to meet the challenge of designing agile antennas.

Periodic structures provide control over the current or field browsing them. Among the structures offering the most application in the field of antennas, it is possible to mention meta-materials, Electromagnetic band Gap (EBG) structure or Frequency Selective Surface (FSS) structure. Since the objectives of this thesis are conception and developing a new class of switched beam reconfigurable antennas based on periodic structures, the relevant reported contributions on this application are reviewed and discussed in this chapter.

3.2. Periodic structures

In the past two decades, an interesting area, widely known as the meta-materials, has increasingly attracted researcher's attention to develop and improve the performance of electrical components in RF, microwave and high frequency [62].

Different structures are used in this type of application and depending on how they deal with electromagnetic waves, this material can be realized as Double Negative (DNG) material, Electromagnetic Bandgap (EBG) structures or Photonic Bandgap (PBG) material and Frequency Selective Surfaces (FSS). They are constructed of an array of periodic elements which can be metallic, dielectric or a composite material of metal and dielectric arranged in one, two or three dimensional pattern [63].

The shape of the element, the texture of the array, the electrical parameters of the used

material, and the distance between elements in the array defines their electromagnetic properties. All these materials might treat the EM wave in different ways with different incident angles. For instance, DNG materials have received considerable attention in developing scanning beam antennas, lens antennas, and microwave filters. [64] In response to the incident electromagnetic waves, DNG materials provide negative dielectric constant and dielectric permeability. The periodicity of the array elements in these types of periodic structures is much smaller than the operating wavelength.

Alternatively, PBG or EBG materials are another type of meta-materials that prohibit the propagation of incident waves across a range of frequency band. The periodicity of the array in these materials is in the range of a half wavelength. They have found intense applications in antennas towards the enhancement of the gain, the suppressions of the surface waves as high impedance ground surface or AMC, the creation of band stop response in microwave filters and in electromagnetic shielding applications [65], [66].

Recent contributions on the application of these materials in antennas and microwave have been described in [6]. FSS are a kind of planar periodic arrays of metallic patches or perforated conductors with a particular pattern with their impact on either one or both of amplitude and phase of the incident waves. They have found considerable applications in antennas, filters, polarizers, radomes, and electromagnetic shielding [68], [69].

The subject of interest in this thesis is the development of the reconfigurable antenna that depends on EBG and FSS structures and its ability to change and modify its nature. Thus, it is necessary to analyze the behavior of these structures and to study the effects of their parameters in order to obtain the best performances.

3.2.1. Analysis of periodic structures

In recent years, the periodic structures known as Meta materials have found great interest in the field of telecommunications because of its interesting spectral properties which make it possible to create radiofrequency devices and to improve the characteristics of the antennas. They make it possible to create materials with double permittivity and permeability [63].

3.2.1.1. Structure Electromagnetic Band Gap

Electromagnetic with bandgap are structures imported from applied optical physics. Photonic crystals are meta-materials periodic structures that alter the propagation of electromagnetic energy and give rise to forbidden propagation bands resulting in a non-linear phenomenon between group velocity and phase velocity. Regardless of the nature of

the wave, wave propagation in a periodic medium has been studied for several years [70] - [71].

The interesting phenomenon in a periodic structure is the filtering of waves, which allowed, in the field of optics, the creation of the Bragg mirror which aims to control the propagation of light. We also find photonic crystals that are optical materials that have found a lot of interest thanks to their crystallized structures that control the propagation of light [72]. These structures are characterized by their forbidden bands that block the propagation of light, hence the name Band Gap Materials. Among the first works developing PBG structures, it is possible to quote those of Yablonovitch; he proposed a material capable of optimizing spontaneous emission by imagining a three-dimensional structure illustrated by *Figure 3.1*.

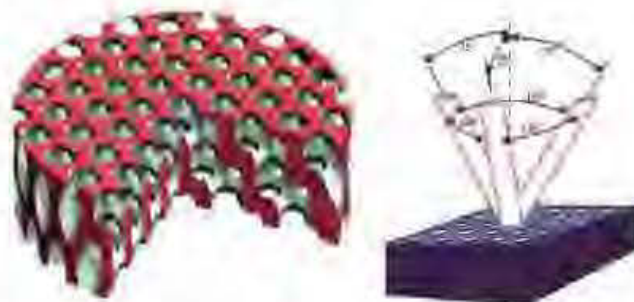


Figure 3.1 Yablonovitch structure. [72]

More advanced structures have since emerged, such as the so-called woodpile structure [71] as shown in *Figure 3.2*.

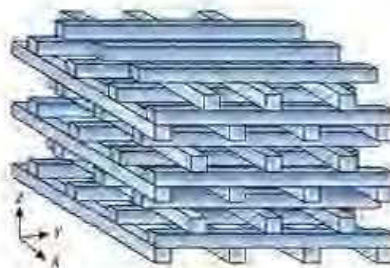


Figure 3.2 Woodpile structure [71]

In the microwave field, light is no longer the propagating wave, and we are no longer talking about PBG structures but electromagnetic Band-Prohibited structures.

In 1919, Yablonovitch began to use periodic structures in the microwave band and in the same year, Marconi and Franklin did the first work which deals with antennas by periodic structures to improve wireless telegraphs [73].

The EBG structures are presented as subsets of meta-materials that have been of great interest to researchers in the microwave field and especially the antenna, [74] - [75].

These artificial periodic structures also allow the creation of the so-called frequency Selective Surface Surfaces (FSS) which are a subgroup of the EBG structures.

3.2.1.2. Theoretical notions

Periodic structures are characterized by the repetition of a unit cell. The periodic surfaces are analyzed by applying the Bloch-Floquet's theorem on the unit cell.

According to this theorem, the field in an infinite periodic medium is linked to the other fields by a factor $e^{j\gamma}$ where γ is the propagation constant. We will provide some of the theoretical principles for the study of bandgap structures. These principles are not exhaustive, but they are often sufficient to address the recurrent characteristic of EBG structures and their periodicity.

The propagation in this kind of structures is considered parallel to the axis of periodicity; therefore, one of the most appropriate means for their study is Floquet's theorem.

3.2.1.2.1. Floquet's-Bloch's modes

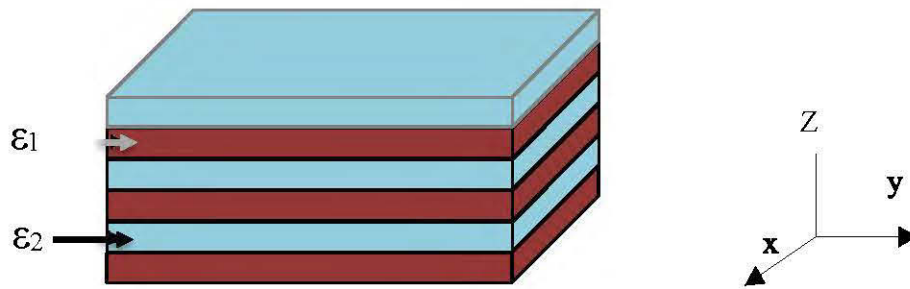


Figure 3.3: One-dimensional periodic structure [75]

Floquet's theorem supposes that the solution of the propagation equation, whose coefficients are periodic functions, must itself be periodic; solutions linearly independent of this differential equation are periodic. Consider the propagation in the medium described in *Figure 3.3*; suppose that the wave propagates along the z axis. The simplified wave equation in such a medium is written:

$$\frac{d^2 E(z)}{dz^2} + \varepsilon(z)k^2 E(z) = 0 \quad (3.1)$$

the permittivity ε being periodic along the z axis,

$$\varepsilon(z + d) = \varepsilon(z) \quad (3.2)$$

d being the period. Floquet's theorem allows us to write

$$E(z) = F(z)e^{\pm\gamma z} \quad (3.3)$$

where $\gamma = \alpha + j\beta$ is the propagation constant of the system. The attenuation. $F(z)$ being a periodic function will not consider, the development of the Fourier series leads to the following:

$$E(z) = Fne^{j\left(\pm\beta + \frac{2n\pi}{d}z\right)} \quad (3.4)$$

The elements of this series are called Floquet's modes or spatial harmonics [76].

The group speed remains constant for all modes, since the frequency and the spatial period are completely independent and it is given by:

$$Vg = \frac{\partial\omega}{\partial\left(\beta + \frac{2n\pi}{d}\right)} \quad (3.5)$$

On the other hand, the phase velocity is different from one mode to another and it is written as:

$$Vp = \frac{\omega}{\left(\beta + \frac{2n\pi}{d}\right)} \quad (3.6)$$

The dispersion diagram illustrates the propagation of constant β of the modes in the direction of periodicity as a function of frequency for a periodic one-dimensional structure. For the case with two or three dimensions, the diagram becomes complicated and requires introducing a new diagram called "Brillouin diagram" which makes it possible to identify zones.

3.2.1.2.2. Dispersion diagram (Brillouin diagram)

This is a graphical tool illustrating the propagation of surface waves to show the "Band Gap" feature of the surface as a meta-material for which frequency bands will be identified. has a wave propagation. In this case, the surface is considered as a 1D period structure whose period P is obtained along the y axis. The surface waves are presented by Floquet's spatial or harmonics whose total surface electric field is written as follows [77]:

$$E_{(x,y,z)} = \sum_{n=-\infty}^{\infty} A_n e^{jk_{yn}y} e^{jk_{zn}z} e^{-j2\pi ft} \quad (3.7)$$

where A_n is the complex amplitude of the nth harmonic, $k_{zn} = \sqrt{K_0^2 + K_{yn}^2}$, is the transverse wave number and $K_{yn} = \beta n - j\alpha = \beta_0 + \frac{2\pi n}{P}$, is the complex number of the wave propagating on the surface, α is an attenuation coefficient which makes it possible to control the level of the side lobes and the opening of the main lobe at -3 dB and β is the propagation phase of the waves which allow to control the electronic scanning [78].

✓ Region 1 (Band pass), all harmonics are evanescent waves and heavy waves that propagate on the surface in the following condition:

$$\beta_{yn} > k_0 \quad (3.8)$$

$$K_{yn} = -j\alpha \quad (3.9)$$

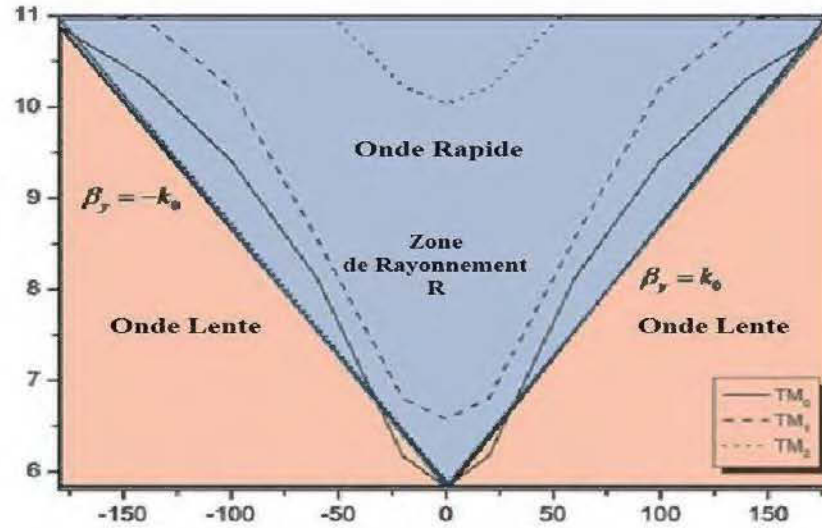


Figure 3.4 Surface wave dispersion pattern of metal strips. [78]

- ✓ Region 2 (Band Stop) is the same as Region 1 except that the k_{yn} propagation constant is complex.
- ✓ Region 3 (Radiant): In this zone, one or more harmonics of Floquet's radiate and fast surface waves propagate in the following condition:

$$\beta_0 > k_0 \quad (3.10)$$

And the propagation constant in the direction y is:

$$K_{yn} \approx \beta_{yn} \quad (3.11)$$

In the case of a 2D Fabry Perot cavity and an excitation of the surface by a normal plane wave, the angle of incidence is zero and normal to the surface, the maximum of radiated power is found when the following condition is satisfied $\alpha = \beta$.

$$R_n : \left(\beta_0 + \frac{2\pi n}{p} \right)^2 < k_0^2 \quad (3.12)$$

The opening of the main lobe can be estimated by the following relation:

$$\Delta \theta_{3dB} \approx 2\sqrt{2} \frac{\alpha}{k_0} \quad (3.13)$$

From the formula connecting the normalized attenuation coefficient to the main beam width at -3 dB, the far field in each Azimuth plane, Plan E, and the Plan H elevation plane, can be estimated as follows [79]:

- ✓ H-Plan

$$E_\theta = \cos(\theta) \cos(\phi) \frac{2j\alpha^{-2}}{\sin(\theta)^2 + j\alpha^{-2}} \quad (3.14)$$

✓ E-Plan

$$E_{\phi} = -\sin(\phi) \frac{2j\alpha^{-2}}{\sin(\theta)^2 + j\alpha^{-2}} \quad (3.15)$$

The reduction of the attenuation coefficient makes it possible to produce very directional lobes in both planes, which increases the directivity. The following relation connecting the directivity with the attenuation coefficient is then obtained:

$$D = 10 \log_{10} \left(\frac{\pi^2}{2\sqrt{2}\alpha} \right) \quad (3.16)$$

The attenuation coefficient α controls the aperture at -3 dB of the main lobe of the radiation pattern. A structure as seen in Figure 3.3 being unidimensional, its resolution is limited by considering a wave vector within a range of length π / d . The truncation in two of the period comes from the symmetry of the solution with respect to the origin. This interval of study is called Brillouin zone; it reports on the relationship between the wave vector and the frequency. In a two-dimensional structure or more, the Brillouin zones are extracted by considering the reciprocal space of the crystal [79].

Let the crystalline structure of *Figure 3.4*. This space G is described by a base D formed by the pair of vectors (d_1, d_2) . This base is called direct base. A reciprocal Gr space of base B can be constructed as:

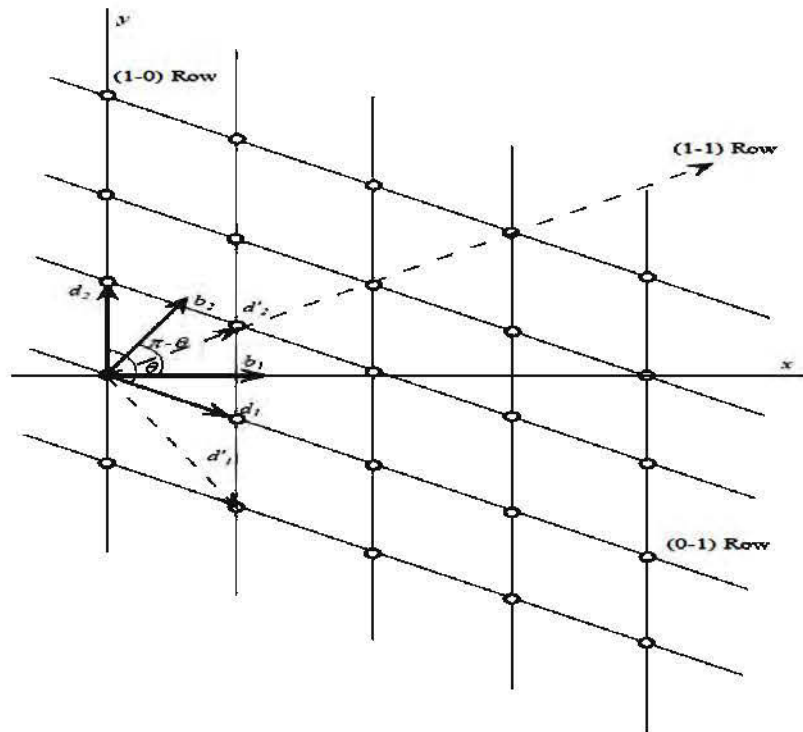


Figure 3.5: Two-dimensional crystalline structure. [78]

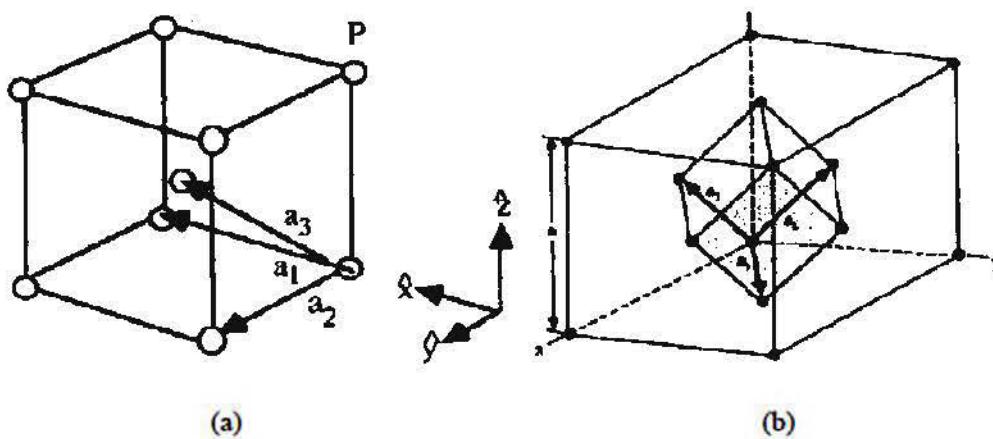


Figure 3.6: (a) Centered cubic cell. (b) Wigner-Zeitz cell

It is possible to write in vector form the spectral transformation given by the equation 2.2. This interpretation is seamlessly exported to a higher dimensional space, such as three-dimensional, as shown in *Figure 3.5*. It makes it possible to describe the basic cell of a three-dimensional centered cubic crystal and its reciprocal space called Wigner-Zeitz cell. The transposition of the problem into a reciprocal space makes it possible to trace the scatter plot in this space. This transposition is a transformation in the spatial domain of the wave propagating in the structure. For each operating frequency corresponds a value of the wave vector according to the propagation direction considered.

The correspondence between the working frequency and the phase constant is translated by the dispersion equation, as well as the correspondence between the group velocity and the phase velocity. *Figure 3.6* illustrates scatter plots for structures ranging from tree-dimensional dimension. It should be noted that often the frequency is presented on the y-axis. The periodicity of the structure makes that the evolution of the curve of the frequency is restricted to an elementary interval. *Figure 3.6 (a)* shows that this interval, for a linear structure, is $[0, \pi / a]$, where a is the linear period of the structure; the symmetry justifies a period $2\pi / a$. This interval is called first Brillouin zone. In a more elaborate structure, the two-dimensional periodicity of the *Figure 3.6 (b)* could be a simple example, the Brillouin areas are the paths elementary elements traveled in all directions in a reciprocal space.

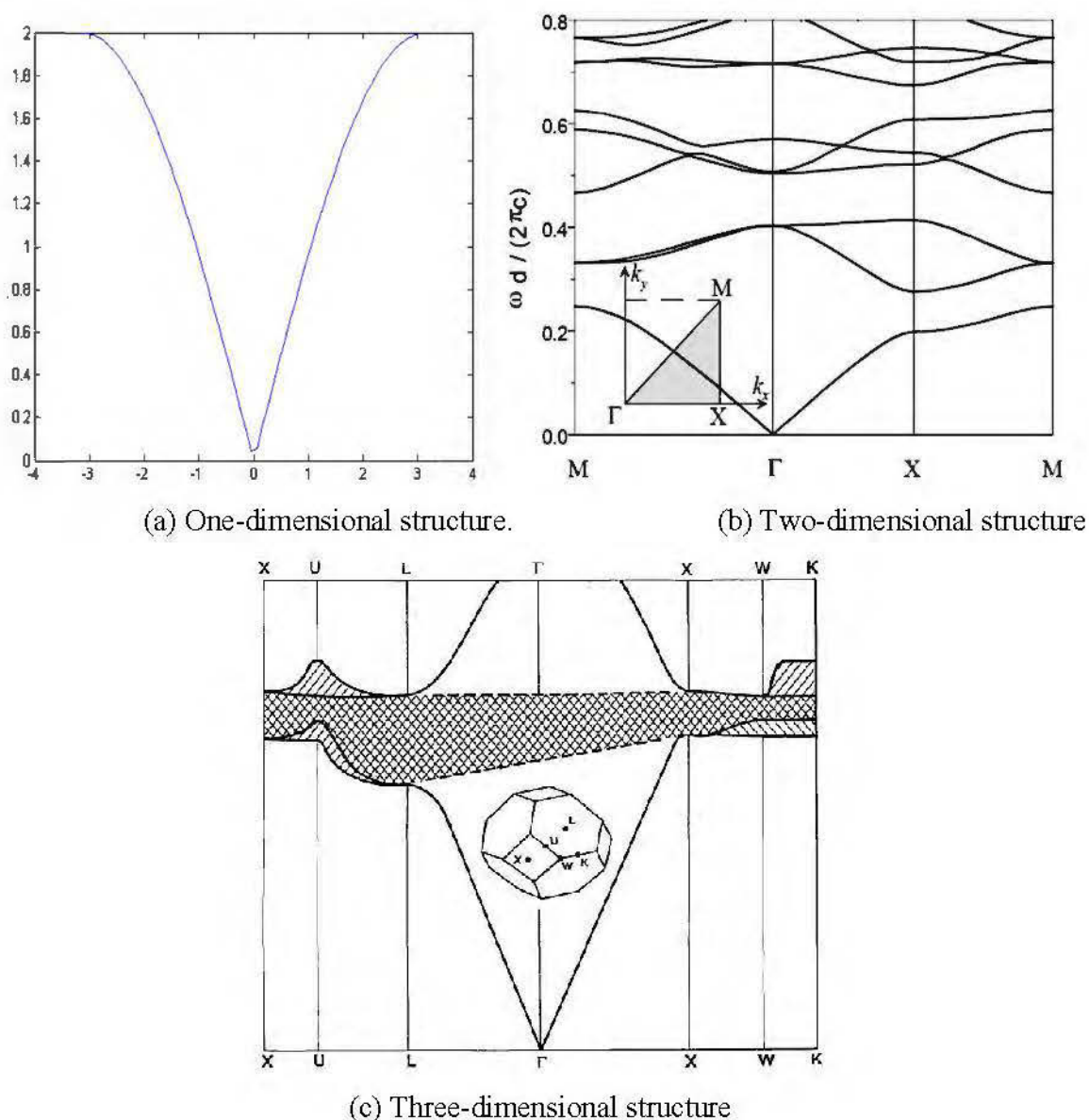


Figure 3.6: Dispersion diagrams [78]

3.2.1.2.3. Fabry-Perot resonator

The Fabry-Perot cage is a resonant cavity applying the principle of reflection between two spaced surfaces and having a given reflection coefficient. The wave is trapped and only a wave having a resonant frequency coinciding with that of the cavity is released. In reality, the selection is not done in frequency, but in terms of wave vector, indeed, the wave released must not only satisfy the condition in frequency, but, moreover, satisfy an angular selection condition. This approach leads to ultra-directive antennas. A Fabry-Perot cavity antenna is considered a two-dimensional (2D) leak wave antenna or a parallel plate guide supporting leaky waves [16-20]. *Figure 3.7* shows the general case of a cavity type antenna Fabry-Perot to 2D.



Figure 3.7 Fabry-Perot cavity

The cavity consists of a low gain source whose vector of the electric field is placed horizontally with respect to the cavity. To obtain the maximum directivity, the condition on the distance h between the ground plane and the semi reflective surface must verify the following condition:

$$\frac{h}{\lambda_0} = \frac{0.5}{\sqrt{\epsilon_r - \sin^2(\theta_i)}} = \frac{0.5}{\cos(\theta_r)} \quad (3.17)$$

where λ_0 is the wavelength, ϵ_r the permittivity of the propagation medium which must not exceed the value 1 and θ_i is the angle of incidence of the wave.

Let the structure of *Figure 3.8*

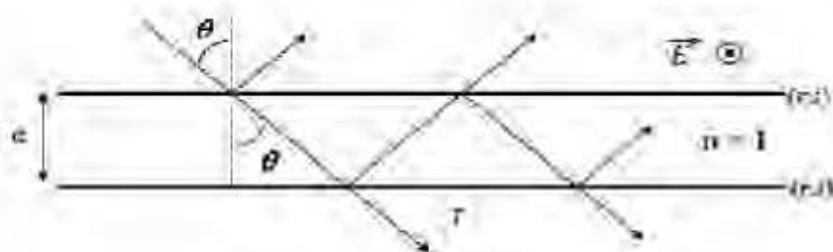


Figure 3.8: Resonant cavity. [70]

A wave is trapped between two identical surfaces, having a reflection coefficient R and distant by a length e . The wave is reflected on one of the surfaces with an angle of incidence θ relative to the normal.

It is possible to write the following:

$$T = \frac{t}{1 - re^{-jkD \cos(\theta)}} \quad (3.18)$$

For a multilayer EBG structure, it is possible to achieve a similar relationship by recurrence, replacing each group of layers by their respective coefficients.

3.2.2. Electromagnetic Band Gap structures

EBG structures have particular electromagnetic characteristics acting as an electric or magnetic wall, radiating structure or decoupling device. At first, the EBG structures were used as a Fabry Perrot resonator. A monopole was placed in the middle of an EBG structure consisting of about ten layers of parallel wire conductors (*see Figure 3.9*). This resulted in a directivity approaching 30 dB.

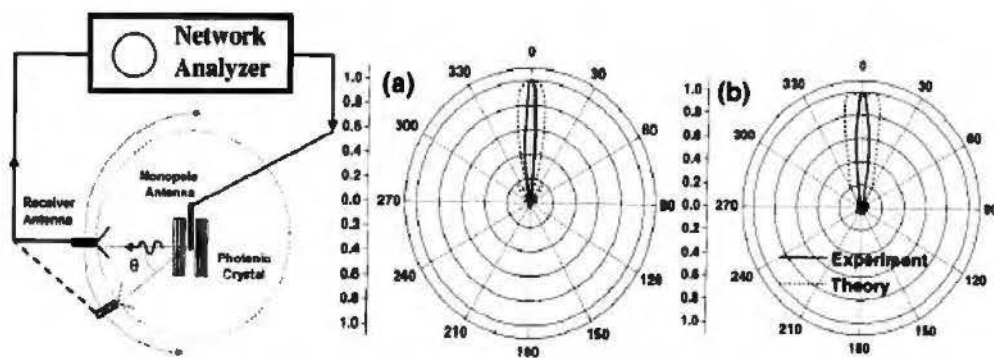


Figure 3.9: EBG antenna of Temelkuran. [78]

In another configuration, a patch antenna has been covered by a structure EBG. The EBG structure has been designed in such a way that the operating frequency is in bandgap; a defect has been introduced into the EBG structure to generate an allowed propagation region coinciding with the operation frequency. This structure thus obtained makes it possible to achieve a gain of 23dBi.

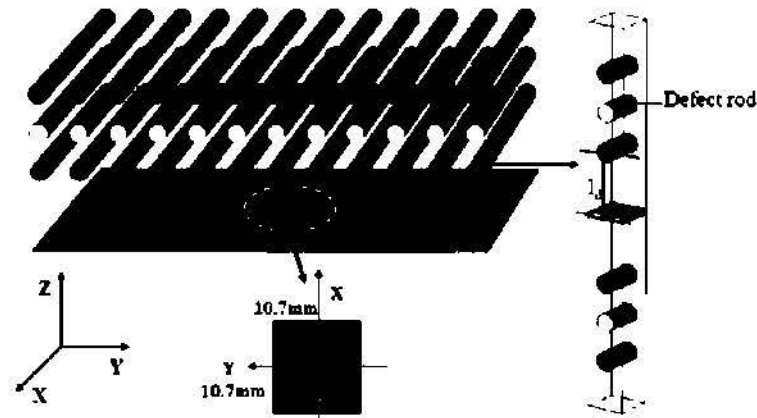


Figure 3.10. EBG antenna with fault. [78]

EBG structures have also been used as a focusing lens for radiation from a weakly directive source in order to achieve gain levels interesting (see Figure 3.11) [Ikonen Tretyakov].

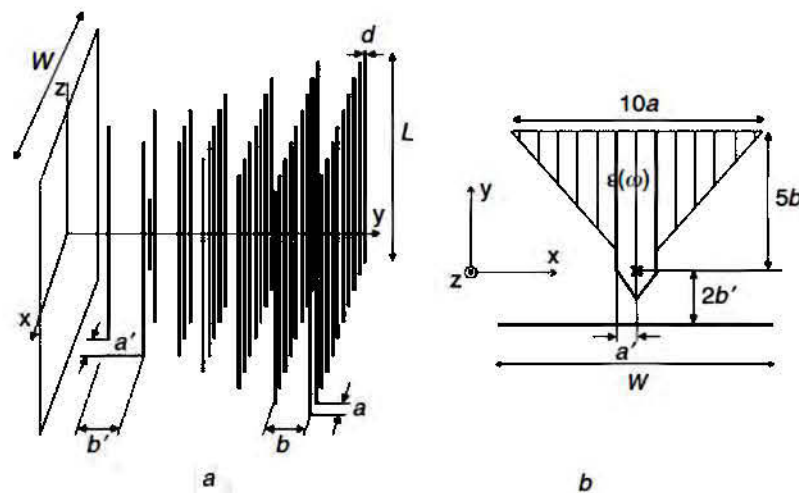


Figure 3.11: EBG Lens Antenna [78]

Finally, it is essential to recall the structures proposed by Boutayeb emulating aperture antennas using cylindrical EBG structures with a defect reminiscent of a horn antenna. This type of approach has the advantage of guaranteeing antennas with a wide frequency band, in comparison with the EBG antennas mentioned above.

3.2.3. Frequency selective Surface structures

FSS surfaces are generally referred to an infinite 2D periodic structure and appeared with Marconi and Franklin in 1919 for the design of a semi-reflective reflector [79]. These surfaces are characterized by their filtering behavior with the EM incident waves. They transmit or reflect waves in well-defined frequency bands. This spatial filtering feature makes it possible to create many devices that enhance the characteristics of the antenna

[80]. Often they are periodic structures illuminated by a wave parallel to their normal and could act as a low-pass, high-pass, band-pass or band-reject filter. This characteristic opens a wide variety of applications for each FSS design. During the 1960s, they found much interest in military field. One of the important applications in military is the stealth technology that reduces the object detection by the enemy. FSSs are used for this application because it reduces the radar cross section in communication systems when covering an object. FSSs have been implemented on aircrafts and warfare ships and other military weapons [80].

FSSs are used to absorb the radiant energy as a function of the frequency or change of the polarization of the wave. The unit cell of the surface is designed considering the direction of the electric field of a plane wave that can be either Transverse Electric (TE) or Transverse Magnetic (TM) [81]. FSS structures also allow creating high impedance surfaces characterized by magnetic walls that do not exist in nature. Among the most common FSS structures is the comb structure [Stutzman]. Sievenpiper et al. proposed a more compact approach leading from the plane of mass by converting it into HIS surface as shown in *Figure 3.12*.

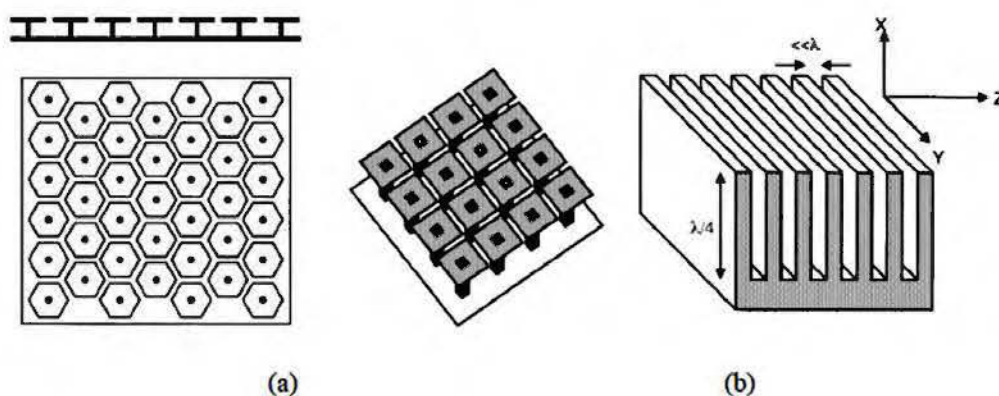


Figure 3.12. High Impedance Surface: (a) Mushroom cell, (b) Comb teeth. [81]

Waves that propagate on an HIS surface will be reduced compared to a conventional ground plane. This feature allows the creation of Perfect Magnetic Conductors which is characterized by a zero phase of its coefficient of reflection in a well-defined frequency band and reduce the size of the antennas, Figure 1.8, widen their bandwidth, increase their directivity and finally decrease their coupling [82-83].

Another application of FSS structures concerns magnetic walls. A magnetic wall does not exist in nature; however, it was possible to synthesize some prototypes using composite surfaces. This kind of entity have a high impedance and an angle of reflection between -

270° and -90°. Several studies have been conducted for the synthesis of AMC (Artificial Magnetic Conductor) [Yang, Feresidis, Rahman]. *Figure 3.13* shows an example of a wall artificial magnetic and its frequency response [Zhang].

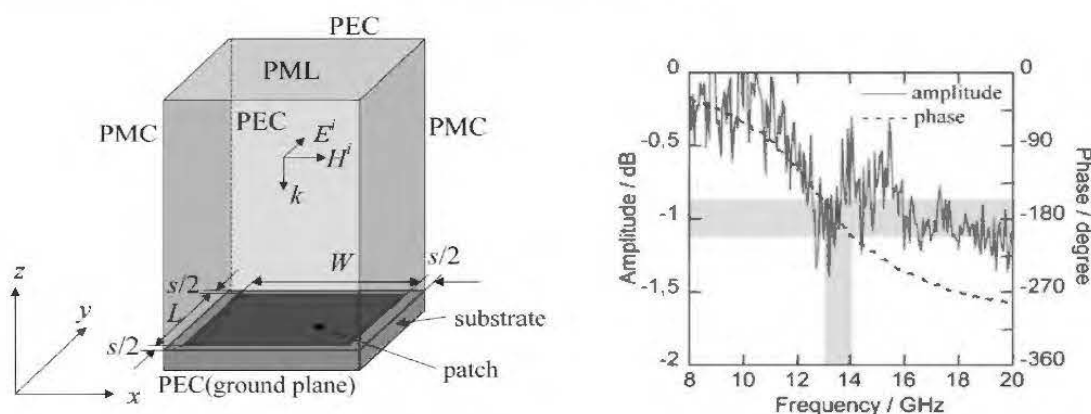


Figure 3.13 Artificial Magnetic Wall. [82]

3.2.3.1. Passive periodic structures

This section deals with the study of passive FSS structures. The goal is to present two passive and geometrically close FSS structures with dual electromagnetic responses at particular frequency bands. The first structure is an arrangement of continuous parallel metal strips. The width of the bands, their spacing, their number and their length are all parameters which have an effect on the electromagnetic behavior of these bands. The second structure examined is a parallel arrangement of discontinuous bands; two parameters are added to the previous case of continuous bands, namely the size of the discontinuity and its repetition pitch. Beyond the geometric complementarity existing between the two structures with continuous and discontinuous bands, there is a correlation between their electromagnetic responses.

Consider the transmission coefficient defined as the ratio between the magnitude of the transmitted wave through the FSS structure and the magnitude incident wave. It appears that the continuous band structure is opaque at low frequencies. As the frequency increases, the continuous band structure becomes invisible and the transmission coefficient changes to unity. On the other hand, the discontinuous strip structure displays a relatively opposite behavior. In fact, the discontinuous bands allow the propagation of the electromagnetic waves passing through them at low frequencies. They then tend to block them and become opaque around a resonant frequency.

3.2.3.1.1. Continuous band FSS structures

The structure described in *Figure 3.14*; A layer of metal strips periodically arranged parallels are illuminated by a plane electromagnetic wave TM, the electric field polarized

parallel to the metal bands [Tretyakov, Analytical Modeling]. An elementary cell is periodically reproduced at infinity. In this configuration of infinitely long continuous bands, two parameters are analyzed namely the horizontal repetition period and the width of the bands.

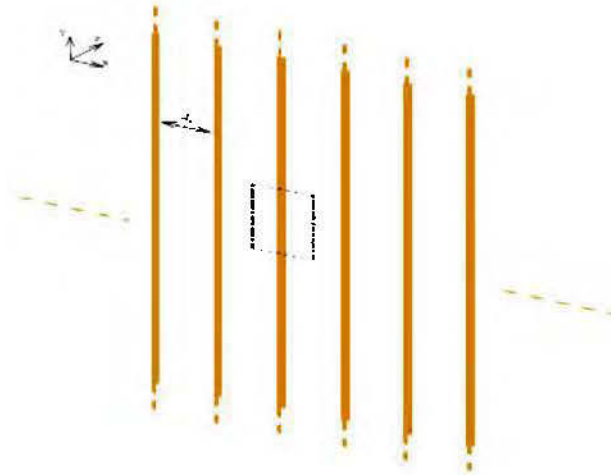


Figure 3.14 Periodic continuous strip structures [83]

The FSS structure considered as described above, is an arrangement of metal strips infinitely long and spaced periodically. The period of the structure defines a frequency band where only one mode appears. Indeed, the structure begins to be opaque to incident electromagnetic radiation, the conditions around metal bands disturbing the propagation at these low frequencies; when the frequency increases, the structure becomes more permissive and its invisibility more effective. However, this invisibility is not perennial, it is interrupted by a sudden rupture of its evolution by a resonance inherent in the inter-band distance; this distance corresponding to the half-length of the frequency of cutoff as shown in *equation 3.19*.

$$f_{\max} = 2 \cdot \frac{c}{d_x - e/2} \quad (3.19)$$

The band width of acts in a subtler way on the response of the FSS structures. It has the effect of controlling the progression slope of the structure from its opaque state to its translucent state. This parameter makes it possible to regulate a frequency band where the structure maintains a uniform behavior.

- *Electrical model*

The incident wave illuminating the structure is of TM polarization, the electric field is thus parallel to the conductive strips. These bands being relatively narrow, this electric field makes it possible to generate an induced current. The associated magnetic field is parallel

to the plane of the surface and perpendicular to the discontinuous bands, the electrical model of the structure can thus be reduced to a parallel arrangement of electric coils (see *Figure 3.15*).

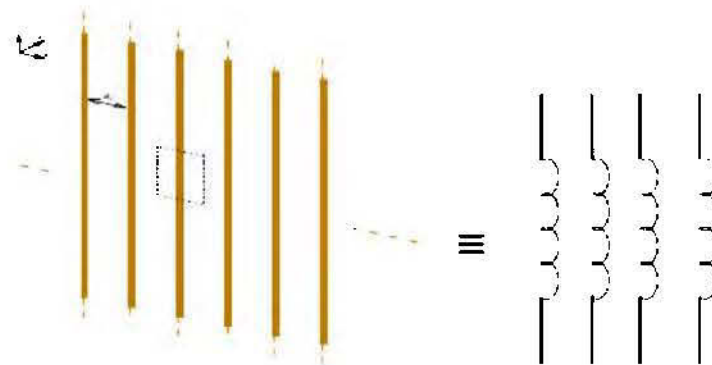


Figure 3.15 *Electrical Model of a Continuous Band Structure.* [83]

In such a model, the coils are likened to a short circuit in low frequency, the FSS surface is similar to an electrical wall blocking the propagation and forcing the electric field to cancel itself on contact. At high frequencies, the coils are open circuits transparent to the electric field. This model effectively translates the response of the continuous band structures described previously.

3.2.3.1.2. Discontinuous bands FSS Structure

Now consider the structure described in *Figure 3.16*. Geometrically, this structure is close to the previous structure with continuous bands. Discontinuities are periodically inserted on each of the metal strips.

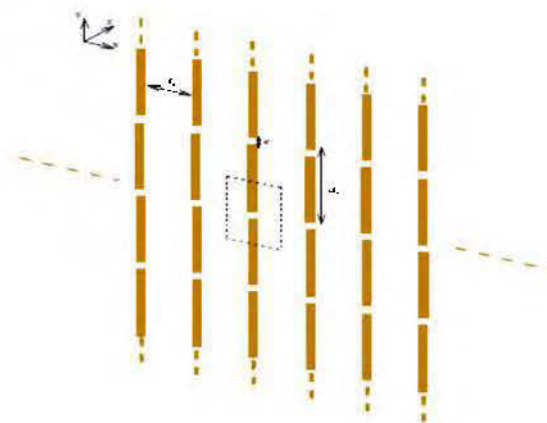


Figure 3.16: *Periodic structure with discontinuous bands.* [83]

The discontinuous band FSS structure has a different electromagnetic response compared to the continuous band. The structure is not opaque at low frequencies but rather invisible to illumination by transverse electromagnetic waves, the discontinuities authorizing the existence of an electric field on the plane of the structure. As the frequency

increases, the structure tends to block the spread. This mutation reaches its culminating point at a resonant frequency defined by the length of the discontinuous band. At resonance, all the incident energy is reflected.

$$f_{disc} = 2 \cdot \frac{c}{d_y - e/2} \quad (3.20)$$

The equation 3.2 teaches us that this period is not the only one responsible for this regulation of the resonant frequency; the longitudinal distance between two successive discontinuous bands acts on this resonance frequency. Indeed, the length of the discontinuous bands being equal to the longitudinal period decreased by the difference between two successive bands, this length corresponds directly to the resonance frequency of the discontinuous bands. Thus, the more the bands are moving away and the distance e is growing, the shorter the bands, and the higher the resonant frequency.

- *Electrical model*

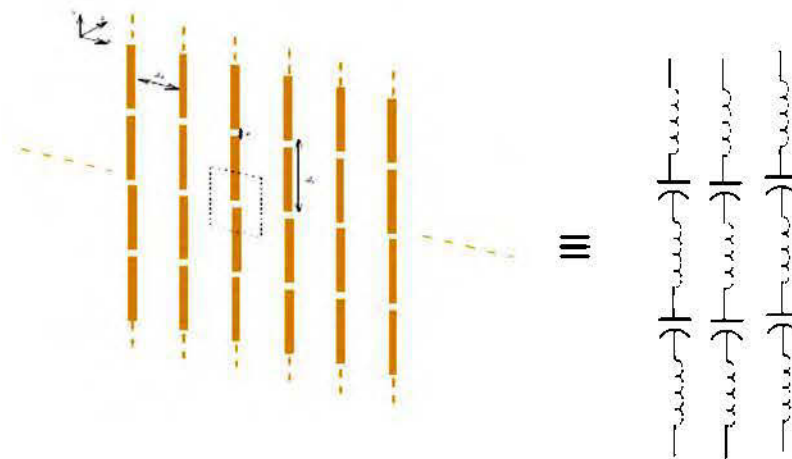


Figure 3.17 *Electrical model of a discontinuous strip structure.* [83]

In the same way as for continuous band structures, the conductors of the discontinuous band FSS structure can be likened to coils. However, the periodic discontinuity reveals a capacitive effect between two successive bands as shown in *Figure 3.17*. Such a circuit has rejection filter properties blocking propagation at the resonance frequency generated by the juxtaposition of a coil and capacitance.

3.2.3.2. Active FSS Structures

Geometric complementarity between continuous band structures and discontinuous as well as the duality of their electromagnetic responses allow to consider a control on the propagation of electromagnetic waves.

Consider the structure described in *Figure 3.18*. Inserting an active element capable of switching between two continuous and discontinuous electrical states in discontinuous

bands, in this case a diode in our case, ensures the switching between the two dual states and it will thus be possible to transform the structure between a configuration emulating an electric wall and another authorizing the spread.

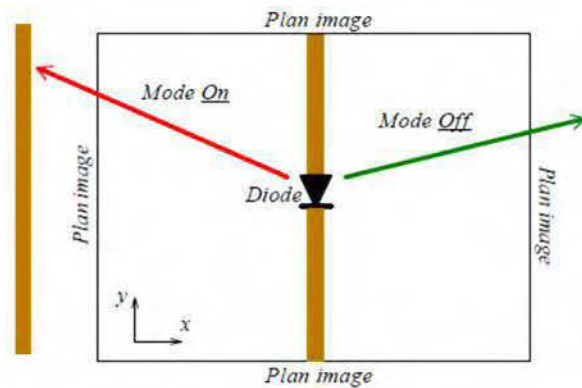
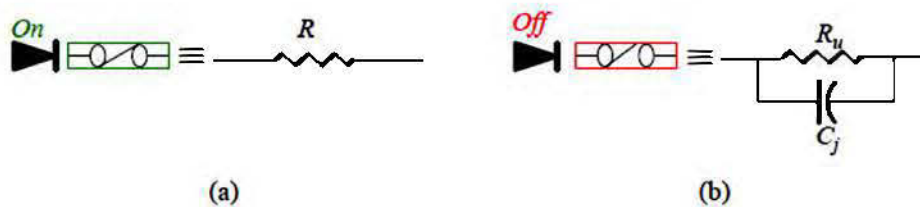


Figure 3.18 Active FSS Structure. [83]

- *Electrical model of the diode*

The diode is an electrical device that ideally switches between two states complementary to an open circuit and a short circuit. However, any electrical element has spurious effects. These effects can inductive, because of the length of the conductor, or capacitive, because of the coupling between the conductors, or ohmic, due to the thermal effect of the current flowing through the conductor, or due to the contacts. The diodes also exhibit undesirable phenomena in both passing and blocking mode; their occurrence leads to the consideration of electric models in both modes.



(a): *passing mode*; (b): *blocking mode*

Figure 3.19 Equivalent electrical model of the diode. [83]

In the On state, only a weak resistance is present. It comes mainly from ohmic contacts; it remains globally around a few ohms. In off state, a capacitive effect appears; this effect results from the coupling effects between the connectors and the oxide layer. A current also exists and this effect is modeled by a resistance R_u of a few tens of kilos ohms. These values, however, depend on several parameters such as working temperature, operating frequency, the value of the bias current and the dynamic current, and so on.

The insertion of a diode in blocking mode would lead to a frequency shift in the electromagnetic response of discontinuous FSS structures. The high resistivity of the diode in off state introduces a loss in the response of the structure without affecting its frequency rate; this loss is naturally of a thermal nature. The capacitive nature of the diodes as for it acts on the frequency response interval of the structure; the response of the structure is shifted to low frequencies. Indeed, it is commonly accepted that one of the techniques for reducing the dimensions of an antenna is to include a load of capacitive nature at its end or inductive at its input; thus, the discontinuous bands being charged with the capacitive charges have their resonant frequency decrease, and because of this, the whole electromagnetic response of the discontinuous EBG structures is transposed towards the low frequencies.

All these parameters being analyzed; it will later use these results for the design of agile antennas based on EBG structures. Several configurations will be explored to meet various requirements such as cost, size, operating band, and performance in gain and agility. These different paths of study will be the subject of the next chapter.

CHAPTER FOUR

DESIGN AND FABRICATION PROCESS OF THE ASBRA

4.1. Project Methodology

This chapter presents the project methodology, the steps of overall designing, simulation, fabrication and measurement of the Adaptive Switched Beam Reconfigurable Antenna (ASBRA) which theory has been discussed in Chapter 2 and chapter 3. The ASBRA is designed from the development of single dipole antenna by numerical method and verified by simulation using Computer Simulation Technology (CST) software; for comparison and validation of the optimized results, Ansoft HFSS software. Then, the parametric study on varying the parameters of antenna is also discussed in this chapter.

The methodology of this project is started by understanding of the reconfigurable antenna, the RF switches and the effect of combination between RF switch and the antenna. The revision on biasing circuit, PIN diode and its equivalent circuit are deeply studied in order to reveal its effect on the antenna's performance. Then, the ASBRA is designed and simulated to study the antenna's performance in terms of return loss, current distribution, gain and radiation pattern. When the simulation process shows a good result, the antenna is fabricated using wet etching technique.

The antenna is fabricated on Flame Retardant 4 (FR₄) laminate board with dielectric constant (ϵ_r) of 4.5 and loss tangent ($\tan \delta$) of 0.019. Other equipment such as a UV unit, transparency, etching chemical and ferric chloride acid were used during the fabrication process. Then, the drilling process is continued by drilling the hole at transmission line to connect the biasing network at the back of the antenna. A copper via is placed through each hole and punched to ensure that the copper via is stable. After that, the PIN diodes were embedded into the antenna using soldering tools. After soldering the components together, the multimeter was used to check the connectivity of the components and the antenna. After all fabrication process is done, the measurement process is continued to get results such as return loss, received gain and radiation pattern. Finally, both simulated and measured results is compared and analyzed for documentation.

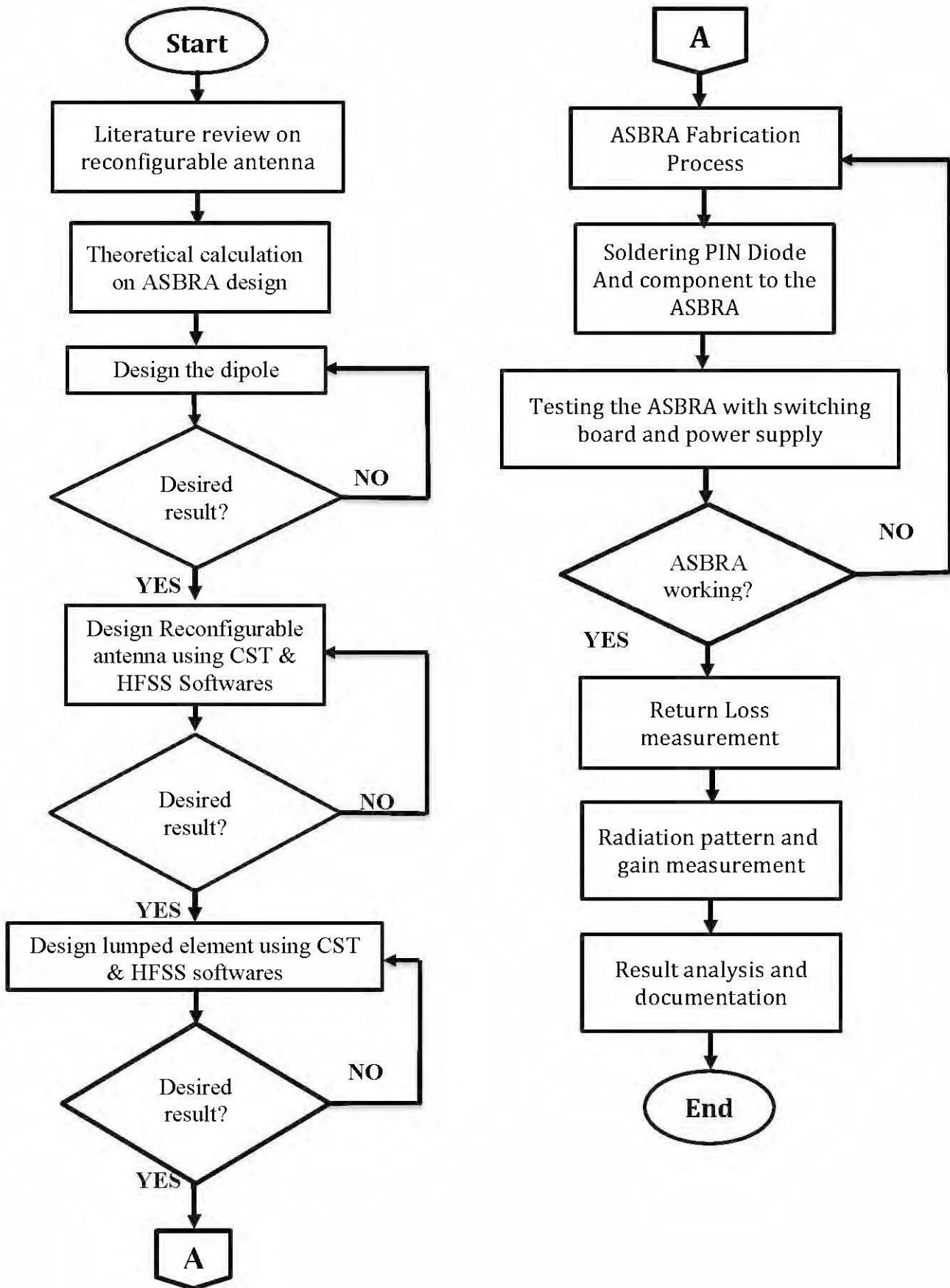


Figure 4.1. Flow chart of overall process of the ASBRA

4.2. Cylindrical Frequency Selective Surface Screens

In the perspective of achieving agility of the radiation pattern in the azimuth plane, it is intuitive to consider a structure with axial symmetry. The cylindrical reflector is a geometrical shape admitting an axis of revolution and a uniformity along this axis as proposed in *figure 4.2*.

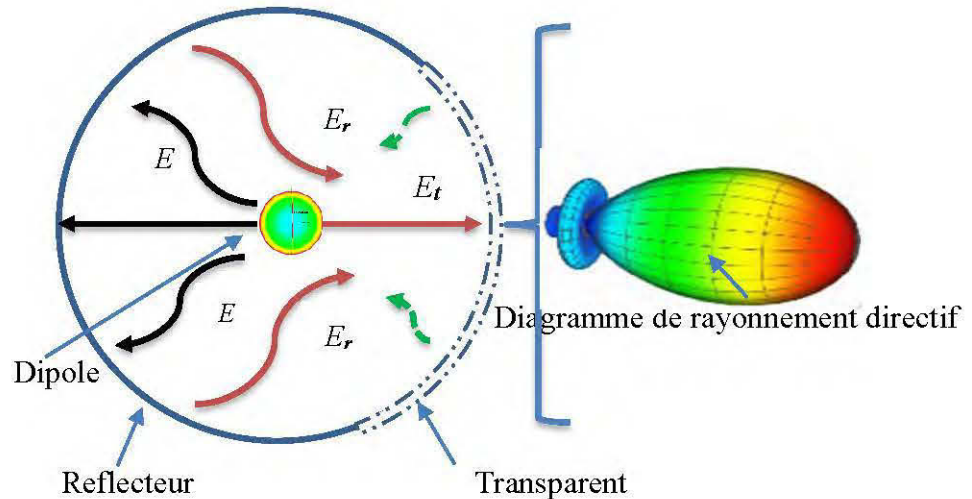


Figure 4. 2. Geometry of the proposed active reconfigurable cylindrical FSS antenna [45]

In this configuration, the controllable partially reflective/transparent surface is illuminated by a simple dipole radiator placed at the center of the cylinder. To realize a directional beam, a part of this cylinder is a reflector, while the other part is transparent for the waves emanated from the dipole and the ones reflected from the other opaque part. By constructive interactions between these waves, a directive radiation-pattern is obtained in front of the reflector. Therefore, the directive beam is turned into a high gain directional pattern. For sweeping the direction of the radiation, the transparent part of the reflector is moved around the cylinder by sequentially activating/deactivating the relevant unit cell elements on the FSS surface. By this technique, the pattern can be easily swept in the azimuth with a certain step dictated by the number of the active elements on the circumference of the cylinder. Alternatively, when the entire cylinder surface is transparent for the dipole radiator, the overall antenna radiation is expected to be only the one of the dipole resonator.

4.2.1. Design of cylindrical reflector.

The radiation of the antenna is based on the reflector principles; the overall antenna dimensions are calculated, then the perfect electric conductor is replaced with reconfigurable partially reflective surfaces. In the radiation geometry, the reflector is illuminated by a dipole antenna at the center of the cylinder as shown in *figure 4.3*.

The initial radius and length of the circular reflector are mathematically calculated based on the design guidelines of a corner-reflector antenna with an apex angle of 90° [84].

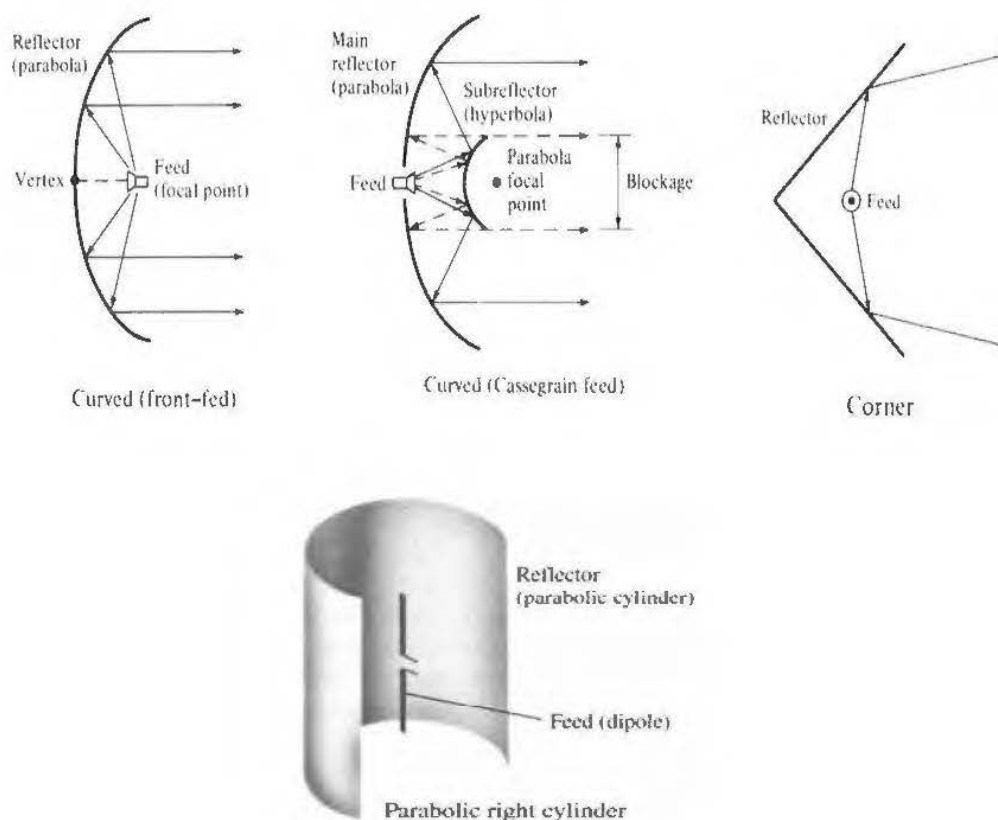


Figure 4.3 Geometry of a corner reflector into a semi-cylindrical reflector antenna. [84]

According to the optical ray tracing theory [84], a source placed at R distance from its reflector generates a low side/back-lobe level directional beam and the open aperture is large enough to capture the most electromagnetic waves emanated from the source. In fact, depending on the distance of the dipole to the reflector, the reflected waves from the side sheets of the corner reflector can be in phase. Moreover, this distance substantially dictates the existence of the secondary lobes of the radiation pattern and also the radiation resistance of the corner-reflector antenna.

An approximate value of the radius R can be calculated by considering the required constructive phase relation of the interfered electric fields. It means that the interactions between the waves reflected from the cylinder and the ones emanated directly from the dipole must be in-phase to achieve a directive radiation-pattern in front of the reflector. To determine this relation, the scattering mechanism in *Figure. 4.3* is considered. It is supposed that an infinitely long cylinder is excited by an infinite thin dipole at its center. Because of geometrical symmetry around the axes of cylinder, almost entire inner surface of the

cylinder is illuminated with co-phased electric fields. To achieve a directive radiation pattern, the pass phase of reflected fields should be in-phase with the fields emanated from the dipole.

$$\Delta\phi = \varphi_G - \varphi_R = 2k\pi, k = 0, 1, 2, \dots \quad (4.1)$$

where:

$$\varphi_R = 2R \times (2\pi/\lambda) \text{ and } \varphi_G = -\pi. \quad (4.2)$$

This equation can be simplified to

$$R = k\lambda/2 + \varphi_G \lambda/4\pi. \quad (4.3)$$

The minimum value of $R=0.25\lambda$ is achieved for this ideal case. In reality, since R is comparable with wavelength, the reflector is in the near field of the dipole antenna. In fact, the cylinder is illuminated while neither the amplitude of incident waves is uniform, nor they are in-phase. Therefore, the contribution of cylindrical reflector is not exactly -180° . Then, a distance of usually larger than $R=0.25\lambda$ is required to fulfill the in-phase condition of interfered electric fields. This relation is in agreement with the required antenna to distance of $[0.2\lambda-0.8\lambda]$ for a corner reflector at its first dipole position [84].

4.2.2. Source of radiation design

The agility of our antenna is on the azimuth plane of our diagram of radiation. It is therefore natural that the radiation of the basic source should be omnidirectional in the azimuth plane. Thus, we will focus on broadband omnidirectional source of radiation that can be adapted to our structure. The wired dipole is an excellence candidate because of its simplicity and ease of manufacture to produce a uniform radiation pattern in the azimuth plane. The length of the two arms of the dipole is of the order of a quarter wave. At resonance, the impedance of the dipole is equal to theoretically $73 + j42.5\Omega$ [Stutzman].

A dipole with length 76 mm and radius 1.5 mm has been designed. The ratio between the radius of the dipole and its length is 2%. Such a dipole makes it possible to reach a bandwidth of 100% (2.3 GHz to 2.7 GHz) at -10 dB as shown in *figure 4.4*.

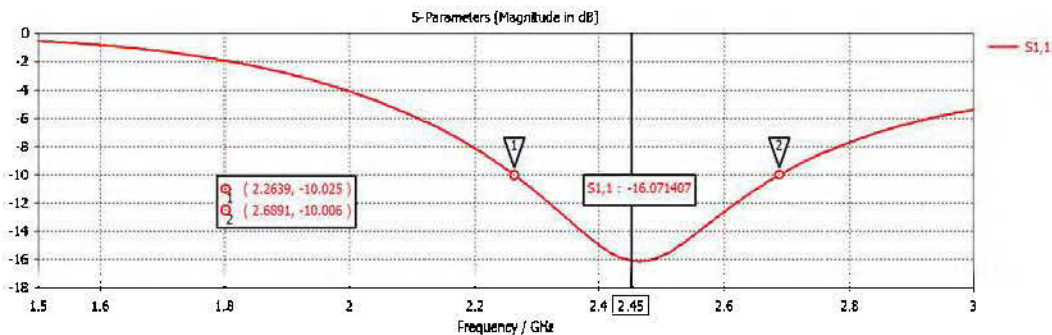


Figure 4.4(a) Frequency response of the dipole

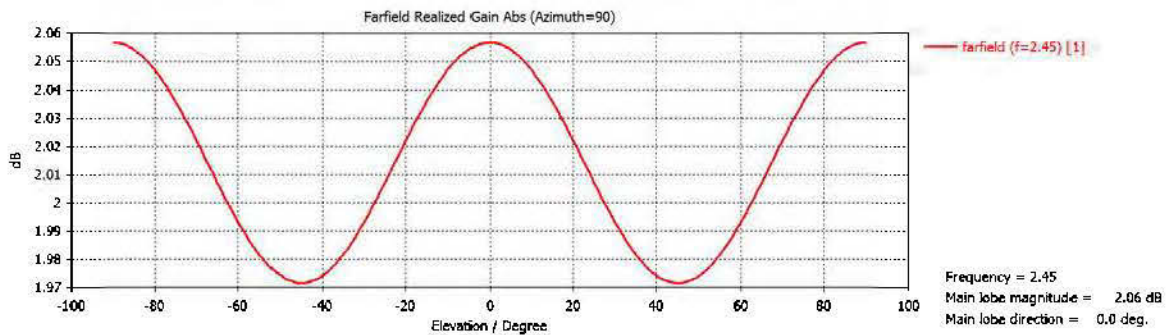


Figure 4.4(b) realized gain response of the dipole

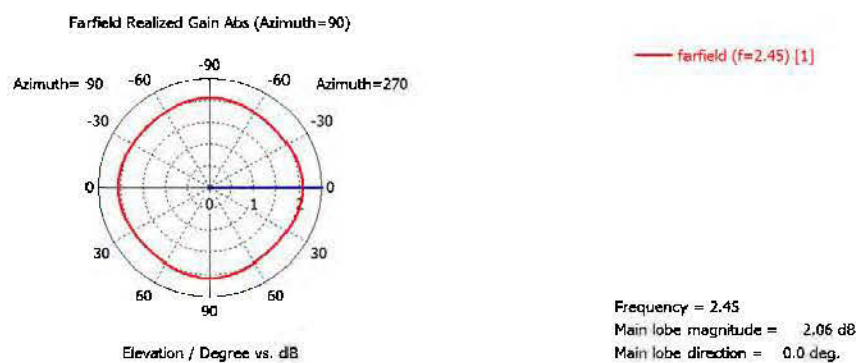


Figure 4.4(c) Radiation Pattern response of the dipole

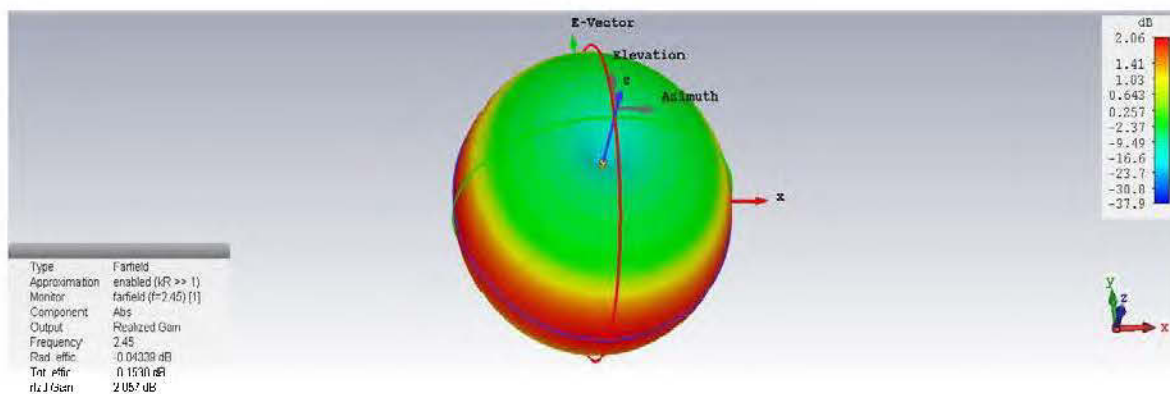


Figure 4.4 (d) Radiation pattern of the dipole in Azimuth Plane (CST)

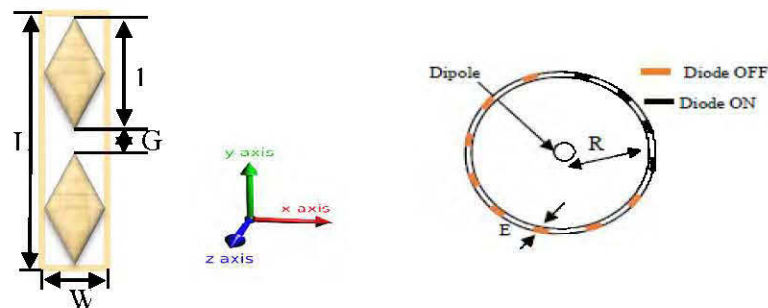
4.2.3. FSS unit cell design

It is worthwhile pointing out that the transmission and reflection coefficients of the unit cell design are obtained on the basis of Floquet's theory for an infinite planar periodic structure, so that the curved cylindrical FSS may change the electromagnetic response. The factors impacting the performance include the structure of the cell unit, the radius of the curvature and the incident angle of the electromagnetic wave [85].

To design a reconfigurable pattern antenna using an FSS structure, the unit cell must have reconfigurable transmission and reflection coefficients.

However, the FSS unit cell proposed in [86-89], in the ON state, the basic unit cell is not fully transparent for the EM waves, which results in a considerable deterioration of the radiation pattern's performance.

Therefore, to improve the transparency level of the unit cell, a new FSS design is proposed with interesting properties in terms of controlling the radiation pattern of the proposed antenna. The proposed unit cell, presented in *Figure 4.5* is composed of metallic and symmetric lozenges shape with discontinuous strip and a gap in its discontinuity. The EM plane waves propagate in the normal Z direction with the E-field parallel to the strip Y direction. In the OFF state, a reconfigurable stopband is noticed around 2.45 GHz.



$$L = 154, Gd = 1.5, l = 76, Gd = 1.9, w = 50, R = 96.5, E = 0.127 \text{ (All dimensions in mm)}$$

Figure 4.5. Fss Unit cell of the ASBRA.

On the basis of the principles of the reflector antennas studied in chapter 3, the dimensions of the proposed antenna can be properly determined. Therefore, the length of the cylindrical FSS should be larger than the wavelength, and the required number of the FSS in each column will be defined according to the height of the unit cell. The total number of the unit cells along the cylinder circumference depends on the width of the unit cell and radius of the cylinder as follows:

$$N = 2\pi R/W. \quad (4.4)$$

N is the number of columns, W is the width of the FSS unit cell, and R is the radius of the cylinder

4.2.4. PIN diode integration

The PIN diode equivalent circuit is an important part in simulation of reconfigurable antenna to support better results in measurement process done by using real PIN diode.

Two types of PIN diode representation are simulated and discussed which are:

- i. PIN Diode Representation using Lumped Element

ii. PIN Diode Representation Using PEC Pad

4.2.4.1. PIN Diode Representation using Lumped Element

In Figure 4.8, the design and simulation setting of the ASBRA antenna incorporated with lumped element data in CST simulation software. The PIN diode equivalent circuit is based on Micro semi technology [90] that was discussed in Chapter two. The equivalent circuit of PIN diode for forward bias consists of a series combination of the series resistance (R_S) and an inductance (L_S). In CST simulation software, there are two types of circuit which are RLC-Serial and RLC Parallel as shown in *Figure 4.6*. The values of lumped elements in ON and OFF modes are shown in *Table 4.1*.

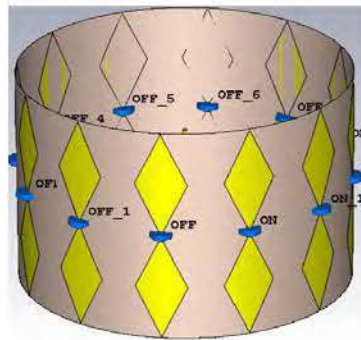


Figure 4.6 (a) ASBRA representation using lumped element in CST.

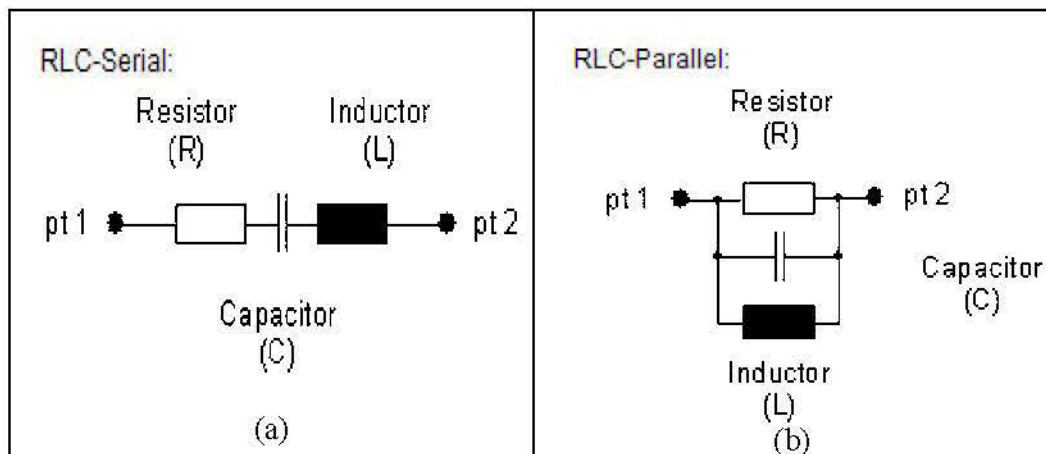


Figure 4.6 (b) Pin diode electrical model (a)RLC-Serial (b) RLC-Parallel.

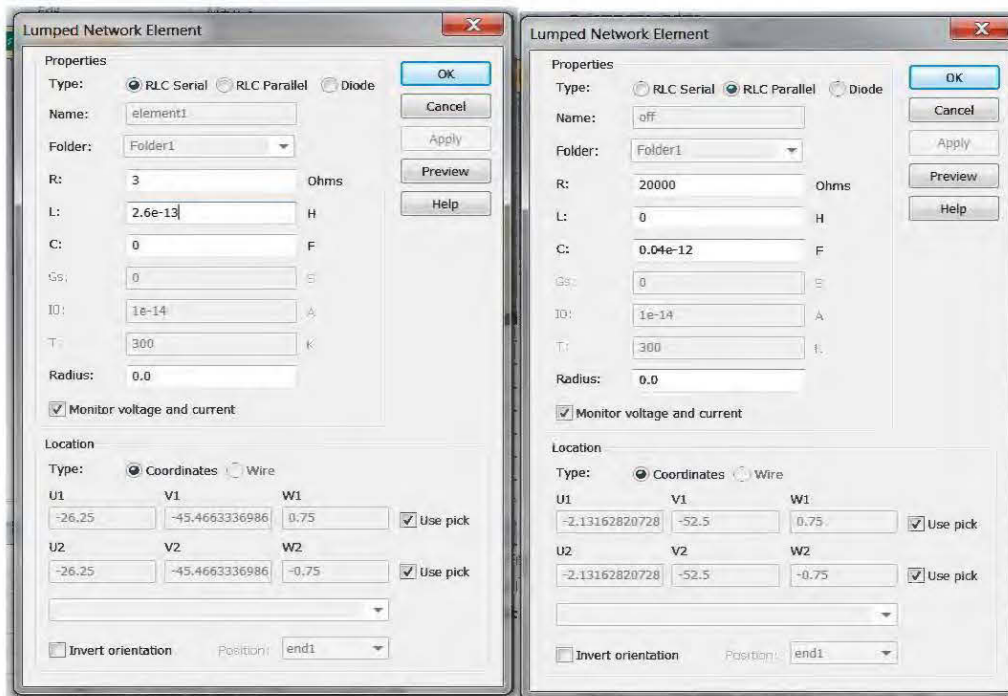


Figure 4.6 (c). lumped element circuits that are developed in CST software

<i>Pin Diodes States</i>	<i>Resistor (R)</i>	<i>Inductor (L)</i>	<i>Capacitor (C)</i>
<i>ON</i>	3Ω	$2.6e-13 H$	$0 F$
<i>OFF</i>	$20 k\Omega$	$0 H$	$40 fF$

Table 4.1 The value of lumped elements as a PIN diode

4.2.4.2. PIN diode representation using PEC pad

The other type of PIN diode representation in simulation process is using a PEC pad. It is represented as an open or short of the transmission line as shown in *Figure 4.7*. The OFF state is represented by the 1mm x 3mm metal stripe and the absence of the metal strip represents the ON state. This type is easier than the lumped element circuit because the simulation is faster and more accurate. This principle of operation has also been used by other researchers as reported in [91-93].

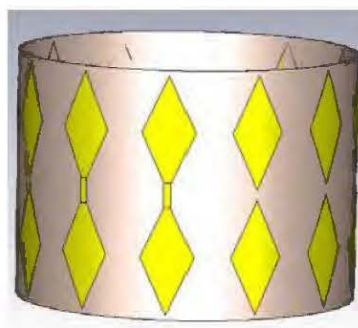


Figure 4.7: ASBRA representation in CST using PEC pad.

4.3. Parametric study of the ASBRA

The desired functionality of the ASBRA is the product of several parameters such as cavity size, dipole size, lumped elements specifications, type of substrate, band gap size the number of FSS elements... that mainly affects the reflectivity of the FSS structure.

We firstly considered the default parameters such as:

- i. The dipole is considered in the range of:
 - a. distance to the reflector is chosen in the range of $0.2\lambda < R < 0.8\lambda$.
 - b. the length of $0.5 \leq L \leq 0.6 \lambda$
 - c. the radius of 3mm to guarantee a 10% bandwidth for the dipole.
- ii. The FSS Unit cell is chosen in the range of
 - a. the length of $0.5\lambda < l < 0.7\lambda$
 - b. the Width of $0.2\lambda < w < 0.4\lambda$
 - c. the periodicity of 30° .
 - d. the distance between columns of $0.08\lambda < w < 0.1\lambda$
 - e. the copper material of the thickness of 0.017 mm
- iii. The gap for the diode's insertion is chosen between $0.01\lambda < Gp < 0.03\lambda$
- iv. The reflector size is chosen by:
 - a. the height of $0.5\lambda < H < 2\lambda$;
 - b. the width of $3\lambda < W < 5\lambda$;
 - c. the thickness of $0.127 \text{ mm} < T < 0.254 \text{ mm}$;(real substrate size available)
 - d. the material chosen is FR-4 with dielectric constant, $\epsilon_r = 4.7$, loss tangent 0.019 and Rogers R03003 with dielectric constant, $\epsilon_r = 3$, loss tangent 0.001.
- v. The Pin diode is chosen with the specifications of the lumped elements of:
 - a. Model GMP4201($R_s=2.3\Omega$, $R_p=30k\Omega$, $C_p=180pF$)
 - b. Model MA4AGBLP912 ($R_s=4\Omega$, $R_p=20k\Omega$, $C_p=0.025pF$)

We start our design with a structure whose FSS elements are discontinuous and the dipole placed in the surrounding of FSS structure has a radius of 3 mm, a height of 60 mm, and a gap of 2 mm between its arms, with the best radiation characteristics in the desired frequency around 2.45 GHz. The ASBRA has twelve columns each subtending an angle of 30° at the circle center. Each vertical column contains a unit cell. Consequently, twelve pin diodes are required. The unit cells are placed cylindrically around the dipole with an angular periodicity of 30° and radius of 90 mm ($3\lambda/4$) on a substrate R03003 with a

thickness of 0.127 mm. To reconfigure the antenna beam from an omnidirectional dipole into a directional one, the diodes on the FSS columns will switch in the ON and OFF states. This diode is modeled as lumped elements in *Table 4.1* (Model GMP4201).

The final design values are determined by a compromise between the acceptable size, gain, and bandwidth of the antenna.

4.3.1. Effect of the radius of the Cylindrical Reflector

To study the effect of the radius on the radiation patterns and directivity of the antenna, the angular periodicity varied. The same transversal period means the transmission and reflection coefficients of the FSS structure are the same. To keep the transversal period fixed when the radius of the cylindrical structure changes, the ϕ_{FSS} must be modified

The transversal periodicity is defined by:

$$dx = R \cdot \phi_{FSS} \text{ (rad)} = R \cdot \phi_{FSS} \text{ (deg)} \cdot \frac{2\pi}{180} \quad (4.5)$$

We demonstrate this in the following four cases:

- $R = 48.25$, $\phi_{FSS} = 40^\circ$, $dx = 101.05$ mm, $N_{FSS} = 6$
- $R = 72.37$, $\phi_{FSS} = 40^\circ$, $dx = 101.05$ mm, $N_{FSS} = 9$
- $R = 96.5$, $\phi_{FSS} = 30^\circ$, $dx = 101.05$ mm, $N_{FSS} = 12$
- $R = 120.06$, $\phi_{FSS} = 30^\circ$, $dx = 101.05$ mm, $N_{FSS} = 15$

In other case transversal periodicity of the FSS structure is changed. In both cases, the radiation patterns are compared. We will begin by considering several parameters namely reflection coefficient, the directivity, the level of back lobe, and the beams of the radiation pattern in the planes of elevation and azimuth at 2.4 GHz. The structure is recalling a configuration similar to a cavity; it is particularly sensitive to the radius of the cylinder as shown in *Figure.4.8*. Nevertheless, due to the symmetry of the proposed ABSRA system, a small discrepancy of the electromagnetic performance between the infinite planar FSS and cylindrical FSS can be expected as long as their tangential dimensions are the same [94]. Since the parameter R is the major factor that determines the overall dimension of the cylinder and mainly influences the radiation performance of the antenna, it is necessary to firstly optimize the horizontal tangential periodicity which defines by *Eq. (4.4)*. For simplification, the parametric studies were developed by using an equivalent metallic reflector in the columns switched to reflecting state. It is clearly observed in *figure 4.8 (a)* that the structure is highly reflective for such FSS transverse and describes the evolution

of the resonant frequency in function of the radius. This frequency evolves in opposition to the ray. For a 100mm radius, the first resonance occurs around 1.9 GHz, at 90 mm it is 2.3 GHz, 1.7 GHz at 115 mm and 2.45 GHz at 96.5 mm.

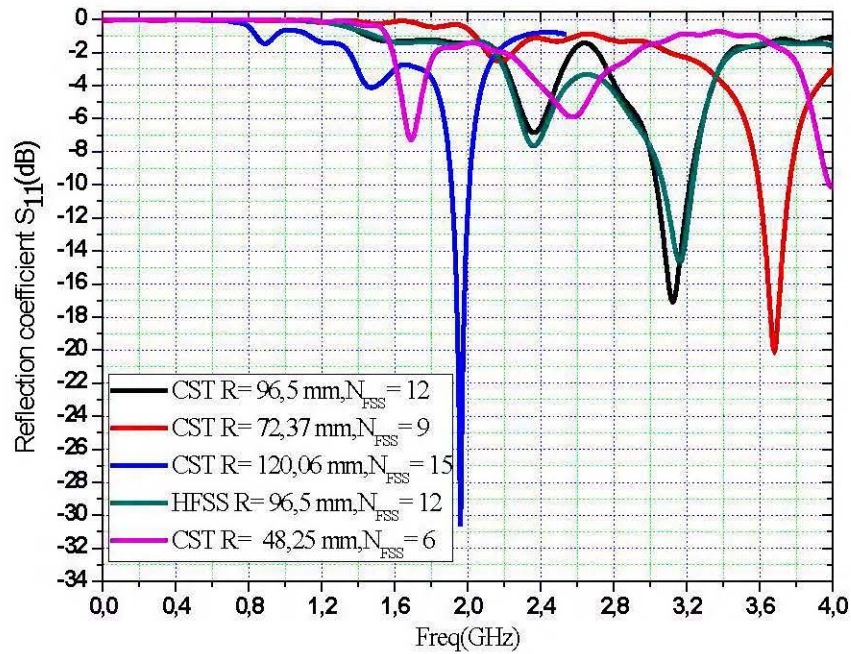


Figure 4.8(a). Effect of the radius R on the resonance frequency of the cavity.

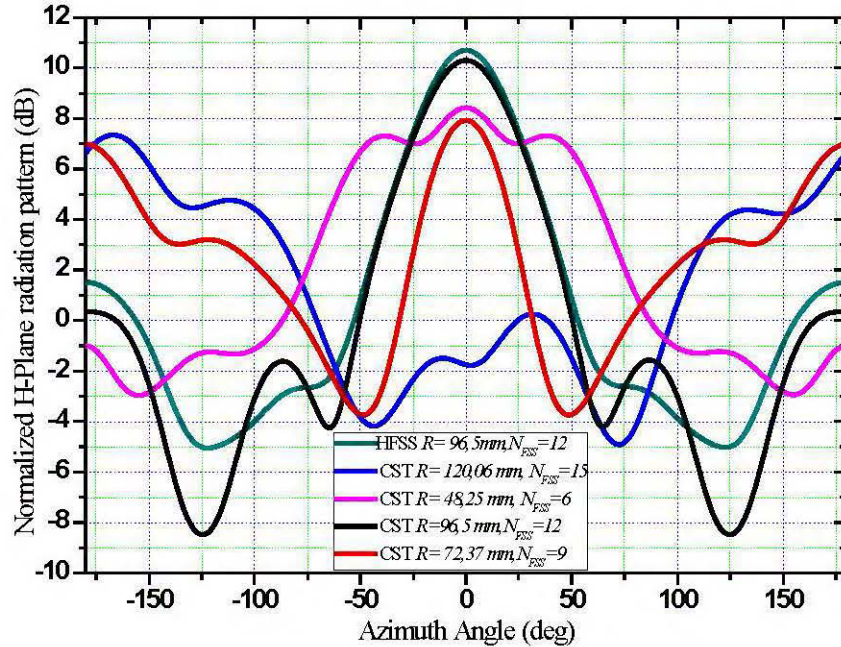


Figure 4.8(b). Effect of the radius R on the H-plane radiation pattern of the cavity.

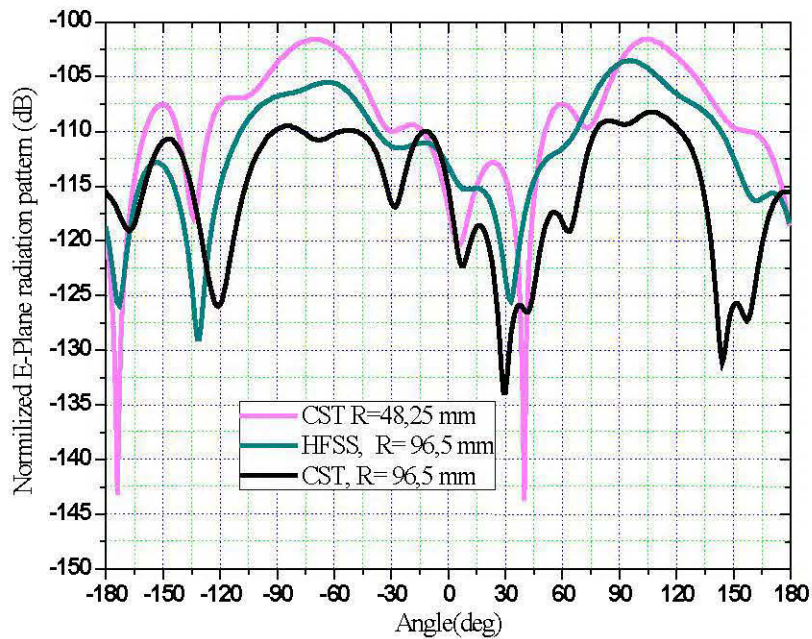


Figure 4.8(c). Effect of the radius R on the E-plane radiation pattern of the cavity.

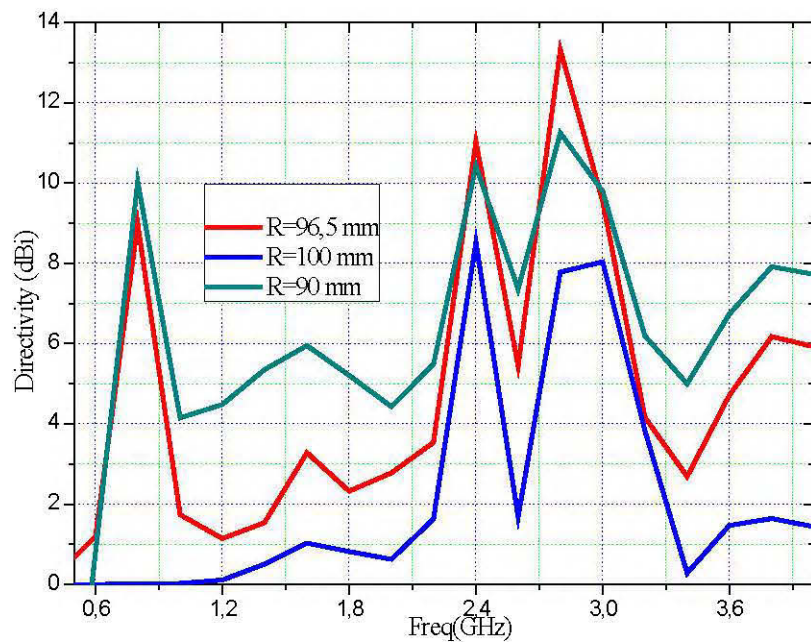


Figure 4.8(d). Effect of the radius R on the E-plane radiation pattern of the cavity.

Figure 4.8 (b) and Figure 4.8 (c) illustrate the H-plane and E- plane of the radiation pattern for different R . The lowest side/back-lobes are found at $R=96.5$ mm. In addition, the resonant frequency increases dramatically with the decrease of R , and is degraded at the desired band. The larger R is the better S_{11} , but the lower the directivity. Therefore, as long as it is acceptable level of S_{11} is achieved for a small value of N_{FSS} , matching will be acceptable at larger L_{FSS} .

Considering all radiation characteristics seen in the above results, the optimal value of our applications is the radius of the cylindrical reflector being equal to 96.5mm.

4.3.2. Effect of the number of FSS unit cell elements

Here, the transversal period (dx) which refers to the *equation 4.5* changes when the radius R is fixed. We demonstrate this in the following three cases:

- $R=96.5$, $\phi_{FSS}=40^\circ$, $dx=134.7$ mm, $N_{FSS}=9$
- $R=96.5$, $\phi_{FSS}=30^\circ$, $dx=101$ mm, $N_{FSS}=12$
- $R=96.5$, $\phi_{FSS}=24^\circ$, $dx=80.8$ mm, $N_{FSS}=15$

It was attempted to keep the radius of the structure the same as the previous case, but since the (number of columns of strips) must be an integer, the value of R cannot be exactly the same as the previous case. Being fixed a radius of the structure and the dimensions of the dipole, the number of elements FSS retained will act on the nature of the periodic surface and more specifically on its reflection coefficient. Thus, the cavity will react differently depending on the number of continuous elements considered. *Figure 4.9* describes the effect of the number of FSS elements on the behavior of the cavity. When the number of elements is 12 elements, the FSS layer has two resonant frequencies are around 2.3 GHz and 3.1 GHz which gives an excellent first harmonic lobe to be explored in our project.

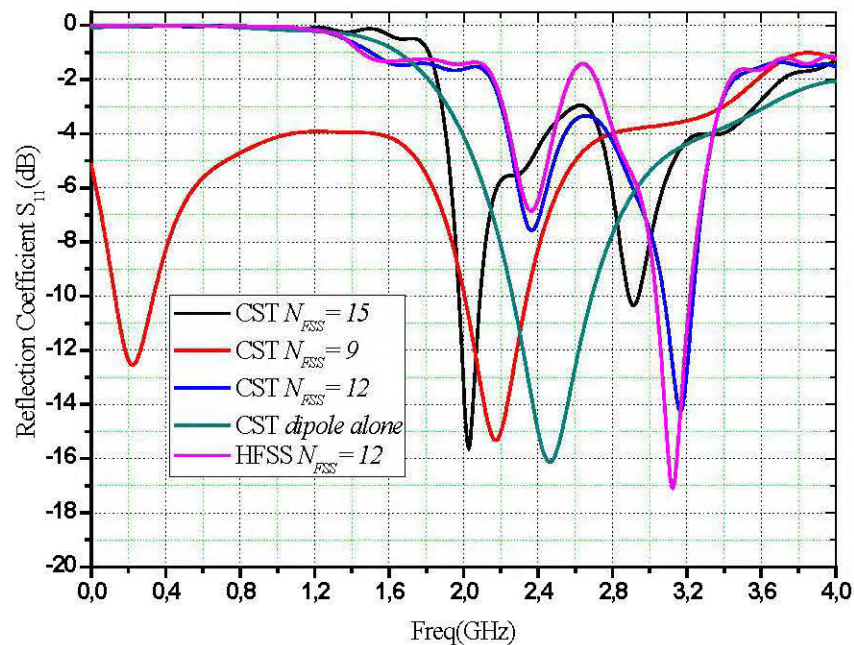


Figure 4.9 Effect of the number of FSS elements ($N_{FSS}=6,9,12,15$).

4.3.3. Effect of width of FSS elements

Besides the radius, other dimensions of the unit cell W_{FSS} and L_{FSS} control the transmission and reflection response of the planar FSS (as shown in *Figure. 4.10*), and hence also influence the radiating characteristics of the ASBRA. It is essential to focus part of the study on the importance sets combinations of W_{FSS} and L_{FSS} of the resonant frequency of 2.45 GHz structure. It is known that the resonant frequency of the band-pass FSS shifts as the width of the unit cell and periodicity changes. However, for a width of 37.5 mm the structure has the resonance frequency disturbed in the 2.4 GHz band.

Therefore, the width of the cylinder can be calculated as:

$$W_{FSS} \approx \frac{2\pi \cdot R}{12} \quad (4.6)$$

where N_{FSS} is the number of unit cell and W_{FSS} the width of unit cell.

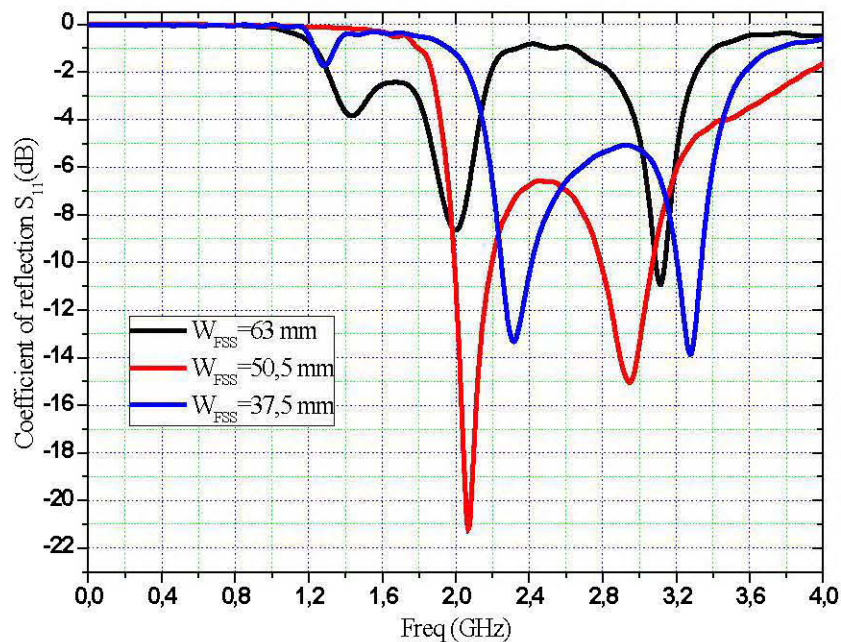


Figure 4.10 Effect of the unit cell FSS width.

4.3.4. Effect of the band gap aperture

In the light of what has preceded, it is intuitive to think that the structure will not be completely closed. The band gap spacing between two contiguous discontinuous strips has the effect of aerating the discontinuous FSS surface making it more transparent. *Figure 4.11* illustrates this phenomenon by showing the S_{11} which are almost identical; note also the slight collapse of the secondary lobes.

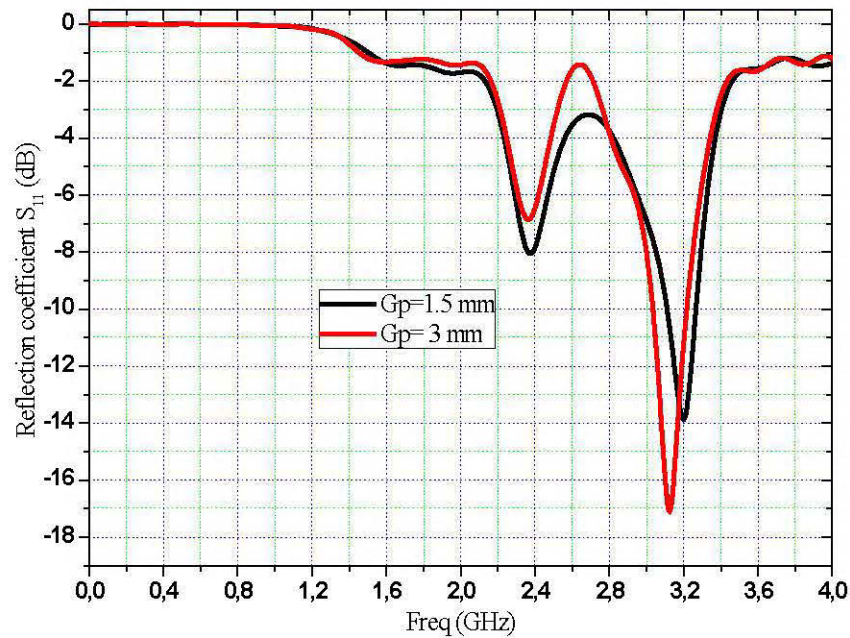


Figure 4.11 Effect of the width of the gap.

The ultimate goal is to achieve a reconfigurability of the antenna radiation pattern by creating a gap which will be truncated at times and will have a leakage region which has the effect of raising the resonant frequency. For all practical purposes, it is important to remember that this spacing corresponds, in practical, to the size of the active element needed to switch between states passing and blocking.

4.3.5. Effect of Lumped elements

It has been demonstrated that a cylindrical FSS structure, combining continuous elements and other discontinuous, has the potential to produce a directional beam. The reconfigurability of such a structure relies on the permutation between passing and blocking states of FSS elements, in a desired direction, and via the use of an active element. The diode is the device selected for this purpose. At high frequencies, however, its behavior involves parasitic effects, the effects of which influence the behavior of FSS surfaces. It was observed in *figure 4.12* that the capacitive nature of the blocking mode diodes was the feature having the most critical effect on the performance of the FSS surfaces. As a result, the diode model MA4AGBLP912 is included in the spacing separating the discontinuous bands. The resistance R_p selected is of the order of 30 k Ω ; it has been noticed that this magnitude has little effect on the response of discontinuous element surfaces, if it is of the order of a few k Ω . The capacitance is varied and its effect on the performances of the cylindrical structure are analyzed.

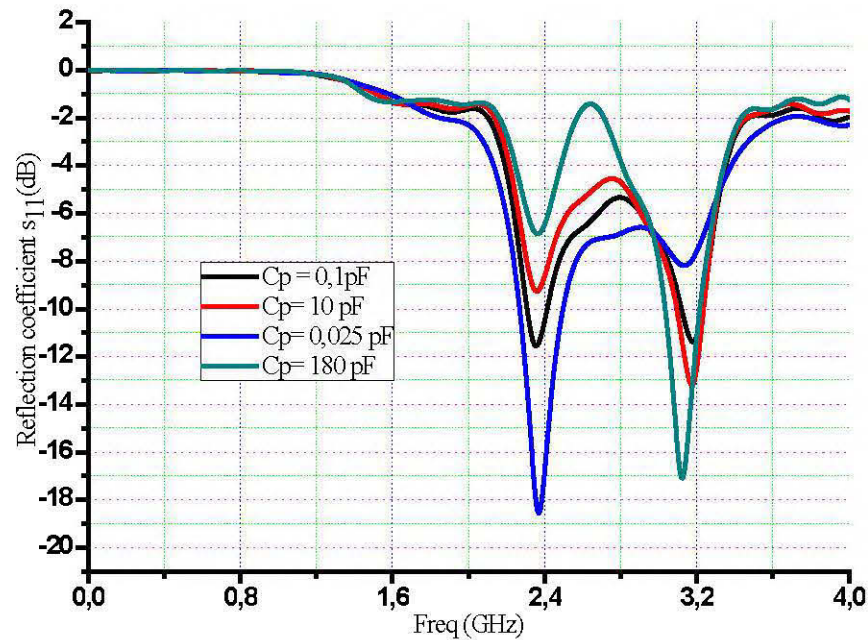


Figure 4.12 Effect of the diode capacitance on the structure.

The initial effect shown in *Figure 4.12* is a slight shift towards the low frequencies of the resonance of the structure. The transparency bandwidth of discontinuous strip FSS structures is reduced and shifted to low frequencies. The beams are still generated for a capacitance of 180 fF, at 2.4 GHz, with a background radiation level of around -12dB, as indicated by the radiation patterns in *Figure 4.13*. The spectral performance of the antenna degrades even more manifested at high frequencies, in the case of diodes with low capacitive effect. By substituting diodes whose capacitance is of the order of 180 pF by capacitance diodes of the order of 0.025 pF, the rear radiation level decrease of 10 dB and the directivity undergoes an inflation of 3 dB as shown in *figure 4.14*

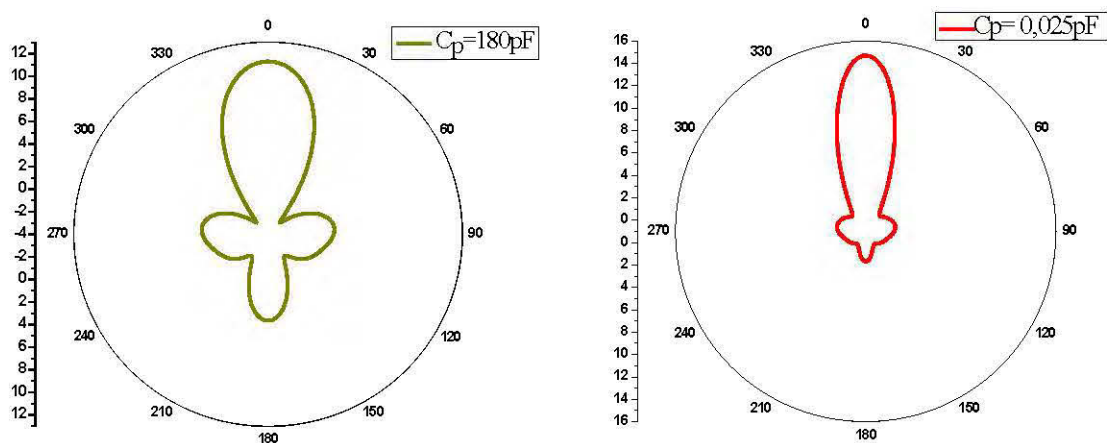


Figure 4.13 Effect of the diode capacitance on the radiation pattern

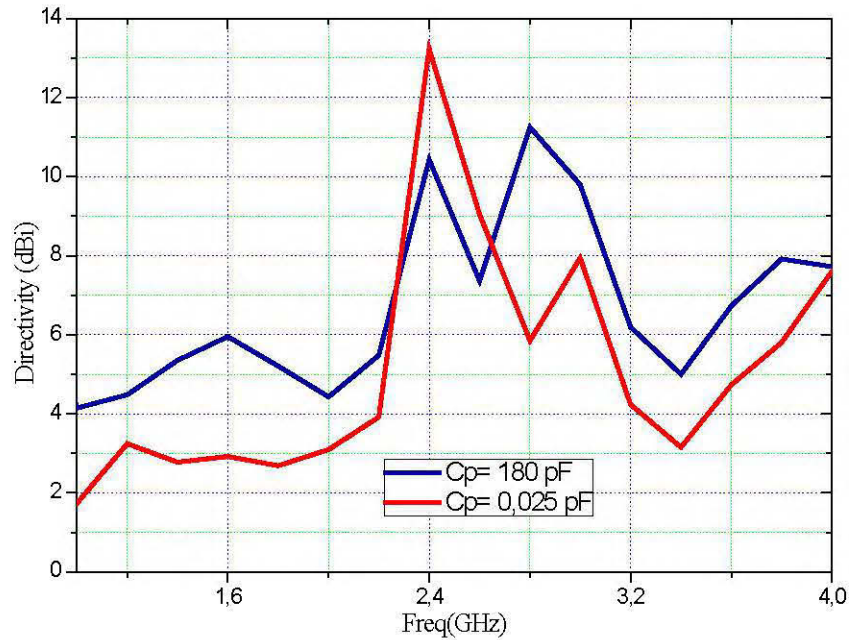


Figure 4.14 Effect of the capacitance on directivity

4.3.6. Effect of the opening angle

When a number of diodes on FSS elements are switched ON, the structure defines an opening angle which depends on the ratio between the number of Pin diodes in the ON states (n) and the total number of diodes (N) on elements FSS. This angle as shown in *Figure 4.15* controls the directivity response of the structure, depending on the frequency.

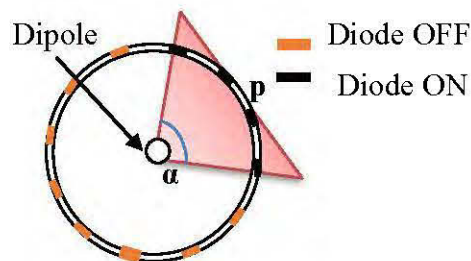


Figure 4.15 Opening angle of the radiating structure.

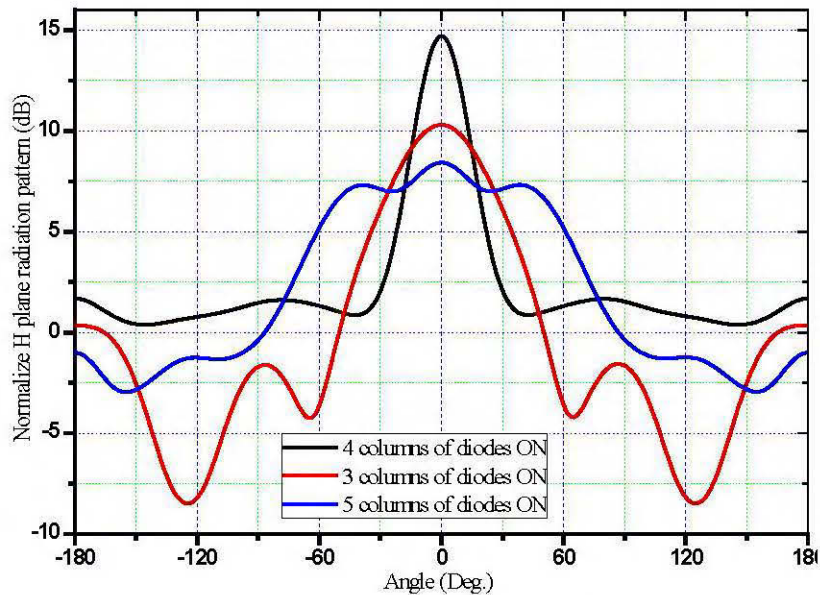
The arc defining the opening angle is described by equation Eq.4.1 below:

$$arc = p \cdot (n + 1) \quad (4.7)$$

The opening angle being the ratio between this arc and the circumference of the cylinder, it follows as well as:

$$\alpha = \frac{arc}{2\pi d} = \frac{n \cdot p}{N \cdot p} \cdot 2\pi \text{ (rad)} = \frac{n \cdot p}{N \cdot p} \cdot 360 \text{ (deg)} \quad (4.6)$$

Figure 4.16 describes the radiation diagrams, at 2.45 GHz, of cylindrical FSS structures having different periodic steps (total number of elements) and different opening angles (ratios of elements in the ON state / total number of elements).



(a): for $\alpha = 90^\circ$, (b): for $\alpha = 120^\circ$, (c): for $\alpha = 150^\circ$.

Figure 4.16: Radiation diagrams in the azimuth plane at 2.45 GHz

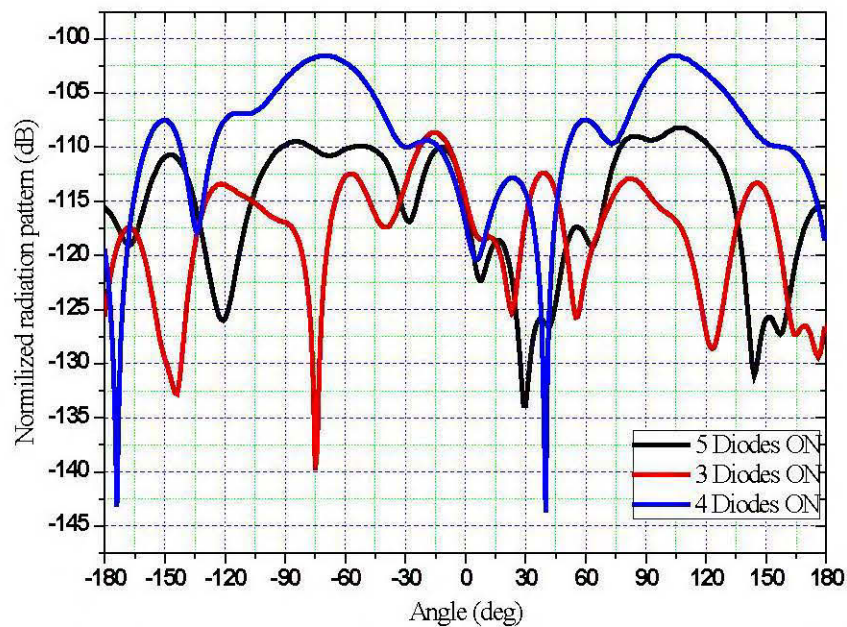
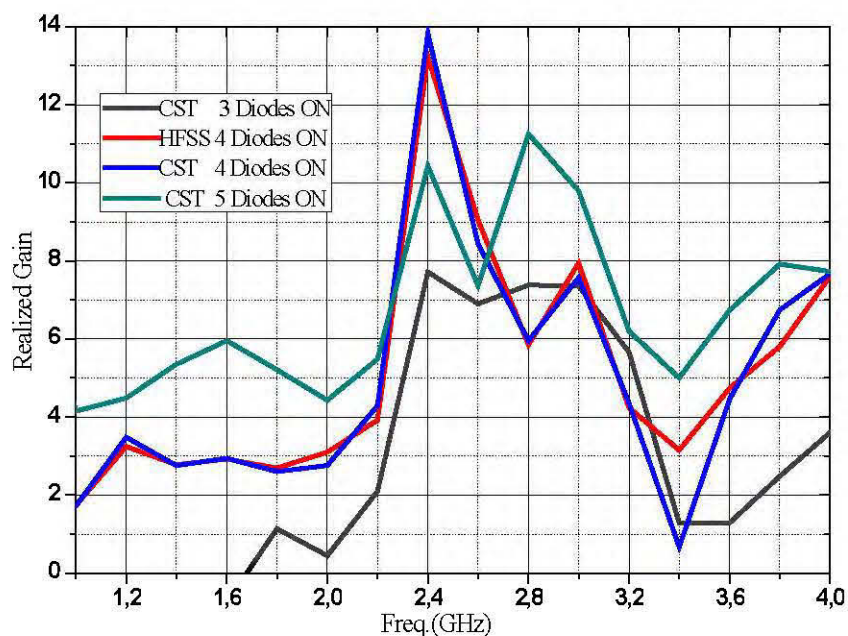


Figure 4.17: Normalized Radiation diagrams in the E-plane at 2.45 GHz

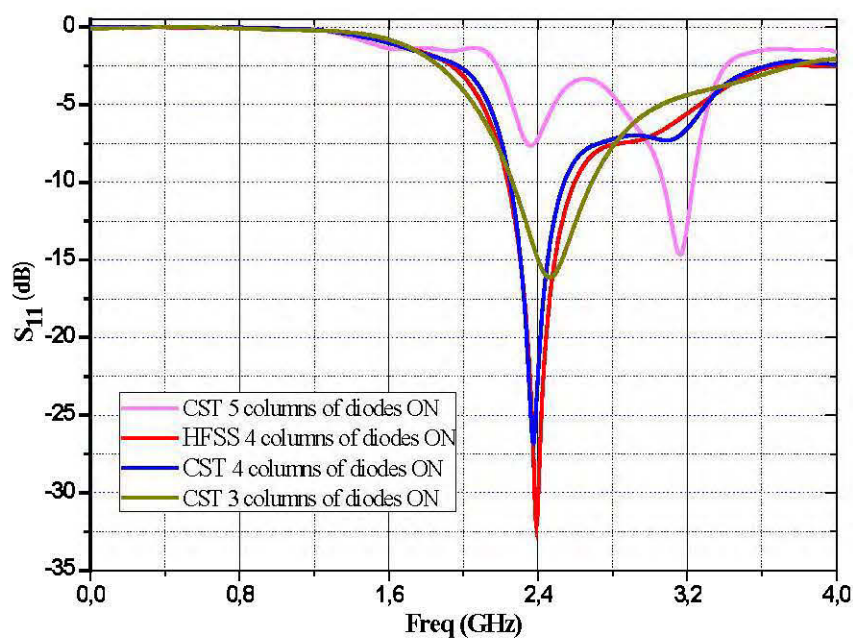
It is equally useful to observe the evolution of the directivity according to the frequency. Figure 4.18 illustrates the spectral progression of the directivity for different angles of opening and the Figure 4.19 illustrates the S_{11} of the opening angle. Therefore, one third

open structure has interesting spectral stability, and an acceptable level of directivity. Of more, the level of back radiation is closely related to the periodic pitch, as evidenced by the curves in *Figure 4.20*. It is equally useful to note that this level also depends on the opening angle; indeed, a structure with a wide opening is less prone to successive reflections on its walls.



(a): for $\alpha = 90^\circ$, (b): for $\alpha = 120^\circ$, (c): for $\alpha = 150^\circ$.

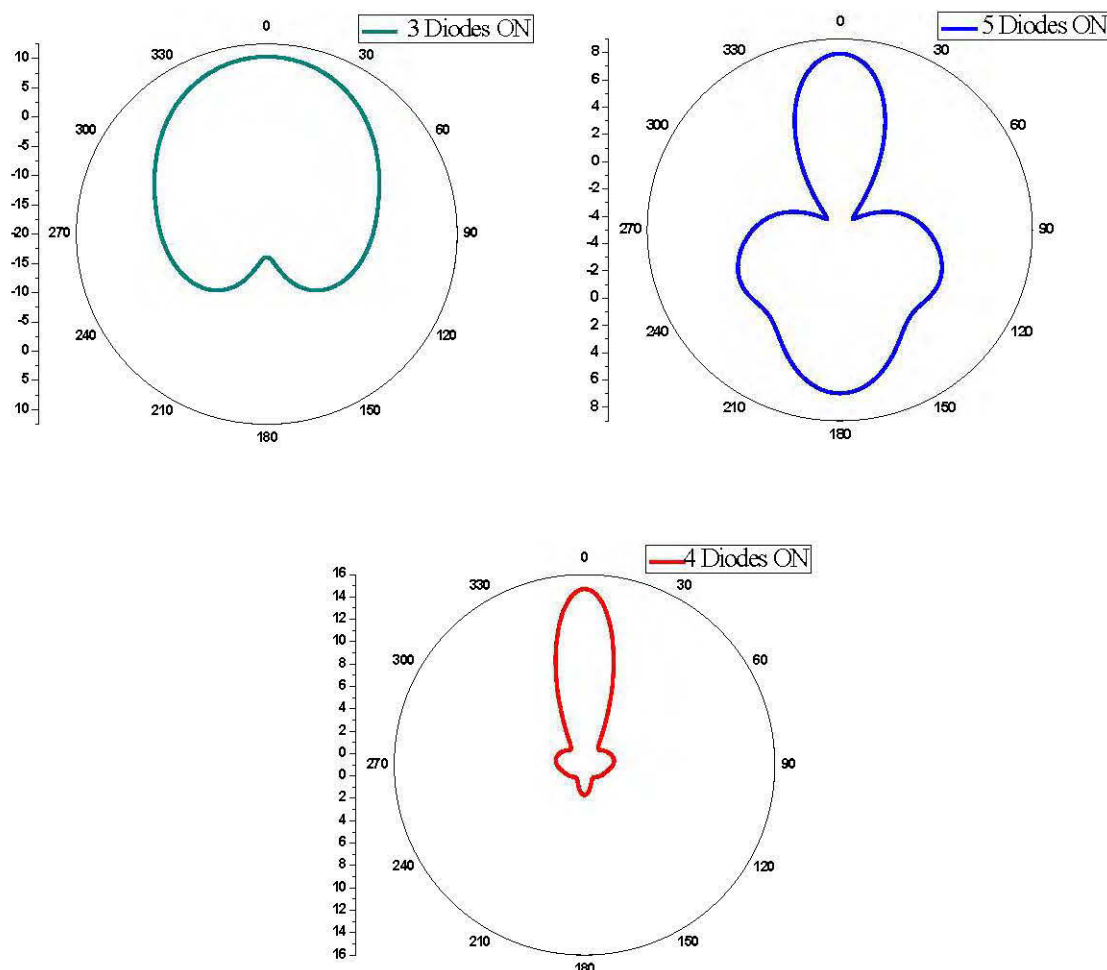
Figure 4.18: Directivity according to the opening angle



(a): for $\alpha = 90^\circ$, (b): for $\alpha = 120^\circ$, (c): for $\alpha = 150^\circ$.

Figure 4.19: S_{11} according to the opening angle

The level of back radiation is closely related to the periodic pitch, as evidenced by the curves in *Figure 4.13*. It is equally useful to note that this level also depends on the opening angle; indeed, a structure with a wide opening is less prone to successive reflections on its walls.



(a): for $\alpha = 90^\circ$, (b): for $\alpha = 120^\circ$, (c): for $\alpha = 150^\circ$.

Figure 4.20: Radiation pattern according to the opening angle

An additional constraint is invited when choosing the opening angle. The section relating to the frequency response of the structure has taught us that the cavity nature of the cylindrical structure had the effect of limiting the useful bandwidth by the amplification of the quality factor. On the other hand, an exaggerated opening angle has the effect of defatting the quality factor and widening the bandwidth of the structure. A multidimensional compromise is thus put in place, combining the cost of the structure and the level of back radiation (not periodic corresponding to the total number of elements), the desired gain (number of elements in ON states) and the frequency bandwidths of the device, adaptation and directivity (opening angle). To show the radiation pattern reconfigurability of the antenna in the azimuth plane, the simulated H-plane radiation

pattern for switching the beam is presented in *Figure. 4.21*. The present radiation patterns correspond to the diode-state configurations shown in *figure 4.22*.

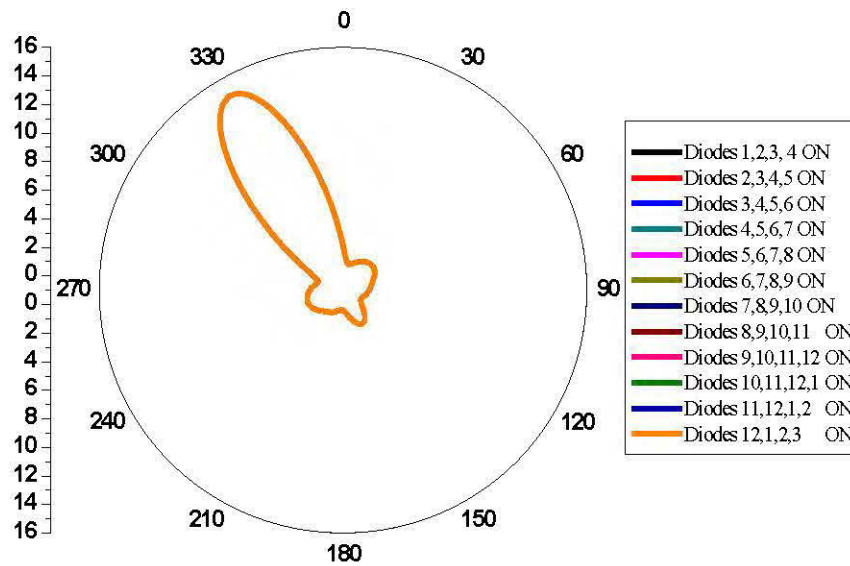


Figure 4.21: Switching beam in the all azimuth angles

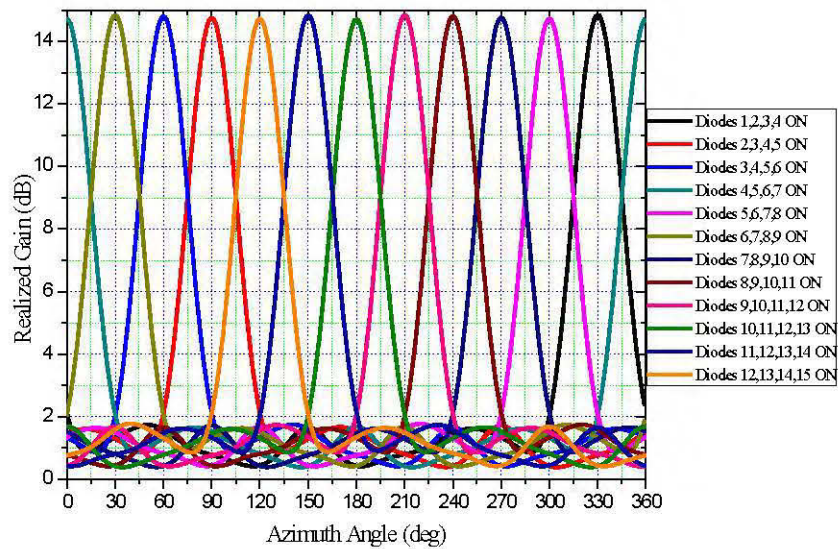


Figure 4.22 reconfiguration in the H-plane

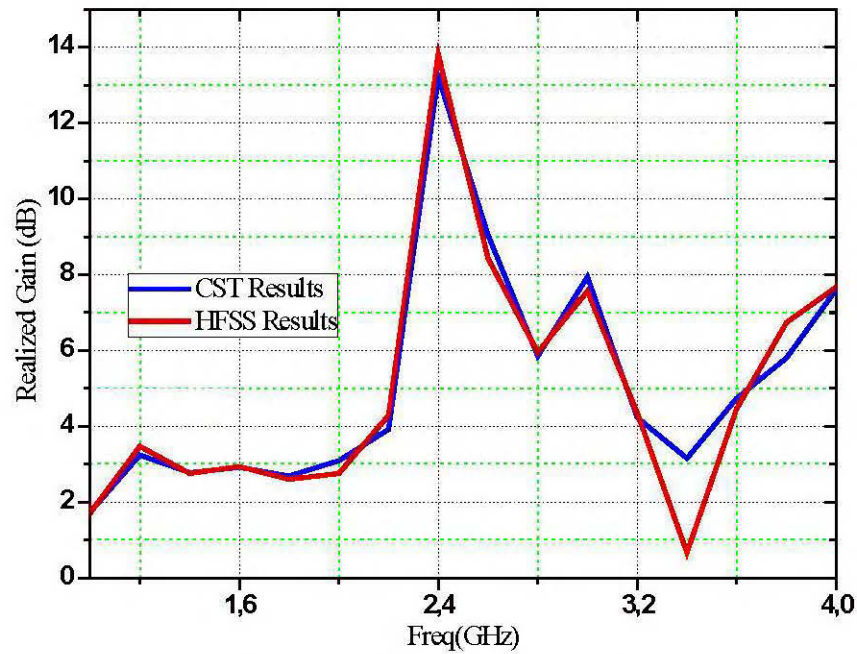


Figure 4.23. Realized gain of the ASBRA

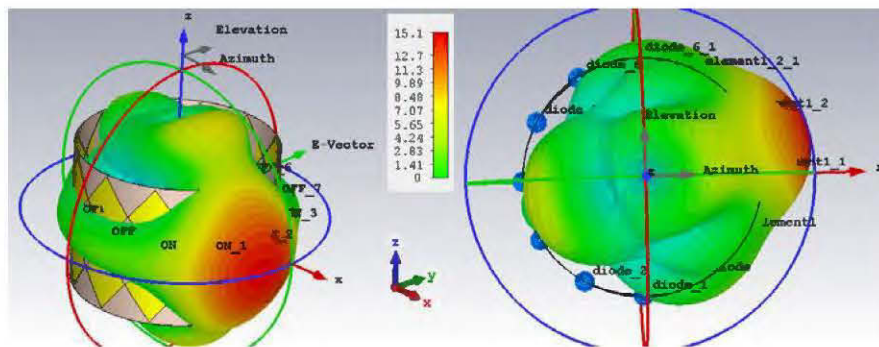


Figure 4.24 ASBRA radiation pattern in CST

As the fabricated prototype in the azimuth plane has cylindrical symmetry, it can be concluded that the other cases will give the same performance as the simulation. It is important to note that the beam spacing in the proposed antenna is equal to $\phi_{\text{FSS}} = 30^\circ$ and it is possible to obtain smaller beam size by optimizing the FSS design for a smaller ϕ_{FSS} .

4.4. Antenna Matching

When the states of diodes are changed from OFF to ON-state, the resonance of the cylindrical ABSRA changes the input impedance of the antenna; therefore, the reflection coefficient at the FSS port is changed. It means, if the antenna is designed to be matched in one state, it loses the matching in another state. The antenna can only be designed to

match the OFF state, while for the ON state, a matching circuit and switches are needed. Therefore, a matching circuit has been designed such that the proposed antenna can be matched for both states without any switching. *Figure 4.25* shows the antenna matching circuit. It is microstrip with a plane at the bottom. The substrate is RT / duroid 5870 with the $\epsilon_r = 2.33$ and $h = 0.8$ mm.

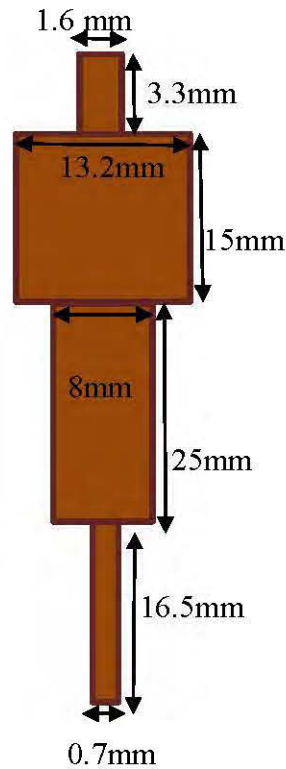


Figure 4.25 matching circuit.

Figure 4.26 shows the simulation for both states without and with matching circuit in the ground plane. As it can be seen, the antenna is matched at working frequency 2.45 GHz. The resonance of the antenna causes narrow bandwidth about 8%. The lower is possible if we design a matching circuit for each state separately.

Figure 4.27. shows that the antenna peak gain is about 14 dB at 2.45 GHz in the ON state and about 4 dB in the OFF state without the matching circuit and the antenna peak gain is about 11.5 dB at 2.45 GHz in the ON state and about 0 dB in the OFF state with the matching Circuit that gives the desired response in terms of realized gain [95].

In the fabricated prototype of the matching circuit, we need to take in consideration the drop in the antenna gain due mainly to the antenna losses including the metallization, substrate, and diodes loss.

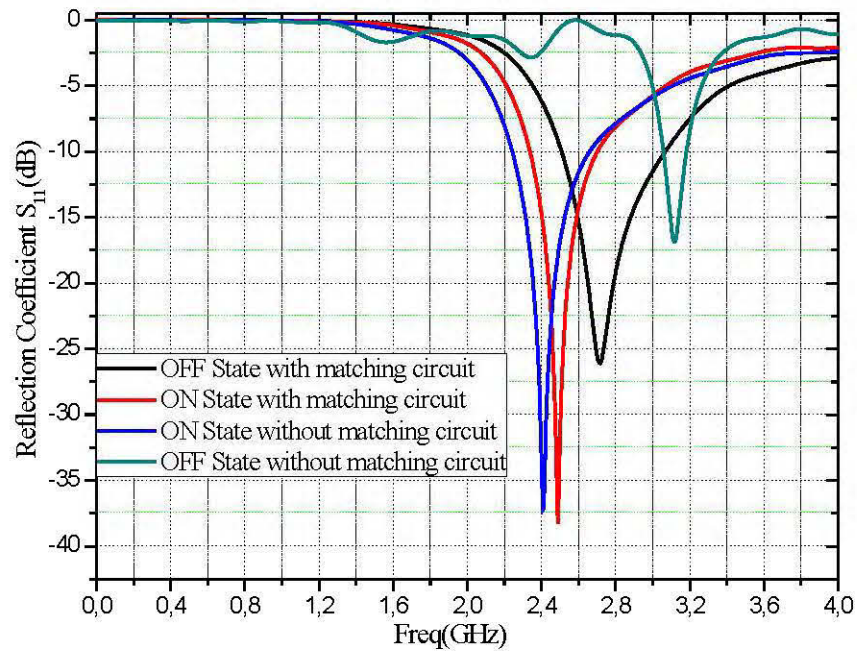


Figure 4.26. Return loss without and with matching circuit.

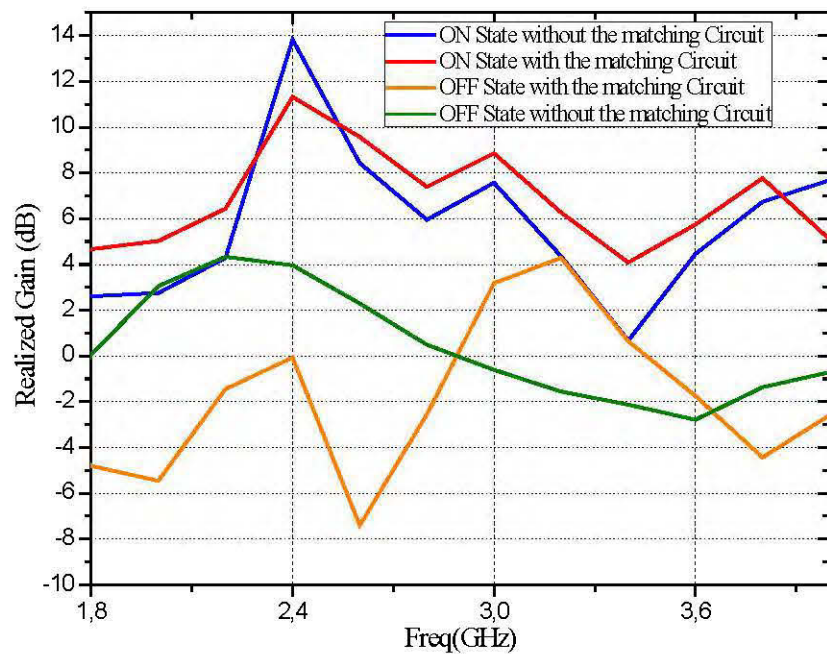
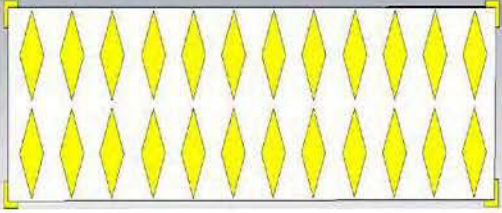


Figure 4.27. Realized gain without and with matching circuit.

4.5. Fabrication Process.

The fabrication process is an intermediate process between the simulation and measurement process. After obtaining such encouraging results in the simulation, the antenna needs to be fabricated in order to measure the real antenna. The wet etching technique was used in this

process. The fabrication process consists of several steps and these steps must be done carefully to get optimum results. *Table 4.6* shows the steps of fabrication process.

No	Picture	Explanation
1		<p>The design's layout was carried out from CST as Gerber files and was printed over transparency. The substrate that will be used is FR-4 board with photo resist layer.</p>
2		<p>Then, this layout will expose under ultraviolet (UV) light over FR-4 board. This step is doing under lightless condition in order to protect the photo resist layer.</p>
3	 	<p>After that, the structure is soaked and etched with the acid developer to remove the positive photo resist layer. This step also is doing under lightless condition.</p>
4	 	<p>Afterward, to remove the copper layer at unused region, the structure was etched using chemical acids. This is the last part of fabrication processes.</p>
5		<p>Then the verification on printed size of the substrate were compared with the designed one</p>

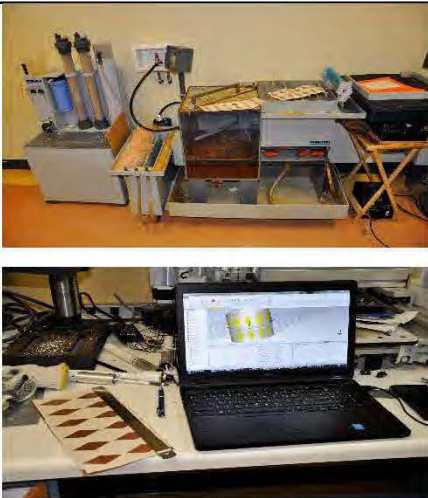
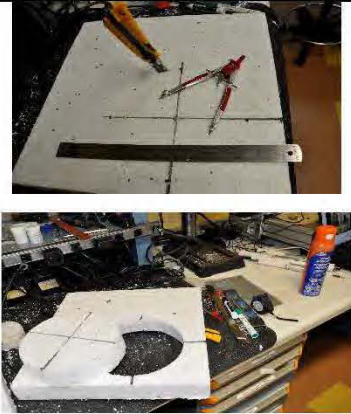
		
6		<p>The Foam were shaped to fill the cavity of the cylindrical out layer.</p>
7		<p>The drilling process with the size of the dipole, then lamination to get the full height of the cavity.</p>
8		<p>Lastly the assembling were made to match the overall ASBRA</p>

Table 4.6 steps of fabrication process

4.6. Measurement Process

After the fabrication process, the antenna is tested and measured to validate the simulation results such as return loss and the radiation pattern. All measurement processes have been done in the Université du Québec en Abitibi-Témiscamingue (UQAT) and at the Télébec underground communications research laboratory (LRTCS) in Val d-Or, Québec.

In order to carry out our measurements, the following materials are required.

4.6.1. Return loss measurements

The equipment that was used in this measurement is Vector Star MS4647A Microwave Vector Network Analyzer (VNA) shown in *Figure 4.28*. The MS4647A VNA is an instrument system that contains a built-in source, test set, and analyzer. Test results are displayed real time on a front panel touch screen or also to a separate video monitor. Screen captures can easily be printed or saved in common graphic file formats. [96]

The MS4647A VNAs provide a maximum frequency range from 70 kHz to 70 GHz for standalone VNAs. Through its front panel user interface, the instrument can be quickly configured to provide either:

- **25,000 Points**

MS4640A Series VNAs have up to 25,000 total test points available, with up to 16 channels, and each channel with up to 16 trace display graphs where each channel is configured as a virtual separate VNA. Each trace can have up to 12 standard markers and one reference marker.

- **100,000 Points**

The VNA can be configured with up to 100,000 total test points, limited to one channel with up to 16 trace display graphs. Each trace can have up to 12 standard markers and one reference marker



Figure 4.28. VectorStar MS4647A VNA Front Panel – Rear panel

The equipment was calibrated to ensure that the equipment gives precise results or in other words can reduce uncertainties during the measurement process. The calibration process is done by using the calibration kit by loading the open, short and broadband terminator. Further step to measure the input return loss for those antennas is to setup the start and stop the frequency range then measure the dipole alone as shown in *figure 4.28*. then finally measure the overall structure as shown in *figure 4.29*.

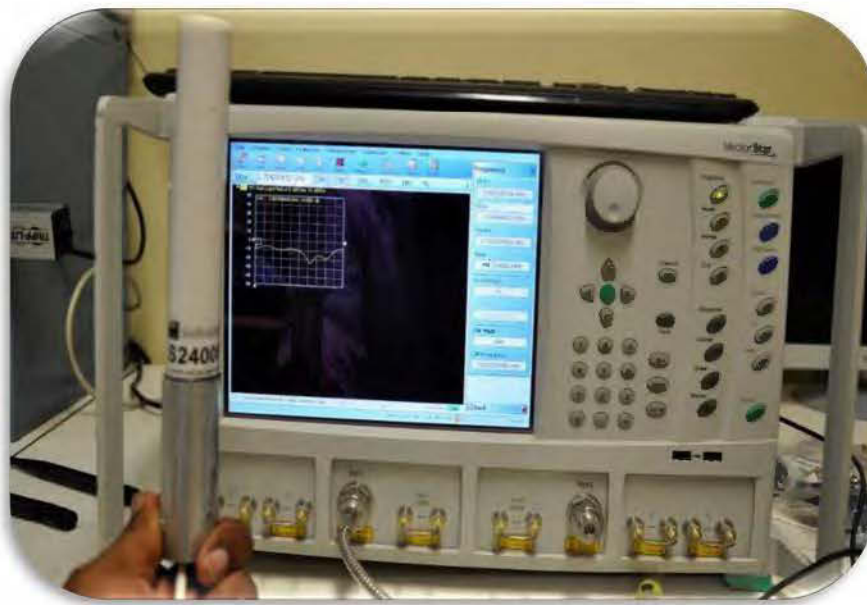


Figure 4.29. Measuring the S_{11} of the dipole alone

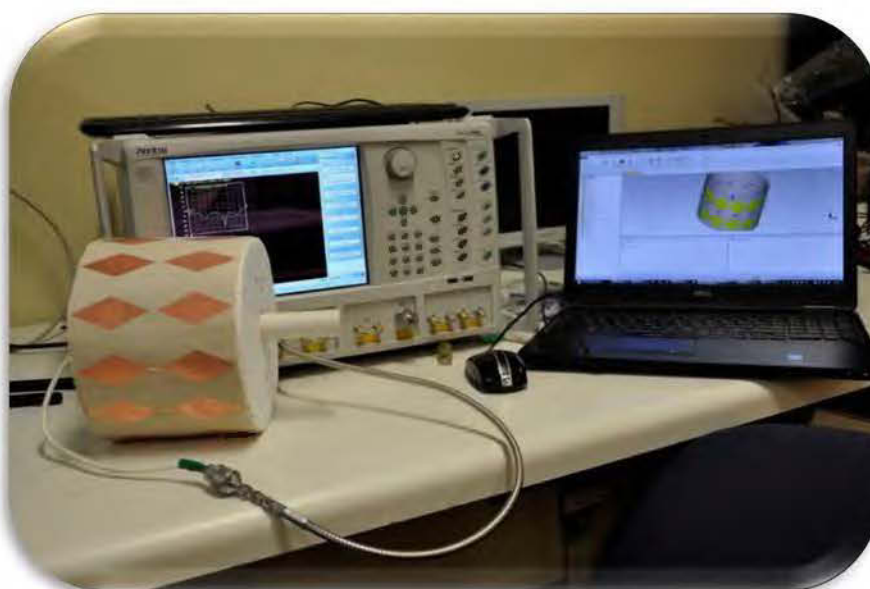


Figure 4.30. Measuring the S_{11} of overall structure

4.6.2. Radiation Pattern Measurement

The measurement of the realized gain of the antenna is conducted by comparing the antenna with the horn antenna as a reference. By lack of the anechoic chamber facilities in the university, the set-up is made in the laboratory as showed in *Figure 4.35* while *Figure 4.31* shows our reference set up picture of anechoic chamber. The proposed antenna is placed as the antenna under test (AUT) to measure the receiving power from the horn antenna. The antenna has been measured, and the power will be received in dBd [98] by varying the frequency range from 2 GHz to 7 GHz. The radiation pattern of the antenna was measured with a 360-degree rotator at the selected frequency bands in the E and H-plane.

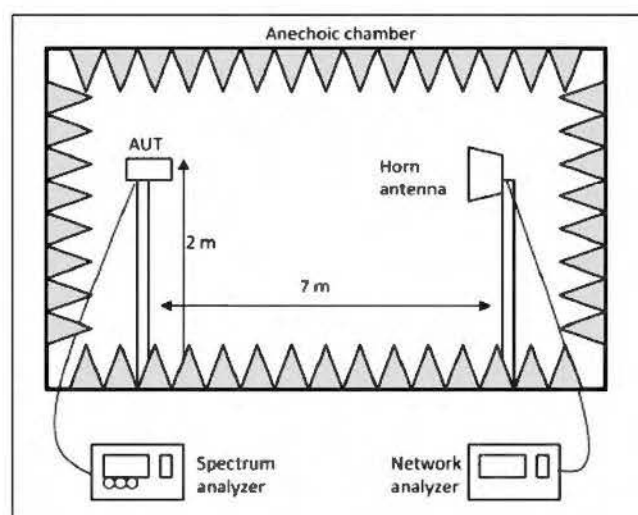


Figure 4.31 Power received and radiation pattern measurement set-up.

Two types of antennas were used during measurements. On the show, a directional antenna was used throughout the duration of the measurement. In reception, a directive and an omnidirectional were used. The omnidirectional antenna used in these measurements is the HGV2406 UB. It has an omnidirectional radiation pattern on the horizontal plane and covers a frequency band from 2.4 GHz to 2.5 GHz with a gain of 3 dBi. The following table presents its specifications. The directional antenna used is a DRG-118 / A. It is a horn antenna whose frequency band varies from 1 GHz to 18 GHz. It is manufactured by ARRA

The low noise amplifier (LNA-Low Noise Amplifier) used is the RLNA01M10G. This amplifier is an RF-Lambda product having a band of frequency from 0.1 GHz to 18 GHz with a nearly stable noise pattern all over the bandwidth. The effects introduced by this

amplifier are eliminated in the post-processing phase by removing from all measurements the measurement of the reference distance that has been taken at 1 m. The following table shows the parameters of LNA. [97]

Frequency (GHz)	Gain (dB)	Puissance maximum (dBm)
0.1-18	30	-16

Table 4.2. LNA Parameters RLNAOIMIOG



Figure 4-32 LNA RLNAOIMIOG

The Anritsu MG3692B RF/microwave signal generator offers the highest output power, best-in-class spectral purity, and fastest switching speed. The Anritsu MG3692B can provide guaranteed +23 dBm at 20 GHz with -94 dBc/Hz phase noise at 1 kHz offset while typically switching at 5 ms per point. This level of performance enables the verification the toughest spectral purity requirements, and greatly reduces test times.



Figure 4.33 Anritsu MG3692B

The Lab-volt 9506-00 Antenna Positioner consists of the mast for the receiving antenna (antenna under test), a drive motor, a signal detector, a variable attenuator, and a shaft encoder. The drive motor is used to rotate the mast while the rotation is controlled by the LVDAM-ANT software via the Data Acquisition Interface. An SMA connector, mounted on the base of the mast, allows a connection to be made between the receiving antenna and the signal detector. This detector provides a signal whose voltage depends on the level of the RF signal received. This signal is available on a connector for connection to the Data Acquisition Interface. The variable attenuator allows adjustments to be made to the sensitivity of the receiving system according to the strength of the received signal, in order to prevent system saturation. This attenuator is controlled by the LVDAM-ANT software via the Data Acquisition Interface. The shaft encoder is coupled with the shaft of the drive motor and provides signals to monitor the rotation of the mast. Two multi-pin connectors on the Antenna Positioner allow connection to the Data Acquisition Interface / Power Supply.



Figure 4.34 The Lab-volt 9506-00



Figure 4.35 The Lab-volt 9506-00 setup in the Laboratory

These different equipments used in the measurements affect (the effects of antennas, cables, amplifiers, etc.) the propagation channel measurements. Some effects are ignored or minimized. Generally, those who cannot be minimized are eliminated by calibration or post-treatment phase.

4.7. Summary

This chapter made it possible to analyze cylindrical structures. First, omnidirectional radiation sources have been developed to meet the need for beam uniformity, and its symmetry in the azimuth plane. Subsequently, a passive periodic structure consisting of a single layer continuous FSS elements was considered. The omnidirectional source was introduced into a cylinder formed by the FSS layer. The cylindrical geometry has been

retained to guarantee an axis of revolution perpendicular to the azimuth plane. It has been found that the radius of the cylindrical structure acts mainly on the frequency response of the antenna. The total number of FSS elements, and the angle of aperture, worked together on the frequency adaptation and the performances of directivity and the level of background radiation. The structures greater directivity, but a lower spectral uniformity. The more open structures, recalling reflector structures, offered a constant directivity as a function of frequency. In addition, Pin Diodes were then used as necessary in the radiating aperture. Their transparent/opaque nature has been exploited. It has been observed that a judicious choice of their gap dimensions could lead to a slight degradation of performance. However, the discontinuous elements affect the frequency of operation of the structure by translating it towards the high frequencies. Lastly, the effect of the active elements necessary for the agility of the beams has been studied. It was noted that the capacitance of the diodes was a critical parameter that had a degrading effect on both the frequency response of the structure as well as its directivity and its level of back radiation. It is therefore important to choose active elements with very low capacitance in order to reduce the necessary number.

The result of simulation and measurement will be discussed and analyzed in the next chapter.

CHAPTER FIVE

RESULT ANALYSIS AND DISCUSSION

5.1. Introduction

The measurement process is very important to validate the simulation result. This process is conducted after the fabrication process has been completed. In this chapter, the simulation result for the Adaptive Switched Beam Reconfigurable Antenna (ASBRA) is presented in terms of return loss, realized gain and radiation pattern. The measurement results are also presented in terms of return loss, realized gain, and radiation pattern. After that, both simulation and measurement results are compared, analyzed and discussed.

5.2. Analysis Result and Discussion of the ASBRA

The parametric study of the ASBRA has been done and presented in Chapter 4 in term of varying the scaling factor of several parameters such as cavity size, lumped elements specifications, type of substrate, band gap size the number of FSS elements... to study the behavior of antenna performance so that a good result in term of return loss and radiation pattern can be achieved. After simulation using CST software is done, the antenna was fabricated using FR-4 board using wet etching technique followed by measurement process. In this part, the simulated and measured results of the ASBRA are analyzed and compared. The photo of the fabricated antenna is shown in Figure 5.4. The overall size of the proposed antenna has a radius of 96.5 mm ($3\lambda/4$) on a substrate FR-4 with a thickness of 0.13 mm and a height of 154 mm.

5.2.1. Input Return Loss

Based on the simulation of the ABSRA software using the CST software, the antenna return loss is less than -10 dB from 2.35 GHz to 2.55 GHz or a bandwidth of 8, 17 % according to the formula in (2.10). The result of the simulation is then validated by comparing with the measurement results. The return loss measurement is performed using the *VectorStar MS4647A VNA*. The *Figure 5.1* shows the comparison of simulated and measured feedback loss for ASBRA antenna. The result of the measurement shows a good agreement between the results of the simulation. The measurement shows that the antenna can operate from 2.35 GHz to 2.65 GHz or 12 % bandwidth compared to -10 dB.

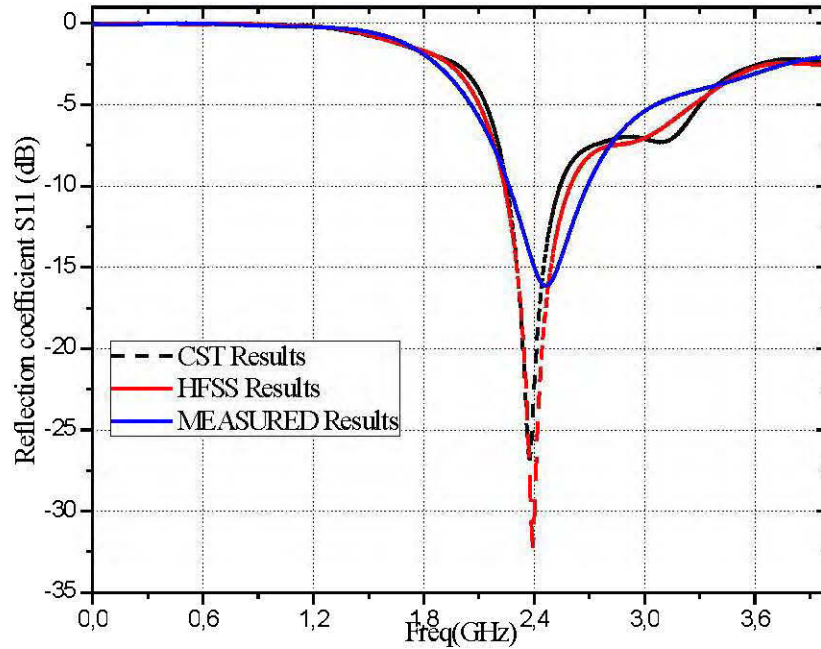


Figure 5.1. Simulated and measured return loss for the ASBRA

$$BW \% = \frac{f_u - f_l}{\sqrt{f_u \times f_l}} \times 100\% \quad (5.1)$$

where:

f_u = upper frequency bandwidth

f_l = lower frequency bandwidth

$$BW(\text{Simulated}) \% = \frac{2.5 - 2.35}{\sqrt{(2.5 \times 2.35)}} \times 100\% = 8.17\%$$

$$BW(\text{Measured}) \% = \frac{2.65 - 2.35}{\sqrt{(2.65 \times 2.35)}} \times 100\% = 12\%$$

The comparison of the simulated and measured loss of efficiency for the ASBRA is shown in Table 5.1.

Parameters	Simulated	Measured
Lower frequency f_l	2.35	2.35
Upper frequency f_u	2.5	2.65
Bandwidth (GHz)	0.15	0.3
Bandwidth (%)	8.47	12

Table 5.1 Comparison of frequency bandwidth between simulation and measurement

Comparing the beam-widths in figure 5.1; it reveals a noticeable difference only for the H-plane pattern. Since the effect of active elements and other losses are considered in the fabricated prototype, this difference basically can be interpreted by the measured gain reduction. This technically confirms the frequency agility of the ASBRA.

5.2.2. Realized Gain

The gain of the antenna is measured using the gain comparison method. The simulated and measured realized gain for the ASBRA with 4 diodes in the ON state are plotted in Figure 5.2. It is shown that the antenna has a good gain at 2.45 GHz for each state. It is worth mentioning that the realized gain for this antenna is about 9.8 dBd for the measured results and 13.8 dB for the simulated results in the ON states and it is 0 dB and 4 dB respectively in the OFF state.

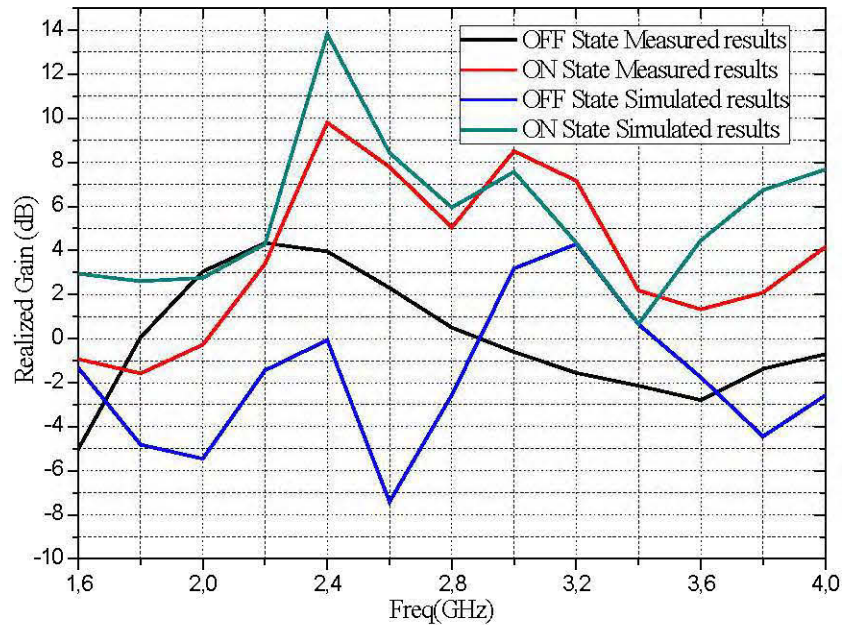


Figure 5.2 Realized gain results for measured and simulated ASBRA

The measurement of received gain of ASBRA is conducted by comparing the ASBRA antenna with the horn antenna as a reference. The measurement set-up is not in the anechoic chamber, so we consider the environment effect by measuring first the dipole alone (*Figure 5.3*) then we measured the all structure (*Figure 5.4*) and finally we divide the vector results using Matlab and Origin pro software to get the final results in dBd (dB referred to a reference dipole antenna) without environmental effect.

It is important to note that the antenna gain is then a measure of the amount of focus that an antenna can apply to the incoming signal relative to one of two reference dispersion patterns [98]. The dBi is the amount of focus applied by an antenna with respect to an "Isotropic Radiator" (a dispersion pattern that radiates the energy equally in all directions onto an imaginary sphere surrounding a point source). Thus an antenna with 2.1 dBi of gain focuses the energy so that some areas on an imaginary sphere surrounding the antenna will have 2.1 dB more signal strength than the strength of the strongest spot on the sphere around an Isotropic Radiator. The dBd refers to the antenna gain with respect to a reference dipole

antenna. A reference dipole antenna is defined to have 2.15 dBi of gain. So converting between dBi and dBd is as simple as adding or subtracting 2.15 according to these formulas:

- $\text{dBi} = \text{dBd} + 2.15$
- $\text{dBd} = \text{dBi} - 2.15$

Specifying antenna gain in dBd means that the antenna in question has the ability to focus the energy x dB more than a dipole.

In our case the realized gain of the measured ASBRA will be $9.8 \text{ dB} + 2.15 = 11.95 \text{ dBi}$.

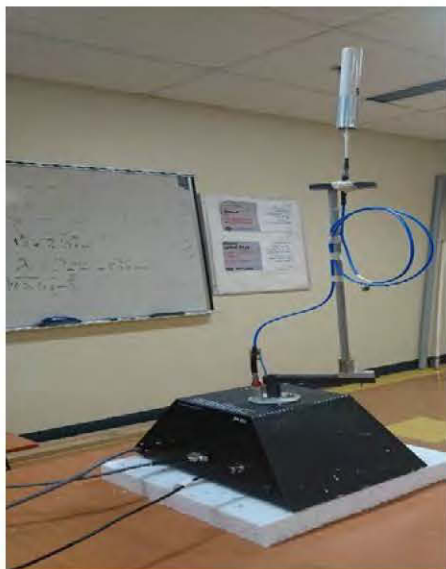


Figure 5.3 Measuring the dipole alone structure

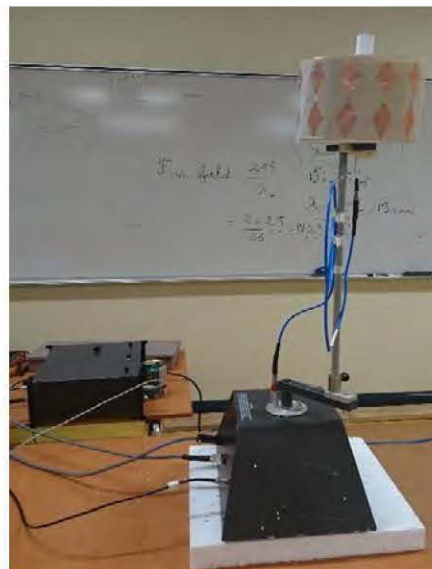


Figure 5.4 Measuring the all structure

The final setup is the same as the radiation pattern setup as discussed in Chapter 4. The ASBRA is placed as the antenna under test (AUT) in ON and OFF mode to measure its receiving power from the horn antenna as a reference antenna with gain of 15 dBi over the range from 0.7 GHz until 18 GHz. The power received in dBm by varying the frequency range from 2 GHz to 7GHz. To evaluate the reconfiguration functionality from directional to omnidirectional case across the operating frequency band, the antenna radiation-patterns are measured when all active elements on the FSS screen are switched ON or OFF, respectively. For the sake of comparison, the measured gain of dipole antenna is provided in *Figure. 5-5*

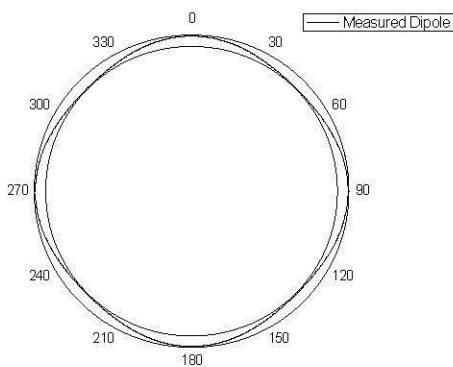


Figure 5.5 Radiation pattern of the dipole Figure

It is observed in figure 5. 6 that the measured radiation pattern has a similar pattern with the simulated and has a directional radiation pattern.

As the fabricated prototype in the azimuth plane has cylindrical symmetry, it can be concluded that the other cases will give the same performance as the simulation.

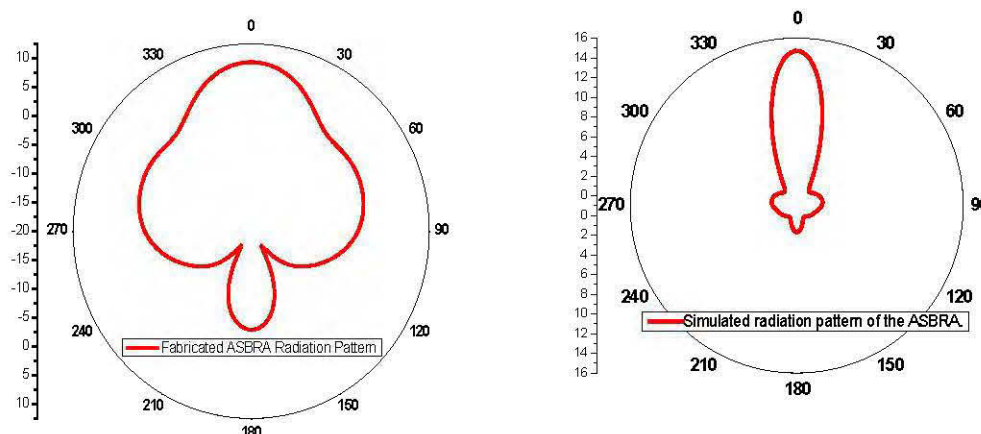


Figure 5.6 Radiation pattern of the Simulated and the Fabricated ASBRA

The simulated and measured results of the ASBRA have been presented and discussed. The simulated result such as return loss, realized gain and radiation pattern has been clearly presented. Then, the measurement process has been done to validate the simulated results and both results have been compared to each other in terms of return loss, received power and radiation pattern. The results show a good agreement between simulated and measurement values.

A summary of achieve results of the ASBRA has been compared to the reconfigurable antennas presented in Table. 5-2, demonstrating the improvements obtained by the earlier proposed antenna.

Table 5.2 Previous researches on reconfigurable antenna

	Title / Authors	Type of reconfigurable Antenna	Back lobe	Bandwidth	Gain	Implementation with real switching
1	Adaptive switched beam reconfigurable antenna for wireless sensor network applications.	Radiation pattern using FSS	- 7 dB	150 MHz	15 dBi	No/Using PEC pad
2	Beam-switching antenna based on active frequency selective surfaces [99]	Radiation pattern using FSS	- 16 dB	400 MHz	11 dBi	No/Using ideal case
3	Electronically sweeping-beam antenna using a new cylindrical frequency-selective surface [100]	Radiation pattern using FSS	- 20 dB	400 MHz	6 dBi	Yes by using PIN diodes
4	Cylindrical slot FSS configuration for beam-switching applications [101]	Radiation pattern using FSS	- 12 dB	0.7-2.7 GHz	8.7 dBi	Yes by using PIN diodes
5	Beam switching antenna based on active frequency selective surfaces [102]	Radiation pattern using FSS	- 12.5dB	500 MHz	12.5 dBi	Yes by using PIN diodes
6	A reconfigurable beam-switching antenna base on active FSS [103]	Radiation pattern using FSS	- 9.5 dB	150 MHz	5 dBi	Yes by using PIN diodes
7	Beam-Switching Antenna with a New Reconfigurable Frequency Selective Surface [104]	Sectoral antenna using FSS	- 14 dB	300 MHz	9.8 dBi	Yes by using PIN diodes
8	High-Gain Reconfigurable Sectoral Antenna Using an Active Cylindrical FSS Structure [105]	Sectoral antenna using FSS	- 13 dB	200 MHz	12 dBi	Yes by using PIN diodes

CHAPTER SIX

CONCLUSION

6.1. Conclusion

The objective of this dissertation were to study, develop and measure an adaptive reconfigurable switched beam antenna (ASBRA) for WSN application intending to enhance the communication performance between nodes in locations difficult to access. The reconfigurable antenna is a promising and an appropriate type of antenna, where through the use of appropriate switches, the antenna can be structurally reconfigured and its resonant dimensions maintained for desired frequency bands. Therefore; the development of the ASBRA has been presented and discussed from the design process, manufacturing process until measurement process. The introduction of the ASBRA including a reconfigurable field study is also presented in addition to the significance of the research objective and the research scopes. These were all explained in detail and the successful outcome of this research is a result of plentiful literature in this particular field, thus we have a better understanding of the ASBRA development. In addition, the concept and the operating behavior of ASBRA have been presented and discussed with the assistance of appropriate figures and tables. To analyze the proposed antenna, numerical simulations were carried out with CST microwave studio which is based on the finite integration method. For comparison and validation of the optimized results, Ansoft HFSS based on the finite element method is also used and which has many applications and bring benefits to researcher for the performance and characteristic of the antenna can be analyzed before proceeding to the manufacturing process besides reducing time wastage.

The design and flow chart of the ASBRA were discussed. The detailed dimension of the ASBRA is included in the simulation process inset feed line and the distance between adjacent patch, which are simulated in order to produce a better result. The design of the ASBRA was then integrated with lumped elements and PIN diode switches to reconfigure the operating frequency from wideband operation to narrow band operation. In the simulation process, two methods to represent the PIN diode which are using lumped element and PEC pad were discussed with some results. Then, the adaptive circuit and DC line were used to compensate the bias of the diode.

The ASBRA was fabricated using wet etching technique on a FR-4 substrate with presented details on manufacturing processes then measured to validate the simulation

results in return of loss, gain and radiation pattern. However, the antenna could be configured in the Azimuth plane with narrowband depending on its application. In addition, a good agreement between measurement and simulation results, antenna gain and radiation pattern were achieved. The results of the antennas are discussed in the graph and tables for better viewing. The ASBRA has saved weight, space and money.

6.2. Key Contribution

The development of the ASBRA has been studied and its performance is analyzed. After hard work on the antenna's development, two key contributions were verified:

1. The performance of narrowband ASBRA is improved by integrating RF switch to have reconfigurability operation.
2. A reconfigurable antenna is design based on real circuit modeling of PIN diode in simulation process using CST software tools. This contribution is replacing the other method by using ideal case which the simulation results are not similar to the measurement results.

6.3. Future Research

In this thesis, some research work has been carried out on the single layer planar and conformal reconfigurable frequency selective surfaces for antenna applications. However, not fully covered in this limited work, some other interesting investigations in this area are still left for future research topics:

1. One of the limitations of this project is that the PIN diode can be operated up to limited capacitance values. The use of high-frequency microstrip could be applied for future research and different technique of feeding such aperture slots can be studied to reduce the effect of PIN diode towards the antenna's performance. Hence, the antenna can operate at a very narrowband operation and it might reduce the size of the antenna.
2. Antenna radiation topology can be interesting future research topic. In this thesis, the antenna radiation-pattern is sweeping only the azimuth angles and it deals with vertical polarized waves. Changing the radiation mechanism to sweep the elevation angles, handling both vertical and horizontal polarizations and proposing a particular method to increase antenna gain by a minimum cylinder height can be recognized as other future research topics in the reconfigurable antenna.

REFERENCES

- [1] Mahmood, S. M., & Denidni, T. A. (2015, July). A novel three-dimensional wideband active frequency selective surface unit-cell. *Antennas and Propagation & USNC/URSI National Radio Science Meeting, IEEE International Symposium on* (pp. 1256-1257). Vancouver, Canada.
- [2] Mahmood, S. M., & Denidni, T. A. (2016, July). Design and implementation of substrate-free frequency selective surfaces. In *Antenna Technology and Applied Electromagnetics (ANTEM), 17th International Symposium on* (pp. 1-2). Montreal, Canada.
- [3] Akyildiz, I. F., & Vuran, M. C. (2010, July). *Wireless sensor networks* (Vol. 4). John Wiley & Sons. (pp. 520-521).
- [4] Akyildiz, I. F., Su, W., Sankarasubramaniam, Y., & Cayirci, E. (2002). A survey on sensor networks. *IEEE Communications magazine*, 40(8), (pp. 102-114).
- [5] Wagner, R. S. (2010, March). Standards-based wireless sensor networking protocols for spaceflight applications. *Aerospace Conference*, (pp. 1-7). Dallas, USA.
- [6] Zhang, S., & Zhang, H. (2012, August). A review of wireless sensor networks and its applications. In *Automation and Logistics (ICAL), IEEE International Conference on* (pp. 386-389). Zhengzhou, China.
- [7] Younis, M., & Akkaya, K. (2008). Strategies and techniques for node placement in wireless sensor networks: A survey. *Ad Hoc Networks*, 6(4), (pp. 621-655).
- [8] Tuna, G., Mumcu, T. V., Gulez, K., Gungor, V. C., & Erturk, H. (2012, July). Unmanned aerial vehicle-aided wireless sensor network deployment system for post-disaster monitoring. *International Conference on Intelligent Computing* (pp. 298-305). Springer, Berlin, Heidelberg.
- [9] Senouci, M. R., Mellouk, A., Senouci, H., & Aissani, A. (2012). Performance evaluation of network lifetime spatial-temporal distribution for WSN routing protocols. *Journal of Network and Computer Applications*, 35(4), (pp. 1317-1328).
- [10] Alazzawi, L. K., Elkateeb, A. M., Ramesh, A., & Aljuhar, W. (2008, March). Scalability analysis for wireless sensor networks routing protocols. *Advanced Information Networking and Applications-Workshops. AINAW 2008. 22nd International Conference on* (pp. 139-144). Okinawa Japan.

- [11] Gilbert, J. M., & Balouchi, F. (2008). Comparison of energy harvesting systems for wireless sensor networks. *International Journal of automation and computing*, 5(4), (pp. 334-347).
- [12] Đurišić, M. P., Tafa, Z., Dimić, G., & Milutinović, V. (2012, June). A survey of military applications of wireless sensor networks. *Embedded Computing (MECO), Mediterranean Conference on* (pp. 196-199). Bar, Monténégro.
- [13] Lee, S. H., Lee, S., Song, H., & Lee, H. S. (2009, October). Wireless sensor network design for tactical military applications: Remote large-scale environments. *Military communications conference. MILCOM. IEEE* (pp. 1-7). Boston, USA.
- [14] Hussain, M. A., & kyung Sup, K. (2009, February). WSN research activities for military application. In *Advanced Communication Technology. ICACT. 11th International Conference on* (Vol. 1, pp. 271-274). Phoenix Park, Dublin.
- [15] Sohraby, K., Minoli, D., & Znati, T. (2007). *Wireless sensor networks: technology, protocols, and applications*. John Wiley & Sons. ISBN 978-0-471-74300-2.
- [16] Alam, M. S., & Abbosh, A. (2016). Planar pattern reconfigurable antenna with eight switchable beams for WiMax and WLAN applications. *IET Microwaves, Antennas & Propagation*, 10(10), (pp. 1030-1035).
- [17] Bona, M., Manholm, L., Starski, J. P., & Svensson, B. (2002, September). Low-loss compact Butler matrix for a microstrip antenna. *IEEE Transactions on Microwave Theory and Techniques*, 50(9), (pp. 2069-2075).
- [18] Bouslama, M., Traii, M., Denidni, T. A., & Gharsallah, A. (2016). Beam-switching antenna with a new reconfigurable frequency selective surface. *IEEE Antennas and Wireless Propagation Letters*, 15, (pp. 1159-1162).
- [19] Balanis, C. A., & Ioannides, P. I. (2007). Introduction to smart antennas. *Synthesis Lectures on Antennas*, 2(1), (pp. 1-175).
Online: <https://doi.org/10.2200/S00079ED1V01Y200612ANT005>
- [20] Capolino, F. (2009). *Theory and phenomena of metamaterials*. CRC press. ISBN 13: 978-1-4200-5426-2, 2009.

- [21] Boutayeb, H. (2003, December). *Etude des structures périodiques planaires et conformes associées aux antennes. Application aux communications mobiles* (Doctoral dissertation no 2942, Université Rennes 1).
- [22] Balanis, C. A., & Ioannides, P. I. (2007). Introduction to smart antennas. *Synthesis Lectures on Antennas*, 2(1), (pp. 1-175).
- [23] Balanis, C. A. (2005). *Antenna Theory: Analysis and Design*” Third edition John Wiley & Sons. Inc. ISBN 0-471-60639-1, (pp. 170).
- [24] Maxwell, J. C. (1881). *A treatise on electricity and magnetism* (Vol. 1). Clarendon press.
- [25] David M. P., (1998) *Microwave Engineering*, 2nd Edition, John Wiley & Sons, Inc., ISBN 0-471-17096-8, (pp. 66-68).
- [26] Balanis, C. A. (2005). *Antenna Theory: Analysis and Design*” Third edition John Wiley & Sons. Inc. ISBN 0-471-60639-1, (pp. 28).
- [27] Krauss, J. D. (1998). *Antennas 2ed.*, (pp. 42-43).
- [28] Institute of Electrical and Electronics Engineers. (1983, June). *IEEE Standard Definitions of Terms for Antennas*. (pp. 15) New York, USA.
- [29] Institute of Electrical and Electronics Engineers. (1983, June). *IEEE Standard Definitions of Terms for Antennas*. (pp. 15) New York, USA.
- [30] Balanis, C. (1997). Aperture antennas. *Antenna Theory, Analysis and Design*, (pp. 575-597).
- [31] Niroo-Jazi, M. (2012, June). *Nimble Radiation-Pattern Antennas Using Agile Frequency Selective Surfaces* (Doctoral dissertation, Université du Québec, Institut national de la recherche scientifique). Montréal, Canada.
- [32] Christodoulou, C. G., Tawk, Y., Lane, S. A., & Erwin, S. R. (2012, July). Reconfigurable antennas for wireless and space applications. *Proceedings of the IEEE*, 100(7), (pp. 2250-2261).
- [33] Alkanhal, M. A., & Sheta, A. F. (2007). A novel dual-band reconfigurable square-ring microstrip antenna. *Progress In Electromagnetics Research*, 70, (pp. 337-349).
- [34] Ismail, M. F., Rahim, M. K. A., Zubir, F., & Ayop, O. (2011, April). Log-periodic patch antenna with tunable frequency. *Antennas and Propagation (EUCAP), Proceedings of the 5th European Conference on* (pp. 2165-2169). Rome, Italy.
- [35] Chen, K. H., Wu, S. J., Kang, C. H., Chan, C. K., & Tarng, J. H. (2009, December). A frequency reconfigurable slot antenna using PIN diodes. *Microwave Conference. APMC. Asia Pacific* (pp. 1930-1933). Singapore.

- [36] Yang, X. S., Wang, B. Z., Wu, W., & Xiao, S. (2007). Yagi patch antenna with dual-band and pattern reconfigurable characteristics. *IEEE Antennas and Wireless Propagation Letters*, 6, (pp. 168-171).
- [37] Monti, G., Corchia, L., & Tarricone, L. (2009). Patch antenna with reconfigurable polarization. *Progress In Electromagnetics Research*, 9, (pp. 13-23).
- [38] Wei, W. B., Liu, Q. Z., Yin, Y. Z., & Zhou, H. J. (2007). Reconfigurable microstrip patch antenna with switchable polarization. *Progress In Electromagnetics Research*, 75, (pp. 63-68).
- [39] Parihar, M. S., Basu, A., & Koul, S. K. (2009, December). Polarization reconfigurable microstrip antenna. *Microwave Conference, 2009. APMC 2009. Asia Pacific* (pp. 1918-1921). Singapore.
- [40] Radi, Y., Nikmehr, S., & Pourziad, A. (2011). A novel bandwidth enhancement technique for X-band RF MEMS actuated reconfigurable reflectarray. *Progress Electromagnetics Research*, 111, (pp. 179-196).
- [41] Ali, M. T., Rahman, T. A., Kamarudin, M. R., Md Tan, M. N., & Sauleau, R. (2009). A planar antenna array with separated feed line for higher gain and sidelobe reduction. *Progress In Electromagnetics Research*, 8, (pp. 69-82).
- [42] Sun, B. H., Zhou, S. G., Wei, Y. F., & Liu, Q. Z. (2010). Modified two-element Yagi-Uda antenna with tunable beams. *Progress In Electromagnetics Research*, 100, (pp. 175-187).
- [43] Nikolaou, S., Bairavasubramanian, R., Lugo, C., Carrasquillo, I., Thompson, D. C., Ponchak, G. E., ... & Tentzeris, M. M. (2006, February). Pattern and frequency reconfigurable annular slot antenna using PIN diodes. *IEEE Transactions on Antennas and Propagation*, 54(2), (pp. 439-448).
- [44] Ou Yang, J. (2008). A novel radiation pattern and frequency reconfigurable microstrip antenna on a thin substrate for wide-band and wide-angle scanning application. *Progress In Electromagnetics Research*, 4, (pp.167-172).
- [45] Huff, G. H., Feng, J., Zhang, S., & Bernhard, J. T. (2003, February). A novel radiation pattern and frequency reconfigurable single turn square spiral microstrip antenna. *IEEE Microwave and Wireless Components Letters*, 13(2), (pp. 57-59).
- [46] Niroo-Jazi, M. (2012). *Nimble Radiation-Pattern Antennas Using Agile Frequency Selective Surfaces* (Doctoral dissertation, Université du Québec, Institut national de la recherche scientifique). (pp. 76)
- [47] Huff, G. H., & Bernhard, J. T. (2006). Integration of packaged RF MEMS switches with radiation pattern reconfigurable square spiral microstrip antennas. *IEEE Transactions on Antennas and Propagation*, 54(2), (pp. 464-469).

- [48] Erdil, E., Topalli, K., Unlu, M., Civi, O. A., & Akin, T. (2007, April). Frequency tunable microstrip patch antenna using RF MEMS technology. *IEEE transactions on antennas and propagation*, 55(4), (pp. 1193-1196).
- [49] Sarrazin, J., Mahé, Y., Avrillon, S., & Toutain, S. (2009, February). Pattern reconfigurable cubic antenna. *IEEE Transactions on Antennas and Propagation*, 57(2), (pp. 310-317).
- [50] Oh, S. S., Jung, Y. B., Ju, Y. R., & Park, H. D. (2010, September). Frequency-tunable open-ring microstrip antenna using varactor. *Electromagnetics in Advanced Applications (ICEAA), 2010 International Conference on* (pp. 624-626). Australia.
- [51] Antonino-Daviu, E., Cabedo-Fabres, M., Ferrando-Bataller, M., & Vila-Jimenez, A. (2007, August). Active UWB antenna with tunable band-notched behaviour. *Electronics Letters*, 43(18), (pp. 959-960).
- [52] Tawk, Y., Albrecht, A. R., Hemmady, S., Balakrishnan, G., & Christodoulou, C. G. (2010). Optically pumped frequency reconfigurable antenna design. *IEEE antennas and wireless propagation letters*, 9, (pp. 280-283).
- [53] Tawk, Y., Albrecht, A. R., Hemmady, S., Balakrishnan, G., & Christodoulou, C. G. (2010). Optically pumped frequency reconfigurable antenna design. *IEEE antennas and wireless propagation letters*, 9, (pp. 280-283).
- [54] Tawk, Y., Costantine, J., Barbin, S. E., & Christodoulou, C. G. (2011, October). Integrating laser diodes in a reconfigurable antenna system. *Microwave & Optoelectronics Conference (IMOC), SBMO/IEEE MTT-S International* (pp. 794-796). Natal, Brazil.
- [55] Mazlouman, S. J., Soleimani, M., Mahanfar, A., Menon, C., & Vaughan, R. G. (2011, February). Pattern reconfigurable square ring patch antenna actuated by hemispherical dielectric elastomer. *Electronics Letters*, 47(3), (pp. 164-165).
- [56] Tawk, Y., Costantine, J., & Christodoulou, C. G. (2010, July). A frequency reconfigurable rotatable microstrip antenna design. *Antennas and Propagation Society International Symposium (APSURSI), IEEE* (pp. 1-4). Toronto, Canada.
- [57] Hu, W., Ismail, M. Y., Cahill, R., Encinar, J. A., Fusco, V. F., Gamble, H. S., ... & Rea, S. P. (2007, July). Liquid-crystal-based reflectarray antenna with electronically switchable monopulse patterns. *Electronics Letters*, 43(14).
- [58] Haupt, R. L., & Lanagan, M. (2013, February). Reconfigurable antennas. *IEEE Antennas and Propagation Magazine*, 55(1), (pp. 49-61).
- [59] Grant, P. D., Denhoff, M. W., & Mansour, R. R. (2004, August). A comparison between RF MEMS switches and semiconductor switches. In *MEMS, NANO and Smart Systems, 2004. ICMENS 2004. Proceedings. International Conference on* (pp. 515-521). Alberta, Canada.

- [60] Christodoulou, C. G., Tawk, Y., Lane, S. A., & Erwin, S. R. (2012, July). Reconfigurable antennas for wireless and space applications. *Proceedings of the IEEE*, 100(7), (pp. 2250-2261).
- [61] Rappaport, T. S. (1996). *Wireless communications: principles and practice* (Vol. 2). New Jersey: prentice hall PTR. ISBN: 0-7803-1167-1, (pp. 48-49).
- [62] Engheta, N., & Ziolkowski, R. W. (Eds.). (2006). *Metamaterials: physics and engineering explorations*. John Wiley & Sons. ISBN 13978-0-471-76102-0, (pp. 10-13)
- [63] Niroo-Jazi, M. (2012). *Nimble Radiation-Pattern Antennas Using Agile Frequency Selective Surfaces* (Doctoral dissertation, Université du Québec, Institut national de la recherche scientifique). (pp. 176)
- [64] Eleftheriades, G. V., & Balmain, K. G. (2005). *Negative-refraction metamaterials: fundamental principles and applications*. John Wiley & Sons. ISBN 13: 978-0-471-60146-3
- [65] Rassokhina, Y. V., & Krizhanovski, V. G. (2009). Periodic structure on the slot resonators in microstrip transmission line. *IEEE Transactions on Microwave Theory and Techniques*, 57(7), (pp. 1694-1699).
- [66] Garcia-Garcia, J., Bonache, J., & Martin, F. (2006). Application of electromagnetic bandgaps to the design of ultra-wide bandpass filters with good out-of-band performance. *IEEE Transactions on Microwave Theory and Techniques*, 54(12), (pp. 4136-4140).
- [67] Abhari, R., & Eleftheriades, G. V. (2003). Metallo-dielectric electromagnetic bandgap structures for suppression and isolation of the parallel-plate noise in high-speed circuits. *IEEE Transactions on Microwave Theory and Techniques*, 51(6), (pp. 1629-1639).
- [68] Munk, B. A. (2005). *Frequency selective surfaces: theory and design*. John Wiley & Sons. ISBN 0-471-37047-9. Pp130-133
- [69] Moustafa, L., & Jecko, B. (2010). Design of a wideband highly directive EBG antenna using double-layer frequency selective surfaces and multifeed technique for application in the Ku-band. *IEEE Antennas and Wireless Propagation Letters*, 9, (pp. 342-346).
- [70] Brillouin, L. (2003). *Wave propagation in periodic structures: electric filters and crystal lattices*. Courier Corporation. (pp. 249)

- [71] Boutayeb, H. (2003, December). *Etude des structures périodiques planaires et conformes associées aux antennes. Application aux communications mobiles* (Doctoral dissertation n0 2942, Université Rennes 1).
- [72] Joannopoulos, J. D., Johnson, S. G., Winn, J. N., & Meade, R. D. (2011). *Photonic crystals: molding the flow of light*. Princeton university press. ISBN 978-0-470-03634-1. (pp. 137).
- [73] Munk, B. A. (2005). *Frequency selective surfaces: theory and design*. John Wiley & Sons. ISBN 0-471-37047-9. (pp. 405)
- [74] Yang, F., & Rahmat-Samii, Y. (2009). *Electromagnetic band gap structures in antenna engineering*, Cambridge university press (pp. 156-201). Cambridge, UK.
- [75] Jackson, D. R., Caloz, C., & Itoh, T. (2012). Leaky-wave antennas. *Proceedings of the IEEE*, 100(7), (pp. 2194-2206).
- [76] Yang, F., & Rahmat-Samii, Y. (2009). *Electromagnetic band gap structures in antenna engineering* (pp. 156-201). Cambridge, UK ISBN 13:978-1-4987-8211-1
- [77] Baccarelli, P., Paulotto, S., Jackson, D. R., & Oliner, A. A. (2007). A new Brillouin dispersion diagram for 1-D periodic printed structures. *IEEE transactions on Microwave Theory and Techniques*, 55(7), (pp. 1484-1495).
- [78] García-Vigueras, M., Guzmán-Quirós, R., & Gómez-Tornero, J. L. (2011, April). Beamwidth control of 1D LWA radiating at broadside. In *Antennas and Propagation (EUCAP), Proceedings of the 5th European Conference on* (pp. 1853-1856). Rome, Italy.
- [79] Garcia-Vigueras, M., DeLara-Guarch, P., Gómez-Tornero, J. L., Guzman-Quiros, R., & Goussetis, G. (2012, March). Efficiently illuminated broadside-directed 1D and 2D tapered Fabry-Perot leaky-wave antennas. In *Antennas and Propagation (EUCAP), 6th European Conference on* (pp. 247-251). Prague, Czech Republic.
- [80] Balanis, C. A. (2008). *modern antenna handbook*, A John Wiley & Sons. Inc., Publication.
- [81] García Vigueras, M. (2012). Analysis and design of hybrid leaky-wave antennas loaded with frequency selective surfaces. (pp. 102-106)

- [82] Wang, S., Feresidis, A. P., Goussetis, G., & Vardaxoglou, J. C. (2006). High-gain subwavelength resonant cavity antennas based on metamaterial ground planes. *IEEE Proceedings-Microwaves, Antennas and Propagation*, 153(1), (pp. 1-6).
- [83] Mateo-Segura, C., García-Vigueras, M., Goussetis, G., Gómez-Tornero, J. L., & Feresidis, A. (2009, November). Analysis of sub-wavelength cavity leaky-wave antennas with high-impedance surfaces. In *Antennas & Propagation Conference. LAPC. Loughborough* (pp. 577-580). UK.
- [84] Kraus, J. D. (1988). *Antennas*. ISBN 0070355487 9780070355484
- [85] Philips, B., Parker, E. A., & Langley, R. J. (1993). Finite curved frequency selective surfaces. *Electronics Letters*, 29(10), (pp. 882-883).
- [86] Bouslama, M., Traii, M., Denidni, T. A., & Gharsallah, A. (2016). Beam-switching antenna with a new reconfigurable frequency selective surface. *IEEE Antennas and Wireless Propagation Letters*, 15, (pp. 1159-1162).
- [87] Bouslama, M., Traii, M., Denidni, T. A., & Gharsallah, A. (2016). Beam-switching antenna with a new reconfigurable frequency selective surface. *IEEE Antennas and Wireless Propagation Letters*, 15, (pp. 1159-1162).
- [88] Li, J., Denidni, T. A., & Zeng, Q. (2015, August). Beam switching antenna based on active frequency selective surfaces. In *Numerical Electromagnetic and Multiphysics Modeling and Optimization (NEMO), 2015 IEEE MTT-S International Conference on* (pp. 1-3). On, Canada.
- [89] Edalati, A., & Denidni, T. A. (2011, July). Beam-switching antenna based on active frequency selective surfaces. *Antennas and Propagation (APSURSI), 2011 IEEE International Symposium on* (pp. 2254-2257). Spokane, USA.
- [90] Tsai, Y. L., Hwang, R. B., & Lin, Y. D. (2012, June). A reconfigurable beam-switching antenna base on active FSS. *Antenna Technology and Applied Electromagnetics (ANTEM), 15th International Symposium on* (pp. 1-4). Toulouse, France.
- [91] Doherty, W. E., & Joos, R. D. (1998). The PIN diode circuit designers' handbook. *Microsemi Corporation*, 1, (pp. 1-137).
- [92] Niroo-Jazi, M., & Denidni, T. A. (2013, October). Electronically sweeping-beam antenna using a new cylindrical frequency-selective surface. *IEEE Transactions on Antennas and Propagation*, 61(2), (pp. 666-676).

- [93] Ramadan, A. H., Kabalan, K. Y., El-Hajj, A., Khoury, S., & Al-Husseini, M. (2009). A reconfigurable U-Koch microstrip antenna for wireless applications. *Progress In Electromagnetics Research*, 93, (pp. 355-367).
- [94] Hamid, M. R., Hall, P. S., & Gardner, P. (2010, December). Frequency reconfigurable log periodic patch array. *Electronics letters*, 46(25), (pp. 1648-1650).
- [95] Mirkamali, A., & Hall, P. S. (2010, April). Wideband frequency reconfiguration of a printed log periodic dipole array. *microwave and optical technology letters*, 52(4), (pp. 861-864).
- [96] https://dl.cdn-anritsu.com/en-us/test-measurement/files/Manuals/Operation-Manual/10410_00266L.pdf
- [97] http://www.rflambda.com/product_node.jsp?cat=43&product_node_name=Low+Noise+Amplifiers
- [98] <http://www.m2inc.com/blog/dbi-vs-dbd/>
- [99] Edalati, A., & Denidni, T. A. (2011, July). Beam-switching antenna based on active frequency selective surfaces. In *Antennas and Propagation (APSURSI), IEEE International Symposium on* (pp. 2254-2257).
- [100] Niroo-Jazi, M., & Denidni, T. A. (2013). Electronically sweeping-beam antenna using a new cylindrical frequency-selective surface. *IEEE Transactions on Antennas and Propagation*, 61(2), (pp. 666-676).
- [101] Liang, B., Sanz-Izquierdo, B., Parker, E. A., & Batchelor, J. C. (2015). Cylindrical slot FSS configuration for beam-switching applications. *IEEE Transactions on Antennas and Propagation*, 63(1), (pp. 166-173).
- [102] Li, J., Denidni, T. A., & Zeng, Q. (2015, August). Beam switching antenna based on active frequency selective surfaces. In *Numerical Electromagnetic and Multiphysics Modeling and Optimization (NEMO), IEEE MTT-S International Conference on* (pp. 1-3).

- [103] Tsai, Y. L., Hwang, R. B., & Lin, Y. D. (2012, June). A reconfigurable beam-switching antenna base on active FSS. In *Antenna Technology and Applied Electromagnetics (ANTEM), 15th International Symposium on* (pp. 1-4). IEEE.
- [104] Bouslama, M., Traii, M., Denidni, T. A., & Gharsallah, A. (2016). Beam-switching antenna with a new reconfigurable frequency selective surface. *IEEE Antennas and Wireless Propagation Letters*, 15, (pp. 1159-1162).
- [105] Edalati, A., & Denidni, T. A. (2011). High-gain reconfigurable sectoral antenna using an active cylindrical FSS structure. *IEEE Transactions on antennas and propagation*, 59(7), (pp. 2464-2472).

PUBLICATIONS

- [1] Leingthone, M. M., & Hakem, N. (2017, July). A reconfigurable beam switching antenna using active cylindrical fss structure. In *Antennas and Propagation & USNC/URSI National Radio Science Meeting, 2017 IEEE International Symposium on* (pp. 2339-2340). Diego, CA.
- [2] Cylindrical Beam Sweeping Antenna Using a New Active FSS structure
(Acceptance date: 27 November 2017. The article was presented in EUCAP 2018 Conference)
- [3] New AMC Ground Plane for 28 GHz Broadband Antenna
(Acceptance date: 2 March 2018. Article to be presented in APS 2018 Conference)
- [4] Reconfigurable Switched-Beam Antenna Using Cylindrical Bow Tie FSS Window.
(Acceptance date: 2 March 2018. Article to be presented in APS 2018 conference)
- [5] Adaptive Switched Beam Reconfigurable Antenna for Wireless Sensor Network Applications
(Acceptance date: 4 April 2018. Journal To be presented in PIERC 2018 conference)